Fakultät für Medizin
Urologische Klinik und Poliklinik

Identification of Molecular Components Regulating the PI3K Signaling Pathway in Bladder Cancer Therapy

Géraldine Ingrid Chalaud

Vollständiger Abdruck der von der Fakultät für Medizin der Technischen Universität München zur Erlangung des akademischen Grades eines
Doktors der Medizin
genehmigten Dissertation.

Vorsitzender: Prof. Dr. Jürgen Schlegel
Prüfende der Dissertation:
1. Prof. Dr. Jürgen E. Gschwend
2. apl. Prof. Dr. Karl-Friedrich Becker

Die Dissertation wurde am 21.08.2019 bei der Fakultät für Medizin der Technischen Universität München eingereicht und durch die Fakultät für Medizin am 01.01.2020 angenommen.

Anhang I

Eidesstattliche Erklärung

Ich erkläre an Eides statt, dass ich die bei der promotionsführenden Einrichtung: Fakultät für Medizin der TUM zur Promotionsprüfung vorgelegte Arbeit mit dem Titel:

Identification of Molecular Components Regulating the PI3K Signaling Pathway in Bladder Cancer Therapy in der Fakultät für Medizin, Urologischen Klinik und Poliklinik des Klinikums Rechts der Isar, Abteilung für experimentelle Urologie unter der Anleitung und Betreuung durch: Univ.-Prof. Dr. med. Jürgen E. Gschwend ohne sonstige Hilfe erstellt und bei der Abfassung nur die gemäß § 6 Ab. 6 und 7 Satz 2 angebotenen Hilfsmittel benutzt habe.

☒ Ich habe keine Organisation eingeschaltet, die gegen Entgelt Betreuerinnen und Betreuer für die Anfertigung von Dissertationen sucht, oder die mir obliegenden Pflichten hinsichtlich der Prüfungsleistungen für mich ganz oder teilweise erledigt.

☒ Ich habe die Dissertation in dieser oder ähnlicher Form in keinem anderen Prüfungsverfahren als Prüfungsleistung vorgelegt.

☐ Die vollständige Dissertation wurde in _____ veröffentlicht. Die promotionsführende Einrichtung

_____

hat der Veröffentlichung zugestimmt.

☒ Ich habe den angestrebten Doktorgrad noch nicht erworben und bin nicht in einem früheren Promotionsverfahren für den angestrebten Doktorgrad endgültig gescheitert.

☐ Ich habe bereits am _____ bei der Fakultät für _____der Hochschule _____ unter Vorlage einer Dissertation mit dem Thema _____ die Zulassung zur Promotion beantragt mit dem Ergebnis: _____

Die öffentlich zugängliche Promotionsordnung der TUM ist mir bekannt, insbesondere habe ich die Bedeutung von § 28 (Nichtigkeit der Promotion) und § 29 (Entzug des Doktorgrades) zur Kenntnis genommen. Ich bin mir der Konsequenzen einer falschen Eidesstattlichen Erklärung bewusst.

Mit der Aufnahme meiner personenbezogenen Daten in die Alumni-Datei bei der TUM bin ich

☒ einverstanden, ☐ nicht einverstanden.

Ort, Datum, Unterschrift

Abstract

Aside from classic chemotherapy, hormone- and antibody-treatment, target therapy is gaining increasing importance in pharmacological cancer therapy.
The PI3K-signaling pathway is one of the most genetically altered cascades in cancer and therefore of major interest for the development of new compounds. Small molecule inhibitors targeting proteins of this pathway are already successfully used in the clinic for different cancer entities. In advanced urothelial carcinoma, clinical trials using these inhibitors have shown limited benefit to date.
In this study we aimed to identify the underlying molecular mechanisms that regulate the PI3K-signaling pathway in bladder cancer in order to explain the limited clinical success and to develop improved treatment strategies.
Previous work has shown that the suppression of both S6K1 and 4E-BP1 phosphorylation is needed to efficiently block cell growth and proliferation in urothelial carcinoma and that the inhibition of PI3K, AKT, mTOR or mTORC1 alone are not sufficient for this purpose.
A possible explanation could be the mTORC1- and PI3K-dependent while AKT-independent regulation of 4E-BP1 in bladder cancer that we have described in this study.
Furthermore we have characterized a novel PI3K/PDK1- mediated feedback loop that leads to reactivation of AKT upon dual PI3K/mTOR inhibition.
To overcome this phenomenon and efficiently suppress 4E-BP1 phosphorylation, simultaneous inhibition of PI3K/mTORC1 and AKT or PDK1 is required and results in reduced cell viability and colony formation and induction of apoptosis.

Key words: bladder cancer, PI3K-signaling pathway, target therapy, 4E-BP1, AKT, mTOR, NVP-BEZ235

Acknowledgements

I would like to express my honest gratitude to the people without whose support this thesis would not have been possible.

First I would like to thank my supervisor Prof. Dr. Gschwend for giving me the great opportunity to prepare my thesis in his department.

My deep gratitude goes in particular to my mentor PD Dr. Roman Nawroth who guided me throughout the whole process of my thesis and was approachable and helpful at all times. His eager support and commitment was highly motivating and created the ideal atmosphere to work on my project. The close cooperation and numerous fruitful discussions always opened up new perspectives and allowed me not only to develop my scientific thinking and critical questioning but also to grow as a person. His lessons on interpreting scientific papers, presenting data, thoroughness in the execution of experiments, troubleshooting and many more have substantially enriched my knowledge and I'm convinced that they will be of great use in my future work as a doctor.

I specially want to thank Dr. Anuja Sathe who has supervised my work in the lab and patiently taught me everything I needed to know from scratch. With her dedication to science, accuracy, perseverance and helpfulness she is a role model not only as a scientist but also as a human being. I was lucky to have worked with such a great person who taught me so many lessons and who I can call a friend now.

I want to extend my thanks to Monika Moissl, Judith Schäfers and Klaus Mantwill for their various assistance and technical support in the lab. I would also like to express a heart-felt thank you to all the lab members of the Holm and the Nawroth group for making the lab a pleasant and cooperative workplace I always felt comfortable in.

Finally, I would like to thank my family for their constant support, love and encouragement that gives me the strength to pursue my objectives in life.

Table of contents

List of Figures

List of Tables

List of Symbols and Abbreviations

AG	Aktiengesellschaft
AGC	Protein kinase A, G and C
AKT	V-akt murine thymoma viral oncogene
AKT Ser	AKT serine 473
AKT Thr	AKT threonine 308
APS	Ammonium persulfate
ATM	Ataxia telangiectasia mutated
ATP	Adenosine triphosphate
BAD	Bcl-2-associated death promoter
Bax/Bak	Bcl-2-associated X protein/ Bcl-2 homologous killer
BCG	Bacillus Calmette-Guérin
Bcl-2	B-cell lymphoma-2
Bcl-xL	B-cell lymphoma-extra large
BEZ	NVP-BEZ235
BLCA; BC	Bladder cancer
Bcl-2	B-cell lymphoma 2
BCA	Bicinchoninic acid
BSA	Bovine serum albumin
°C	Degree Celsius
CA	California
CDK	Cyclin-dependent kinases
CDKN2A	Cyclin-dependent-kinase-inhibitor 2A
CI	Combination index
CIS	Carcinoma in situ
CLL	Chronic lymphatic leucemia
cm	Centimeter
CO2	Carbon dioxide
CST	Cell Signalling technology
Ctrl; C	Control
D	Dose
ddH20	Double distilled H20
Deptor	DEP-domain- containing mTOR-interacting protein
DEVD	Aspartic acid-Glutamic acid-Valine-Aspartic acid

DMEM	Dulbecco’s Modified Eagle’s Medium
DMSO	Dimethylsulfoxide
DNA	Deoxyribonucleic acid
DNA-PK	DNA-dependent protein kinase
DRI	Dose reduction index
DTT	Dithiothreitol
4E-BP1	Eukaryotic translation initiation factor 4E-binding protein 1
E2F3	E2F transcription factor 3
EAU	European Association for Urology
ECL	Enhanced chemiluminescence
EDTA	Ethylenediaminetetraacetic acid
EGFR	Epidermal growth factor receptor
eIF4E/G/A/F	Eukaryotic translation initiation factor 4E/G/A/F
EM	Electron microscope
EORTC	European Organisation for Research and Treatment of Cancer
ERBB2	Erythroblastic oncogene B 2
FAT	Focal adhesion kinase targeting
FATC	C-terminal FAT-domain
FBS	Fetal bovine serum
FDA	Food and drug administration
FGFR3	Fibroblast growth factor receptor 3
FKBP12	FK506-binding protein of 12 kDa
FRB	FKBP12-Rapamycin Binding
G0	Gap 0
G1	Gap 1
GAP	GTP-ase activating protein
GAPDH	Glycerinaldehyd-3-phosphat-dehydrogenase
GC	Gemcitabine, cisplatin
GDP	Guanine diphosphate
GFR	Glomerular filration rate
GmbH	Gesellschaft mit beschränkter Haftung
GmbH & Co. KG	GmbH & Compagnie Kommanditgesellschaft
G-protein	Guanine nucleotide-binding protein
GSK	GSK2334470

GTP	Guanine triphosphate
H2O2	Hydrogen peroxide
HCl	Hydrogen chloride
HEAT	Huntingtin-Elongation factor 3-regulatory subunit A of PP2A-TOR1
HER1/2	Human epidermal growth factor receptor 1/2
HRP	Horseradish peroxidase
HRAS	Harvey rat sarcoma viral oncogene homolog
hrs; h	Hours; hour
IC	Inhibitory concentration
IGF	Insulin-like growth factor
IgG	Immunoglobulin G
IKBKE	Inhibitor of nuclear factor kappa B kinase subunit epsilon
Inc.	Incorporated
INK	INK 128
IRS	Insulin receptor substrate
ISUP	International Society of Urological Pathology
kDa	Kilodalton
l	Litre
LOH	Loss of heterozygosity
Ltd.	Limited
m	Meter
MA	Massachusetts
MAPK	Mitogen activated protein kinase
MDM2	Mouse double minute 2 homolog
MEM	Minimal Essential Medium
MeOH	Methanol
mg	Milligram
MIBC	Muscle invasive bladder cancer
min	Minute
MK	MK-2206
ml	millilitre
mLST8	Mammallian lethal with Sec13 protein 8
mM	millimolar

MN	Minnesota
MO	Missouri
mRNA	Messenger RNA
mSIN1	Mammalian stress-activated protein kinase interacting protein 1
mTOR	Mechanistic target of rapamycin
mTORC1	mTOR complex 1
mTORC2	mTOR complex 2
MVAC	Methothrexate, vinblastine, adriamycin, cisplatin
NaCl	Sodium chloride
NCI-MATCH	National Cancer Institute-Molecular Analysis for Therapy Choice
NEAA	Non-essential amino acids
NF2	Neurofibromin 2
ng	Nanogram
NJ	New Jersey
nm	Nanometer
nM	Nanomolar
NMIBC	Non-muscle invasive bladder cancer
nmol	Nanomole
No.	Number
NSW	New South Wales
NY	New York
NYHA	New-York Heart Association
OH	Hydroxide
PAGE	Polyacrylamide gel electrophoresis
PARP	Poly(ADP-Ribose)-Polymerase 1
PBS	Phosphate buffered saline
PD-1	Programmed cell death protein 1
PDK1	Phosphoinositide dependent kinase 1
PD-L1	Programmed death-ligand 1
pH	Potentia hydrogenii
PH	Pleckstrin homology
PI	Phosphatidylinositol
PI3K	Phosphoinositide 3-kinase
PIP2	Phosphoinositol-4,5-bisphosphate

PIP3	Phosphatidylinositol-3,4,5-trisphosphate
PIK	PIK90
PIK3CA	Phosphatidylinositol-4,5-bisphosphate 3-kinase catalytic subunit alpha
PIKK	PI3K-related-kinase
PKB	Protein kinase B
pNET	Pancreatic neuroendocrine tumor
PR	Partial response
PRAS 40	Proline-rich AKT substrate of 40kDa
Protor-1	Protein observed with Rictor 1
P/S	Penicillin/Streptomycin
PTEN	Phosphatase and tensin homologue deleted on chromosome 10
PUNLMP	Papillary urothelial neoplasm of low malignant potential
PVDF	Polyvinylidene fluoride
RAD	RAD001
rapa	Rapamycin
Raptor	Regulatory associated protein of mTOR
Ras	Rat sarcoma
RB	Retinoblastoma
RCF	Relative Centrifugal Force
RHEB	Ras homologue enriched in brain
Rictor	Rapamycin-insensitive companion of mTOR
RNA	Ribonucleic acid
RNAi	RNA interference
RPMI	Roswell Park Memorial Institute
RTK	Receptor tyrosin kinase
s	Second
S	Synthesis
S6K1	Ribosomal protein S6 kinase beta 1
SD	Standard deviation; stable disease
SDS	Sodium dodecyl sulfate
Ser	Serine
SH2	Src homology 2
shRNA	Small hairpin RNA
siRNA	Small interfering RNA

SLC14A	Solute carrier 14A
STAG2	Stromal antigen 2
SWI/SNF	Switch/sucrose non fermenting
TBK1	TANK-binding kinase 1
TBS	Tris buffered saline
TBST	Tris buffered saline with Tween-20
TCGA	The Cancer Genome Atlas
TEMED	Tetramethylethylenediamine
TERT	Telomerase reverse transcriptase
Thr	Threonine
Tis	Tumor in situ
TNM	Tumor, Node, Metastasis
TOS	Target of rapamycin (TOR)-signaling
TP53	Tumor protein p53
Tris	Tris(hydroxymethyl)-aminomethane
TSC	Tuberous sclerosis complex
TURB	Transurethral resection of the bladder
U	Units
UK	United Kingdom
USA	United States of America
V	Volt
VA	Virginia
VEGF	Vascular endothelial growth factor
VEGFR	Vascular endothelial growth factor receptor
WHO	World health organization
WI	Wisconsin
µg	Microgram
µl	Microlitre
µm	Micrometer
µM	Micromolar
µmol	Micromole

1 Introduction

1.1 Bladder Cancer

1.1.1 Epidemiology and Risk Factors

Being the ninth most common cancer worldwide with 430 000 new cases diagnosed in 2012 and 165 000 attributable deaths (Antoni et al. 2017) bladder cancer is not only a global health issue but also an economical burden (Sievert et al. 2009). The highest incidence was found in well-developed regions such as Europe and Northern America (Cumberbatch et al. 2018). In Germany it is the fourth most prevalent cancer in men and fourteenth in women according to the Robert-Koch-Institute (Koch-Institut 2017). Although bladder cancer is 3-4 times more common in men than in women and the incidence is higher in the white population, the mortality rate is higher amongst women and black individuals who both often show a more advanced stage (Fajkovic et al. 2011, Yee et al. 2011). With a median age of diagnosis at 69 in men and 71 in women, bladder cancer is classified as a disease of the elderly (Volanis et al. 2010).

Smoking is probably the best-studied and most important risk factor in bladder cancer that significantly increases incidence and disease-specific mortality (Cumberbatch et al. 2016). About 50% of all bladder cancer cases are attributed to smoking (Freedman et al. 2011). It was found that workers in the paint, rubber, petroleum and dye industry that are exposed to aromatic amines, polycyclic aromatic hydrocarbons or chlorinated hydrocarbons have an increased risk for bladder cancer. Infection with Schistosoma haematobium, a parasitic worm that causes chronic cystitis, is linked to a special form of bladder cancer, the squamous cell carcinoma, in some regions of North Africa, where this parasite is endemic. Ionizing radiation and the drugs cyclophosphamide and pioglitazone have further been related to a higher incidence of urothelial bladder cancer (Burger et al. 2013).

An increasing number of studies point to the fact that genetic predisposition to bladder cancer plays an important role. Some genetic factors influence vulnerability of external carcinogens, for example alterations in the genes that encode carcinogen metabolizing enzymes, such as N-acetyltransferase, Glutathione-S-transferases and soluble sulfotransferases (Antonova et al. 2015). A correlation between an increased risk of bladder cancer and variation in the SLC14A gene that encodes for urea transporters as well as a role of decarboxylase protein complexes was also described (Garcia-Closas et al. 2011, Cheng et al. 2016).

1.1.2 Classification, staging and prognosis of bladder cancer

In western countries around 95% of bladder malignancies are urothelial carcinomas, but a small subset of non-urothelial carcinomas like squamous cell carcinomas and adenocarcinomas, but also tumors of non-epithelial origin exist (Dahm et al. 2003).

The tumor, node and metastasis (TNM) classification is used for staging of bladder cancer (Brierley et al. 2017) (Figure 1). The T-category is based on the depth of invasion into the layers of the bladder wall (Paner et al. 2017). Non-muscle invasive bladder cancer (NMIBC), mainly Ta papillary tumors of low grade, but also high grade flat carcinomas in situ (Tis) and T1 tumors that reach the lamina propria are found in 75% of patients at diagnosis. The remaining 25% are muscle invasive bladder cancer (MIBC) or metastatic disease (Smith et al. 2014, Sanli et al. 2017). The MIBC comprises stages T2 to T4. The T2 stage is divided up into T2a and T2b, meaning the tumor invades the superficial or the deep muscle respectively, while T3 tumors infiltrate the perivesical structures, and T4 tumors reach adjacent organs and tissues (Witjes et al. 2014). The presence or the lack of regional lymph node invasion is described by the N-category (N0 to N2), and the M-category refers to distant organ metastasis (M0, M1). Hautmann et al. showed that lymph node metastasis is an important risk factor independent of the stage and that it has a negative impact on disease specific survival (Hautmann et al. 2012). For histologic classification of bladder cancer, both the WHO grading system published in 1973 and 2004/2016 should be used according to the guidelines, while advantages and disadvantages are still under discussion (Babjuk et al. 2017, Comperat et al. 2018). The 2004/2016 classification differentiates between papillary urothelial proliferation of low malignant potential (PUNLMP) and low and high grade tumors, according to their propensity for invasion and therefore their aggressiveness (Humphrey et al. 2016). Bladder cancer prognosis is derived from this staging and grading. Although the 5-year survival rate for NMIBC is around 90%, recurrence is common and 10-15% progress to MIBC. Especially Tis and T1 have a high risk of invasion (Knowles et al. 2015). MIBC are of high grade in the majority of cases and have a poor 5-year survival rate of 50%. A progression to metastatic disease occurs in half of the cases (Knowles et al. 2015). Patients with metastasized bladder cancer have a median life expectancy of 14 to 15 months (von der Maase et al. 2005) synonymous with a survival rate of 5% at 5 years (Siegel et al. 2019).

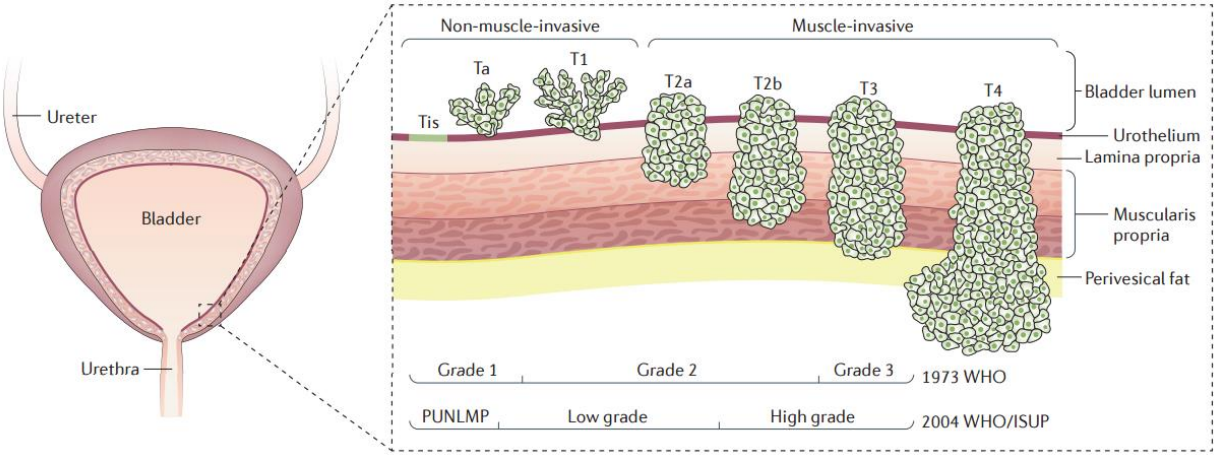

Figure 1: Grading and staging of bladder cancer (Sanli et al. 2017)

1.1.3 Diagnosis and therapeutic strategies of bladder cancer

Painless hematuria is a common first symptom in bladder cancer and should initiate a diagnostic procedure including a complete medical history of the patient, a physical examination and an ultrasound of the kidneys and the bladder as non-invasive diagnostic devices as well as a cystoscopy with histologic evaluation (Babjuk et al. 2017). Despite the ongoing research, no urinary biomarkers are used in the clinic to date. Urine cytology has a high specificity but low sensitivity in the diagnosis of bladder cancer and is recommended especially in addition to a cystoscopy for the detection of high-grade tumors (Oeyen et al. 2019). Tis, Ta and T1- tumors which are NMIBC, can be diagnosed via cystoscopy and histological criteria of the biopsies or the transurethral resection of the bladder (TURB). New techniques like fluorescence cystoscopy or narrow-band imaging can be used to facilitate the visualization and resection of the tumor, especially in case of CIS. According to the EORTC scoring system and risk tables, patients can be categorized in a low, intermediate and a high risk group regarding recurrence and progression. This stratification determines the conditions of adjuvant therapy, for instance the duration of intravesical immunotherapy with BCG or chemotherapy instillation treatment. Radical cystectomy should be considered in cases of elevated risk of tumor progression and is recommended in tumors refractory to BCG treatment (Babjuk et al. 2017).

The therapeutic approach of MIBC consists of radical cystectomy and pelvic lymph node resection. Since the 1980s neoadjuvant cisplatin-based combination chemotherapy, which improves overall survival by about 5%, is recommended. Amongst MIBC patients relapse after treatment is observed in about 50% with two thirds showing distant metastases (Rosenberg et al. 2005, Witjes et al. 2017).

The first-line management of metastatic disease consists of cisplatin-based chemotherapy regimens. The standard schemes are combinations of methotrexate, vinblastine, doxorubicin and cisplatin (MVAC) or gemcitabine and cisplatin (GC) sometimes combined with paclitaxel. These schemes can only be applied after evaluation of the patient’s suitability for cisplatin, based on the GFR, performance score, audiometric loss, peripheral neuropathy and NYHA grade. Carboplatin-based combinations or taxanes that are used in patients not eligible for cisplatin combination therapy have shown inferior results (Witjes et al. 2017). For about 30 years there have been no major improvements in the treatment of bladder cancer and survival-rates (Berdik 2017). Vinflunine was the only second-line treatment option in Europe (Witjes et al. 2017) until the FDA approved atezolizumab, an antibody against the immune checkpoint protein PD-L1 for patients that progressed after cisplatin-based chemotherapy, in May 2016 (Ning et al. 2017). It had shown impressive results with an overall response rate of 15%, compared to 10% overall response of the historical control and an ongoing response in 84% of these patients after 11.7 months (Rosenberg et al. 2016). Nonetheless, the primary endpoint of longer overall survival with atezolizumab could not be met compared to chemotherapy with either vinflunine or taxanes and was around 11 months for both groups in the population with over 5% of PD-L1 expressing immune cells in the tumor (Powles et al. 2018). The FDA-approval for PD-1 inhibitor nivolumab as a second-line

treatment followed in February 2017, based on a study that showed 19.6% objective response rate of this drug (Sharma et al. 2017). Pembrolizumab, durvalumab and avelumab also received their FDA-approval as second-line agents and atezolizumab and pembrolizumab were approved as first-line treatments for patients ineligible to cisplatin-based chemotherapy (Ghatalia et al. 2018). These immune-checkpoint inhibitors are currently subject to further investigation, inter alia the role of combination treatment with immunotherapy and chemo- or target therapy (Tripathi et al. 2018).
Despite this promising new class of drugs, metastasized bladder cancer remains an incurable disease to the present day with limited treatment options, poor survival rates and the imperative need for novel therapeutic strategies (Sanli et al. 2017, Witjes et al. 2017).

1.1.4 Tumorigenesis and molecular biology of bladder cancer

Papillary low-grade NMIBC and solid high-grade MIBC have been described to develop via two different pathways that differ in terms of histopathological and molecular characteristics (Audenet et al. 2018) (Figure 2).
Loss of heterozygosity (LOH) in chromosome 9 is a characteristic and probably early event in both subtypes (Knowles et al. 2015). Low grade papillary urothelial carcinoma derives from urothelial hyperplasia and is linked to genomic alterations affecting cell growth and proliferation, often via the MAPK and PI3K pathway. PIK3CA, STAG2 and TERT mutations are related to this cancer entity and either HRAS or FGFR3 mutations activating the Ras-pathway are found in approximately 82% of NMIBC (Allory et al. 2014, Taylor et al. 2014, Solomon et al. 2016).
MIBC that usually develops from flat dysplasia and carcinoma in situ shows a vast molecular variety in contrast to NMIBC. Frequent mutations affect proteins regulating the cell-cycle, such as RB1 and p53, that are involved in the G1/S transition of the cell cycle or regulating proteins within their pathway, such as MDM2, E2F3 or CDKN2A. The latter might be responsible for the rare event of conversion of low grade papillary tumors into muscle-invasive carcinomas (Knowles et al. 2015). In 2014, The Cancer Genome Atlas research network (TCGA) published a molecular analysis of 131 muscle-invasive urothelial carcinomas in order to identify key mutations and potential therapeutic targets. Three years later, they published a second study with an expanded number of 412 specimens of MIBC (TCGA 2014, Robertson et al. 2017). According to the TCGA, the p53/cell cycle regulation pathway was altered in 89% of all analyzed tumors, and components of the nucleosome remodeling complex were altered in 26%. They also found that epigenetic changes conducted by genes involved in chromatin remodeling by histone modification play an important role, as they were mutated in 52%. In 71% of tumors, genetic alterations in the RTK/RAS/PI3K pathway were detected (Robertson et al. 2017, Rodriguez-Vida et al. 2018). The PIK3CA gene encoding for the p110 subunit of PI3K was found to be altered in 22%, the TSC1 gene in 8% and overexpression of AKT3 was detected in 10% in the TCGA analysis (Rodriguez-Vida et al. 2018)

This and other genomic sequencing studies provide insight in and expand comprehension of the complex genomic landscape of urothelial carcinoma. They allow forming molecular subtypes reaching beyond the original two-pathway-theory and lay the foundation for target therapy in the context of personalized medicine in bladder cancer management (Glaser et al. 2017, Robertson et al. 2017, Inamura 2018)

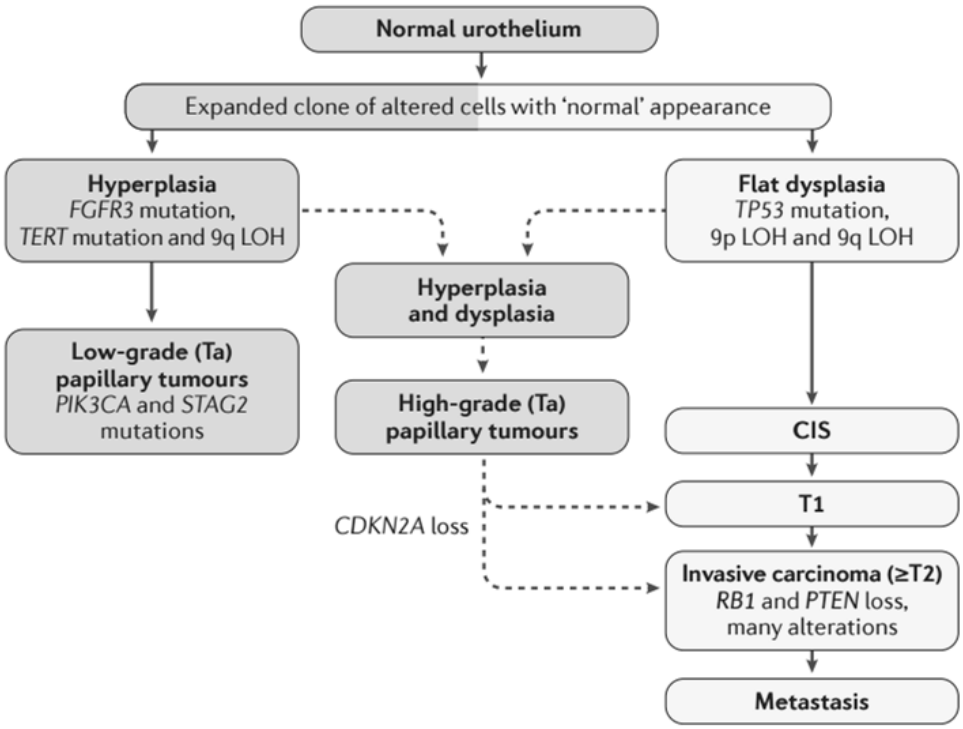

Figure 2: Pathogenesis of bladder cancer (Sanli et al. 2017)

1.2 Target therapy in bladder cancer

The understanding of frequently altered genes in cancer leads to identifying the signaling pathways that are crucial for tumorigenesis and that can therefore potentially be targeted by agents that inhibit proteins of this pathway.
In many cancer entities, such as renal cell carcinoma, lung and breast cancer, target therapy is already an integral part of guideline-based therapy due to the intensified exploration of molecular cancer biology (Lheureux et al. 2017).
With the recent FDA approvals of immune checkpoint inhibitors, target therapy has also found clinical use in bladder cancer treatment, which might be the beginning of a promising development in this direction (Ghatalia et al. 2018). Ross et al. presented a genomic-profile study in 2016 that analyzed 295 high grade and advanced urothelial carcinoma specimens. They found the presence of at least one genomic alteration that could be targeted by therapeutic agents already on the market or in the course of evaluation in clinical studies, in 93% of the cases (Ross et al. 2016). Different target therapies have been tested in clinical trials especially in locally advanced or metastasized urothelial carcinoma. One attempt was to downregulate VEGFR-pathway signaling via specific antibodies, such as Bevacizumab and Ramucirumab

or the use of tyrosinkinase inhibitors like Sunititinib and Pazopanib. Bevacizumab combined with GC in metastatic or inoperable bladder cancer showed promising results in overall survival and response rate but also three deaths related to treatment (Hahn et al. 2011). Ramucirumab combined with docetaxel proved to be successful in a randomized controlled multicenter phase II trial and displayed prolonged progression free survival (Petrylak et al. 2016). Both drugs are currently further examined in phase III trials (NCT00942331; NCT02426125, https://clinicaltrials.gov/). Neither sunitinib nor pazopanib could meet their endpoints in several phase II trials (Gallagher et al. 2010, Grivas et al. 2014, Jones et al. 2017). Targeting the FGFR3-pathway with different inhibitors has shown clinical efficacy in advanced bladder cancer and the FDA granted breakthrough designation for erdafitinib, a pan-FGFR-inhibitor (Iyer et al. 2018).
Regarding the HER2-pathway, trastuzumab did not show beneficial effects on progression-free or overall survival in combination with gemcitabine and cisplatin compared to chemotherapy alone, as shown in a multicenter phase II trial (Oudard et al. 2015). Similarly, lapatinib, inhibitor of HER1 and 2 had disappointing results (Powles et al. 2017). Cetuximab and gefitinib both target the EGFR-pathway that is commonly altered in urothelial carcinoma. In clinical trials they both showed high toxicity (Philips et al. 2008, Hussain et al. 2014). This was just a selection of targeted therapy studies, but many other drugs like Palbociclip, a CDK4/6 pathway inhibitor, the PARP inhibitor Olaparib or the oral histone deacetylase inhibitor mocetinostat, are currently under investigation (Aragon-Ching et al. 2017)
The PI3K-signaling pathway is another pathway that plays an important role in target therapy trials because of its frequent activation in urothelial carcinoma (TCGA 2014, Robertson et al. 2017), and it is also at the center of this study.

1.3 Targeting the PI3K-signaling pathway in bladder cancer

1.3.1 The PI3K signaling cascade

The PI3K/AKT/mTOR signaling pathway promotes cell growth, survival, protein synthesis, metabolism and proliferation (Martini et al. 2014) (Figure 3). As one of the most frequently altered pathways in human cancer, it has a crucial role in tumorigenesis, cellular transformation, cancer progression and drug resistance and is therefore of major interest in the development of new therapeutic agents (Mayer et al. 2016).
The phosphoinositide 3-kinases (PI3Ks) are a family of lipid kinases comprising eight isoforms that are subdivided into three classes according to their structural characteristics and their lipid substrate specificity. They have the ability to phosphorylate the inositol-ring-bound 3’OH-group of three different phosphatidylinositol lipid substrates (PIPs). PI3K class I are heterodimers of a catalytic (p110) and a regulatory subunit (p85). It is the best-studied class and splits into two groups. Class IA PI3Ks, with the catalytic subunits p110α, p110β and p110δ, most often interact with the regulatory subunit p85. They are usually activated by receptor tyrosine kinases (RTKs). Class IB with the catalytic subunit p110γ dimerizes with regulatory subunits p101 and p87 and is activated via G-protein coupled

receptors (Vanhaesebroeck et al. 2010). In cancer, class IA PI3Ks are most frequently involved. The transmembrane domain of activated RTKs can bind the Src homology 2 (SH2) domains of p85 directly or via adaptor proteins such as insulin receptor substrate (IRS) 1/2. This event triggers the accumulation of PI3K heterodimers to the membrane and abolishes the inhibitory effect of p85 on p110. Its catalytic function leads to conversion of phosphoinositol-4,5-bisphosphate (PIP2) to phosphatidylinositol-3,4,5-trisphosphate (PIP3), a reaction that is antagonized by the phosphatase and tensin homologue deleted on chromosome 10 (PTEN) (Engelman et al. 2006, Engelman 2009). Upon loss of PTEN or overactivation of the pathway, PIP3 accumulates at the membrane. It is a second messenger that leads to binding of different proteins with pleckstrin homology (PH) domains, such as phosphoinositide dependent kinase 1 (PDK1) or v-akt murine thymoma viral oncogene (AKT), also known as protein kinase B (PKB). AKT is a serine/threonine kinase and a key molecule in the PI3K-signalling pathway that regulates multiple downstream proteins linked to metabolism and tumorigenesis. It also inhibits apoptosis by direct phosphorylation of the anti-apoptotic factor Bcl-2-associated death promoter (BAD) (Datta et al. 1997). For its full activation, a phosphorylation of its threonine 308 (Thr 308) residue, which is effected by PDK1, is required as well as a phosphorylation of its serine 473 (Ser 473) residue mediated via mechanistic target of rapamycin complex 2 (mTORC2) (Bellacosa et al. 2005, Franke 2008, Courtney et al. 2010, Lim et al. 2015).

The serine/threonine kinase mTOR is a member of the PI3K-related-kinase (PIKK) family and forms two distinct complexes. mTOR complex 2, which acts upstream of AKT and is PI3K-dependently activated (Liu et al. 2015), is formed by six different proteins: mTOR, rapamycin-insensitive companion of mTOR (Rictor), mammalian stress-activated protein kinase interacting protein (mSIN1), protein observed with Rictor-1 (Protor-1), mammalian lethal with sec13 protein 8 (mLST8), and DEP-domain- containing mTOR-interacting protein (Deptor). One of the major downstream targets of AKT is mTOR complex 1, which consists of mTOR, regulatory-associated protein of mTOR (Raptor), mLST8, Deptor and proline-rich AKT substrate 40kDa (PRAS40) (Figure 4) (Laplante et al. 2009). In an activated state AKT phosphorylates tuberosis sclerosis complex 2 (TSC2) that forms the TSC-complex together with TSC1. This complex acts as the GTP-ase activating protein (Garcia-Closas et al.) of the small GTPase Ras homologue enriched in brain (Rheb). Rheb is usually negatively regulated by TSC1/2 and kept in its inactive, GDP-bound state. Is this TSC-complex mediated inhibition of Rheb abolished through activation of AKT, Rheb-GTP accumulates, leading to activation of mTORC1 probably through direct interaction (Dibble et al. 2015). PRAS40 was found to be an inhibitor of mTORC1 by preventing TOS-motif dependent-binding of its substrates to Raptor (Wang et al. 2007). It can directly be phosphorylated by AKT and mTOR, releasing its inhibitory effect on mTORC1 (Oshiro et al. 2007). Raptor regulates the catalytic activity and substrate specificity of mTORC1. It acts as a scaffold protein by binding mTORC1-substrates via their TOS-motif (Nojima et al. 2003, Schalm et al. 2003). Out of those, the two best-described are ribosomal protein S6 kinase beta-1 (S6K1) and eukaryotic translation initiation factor 4E-binding protein 1 (4E-BP1) that have a crucial impact

on protein synthesis and cell growth (Mamane et al. 2006). For its full activation S6K1 is also phosphorylated by PDK1 and can subsequently promote mRNA translation initiation through several downstream effectors (Saxton et al. 2017). It also induces a negative-feedback-regulation of the PI3K pathway via direct phosphorylation as well as expression downregulation of the IRS-1 protein (Harrington et al. 2004).
Once 4E-BP1 is phosphorylated, it releases eIF4E, which can then connect to eIF4G and eIF4A to form the translation initiation complex eIF4F and trigger 5'cap-dependent mRNA translation. These mRNAs encode proteins like cyclin D1, vascular endothelial growth factor (VEGF) or insulin-like growth factor (Harrington et al.) with important functions in cell-cycle progression (Ma et al. 2009). However, 4E-BP1 is not solely regulated by mTORC1 in bladder cancer as previous results of our group have shown (Nawroth et al. 2011).

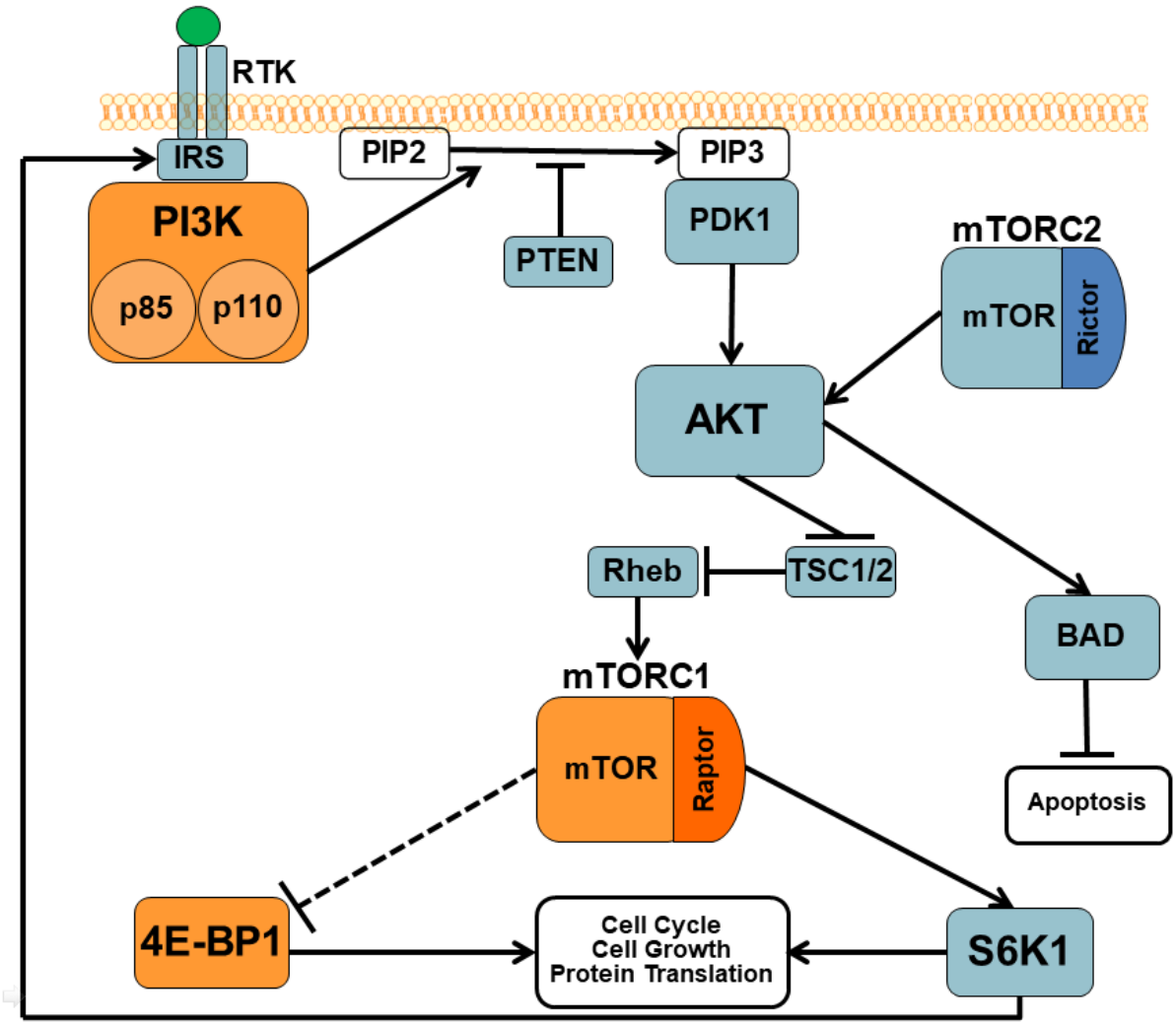

Figure 3: The PI3K/AKT/mTORC1 signaling pathway

1.3.2 Drugs targeting the PI3K-signaling pathway in cancer and in urothelial carcinoma in particular

Many studies, including the TCGA- and Ross-study mentioned above, indicate that the PI3K/AKT/mTOR signaling pathway is frequently mutated in bladder cancer and that crucial proteins of this pathway might be suitable objects for targeted therapy (TCGA 2014, Carneiro et al. 2015, Ross et al. 2016)
There are five groups of inhibitors directed against different key proteins of the PI3K pathway that were developed to counteract pro-oncogenic signal transduction: the PI3K inhibitors, the mTOR inhibitors, the dual PI3K/mTOR inhibitors, the AKT inhibitors and the PDK1 inhibitors (Houede et al. 2015, Sathe and Nawroth 2018).

1.3.2.1 Inhibition of PI3K

There are two classes of PI3K inhibitors: some selectively target specific isoforms of IA PI3Ks like Idelalisib, which targets p110δ and has been approved for CLL and two types of lymphoma. However, the majority are pan-PI3K inhibitors that target all class I PI3K isorforms (Zhao et al. 2017). Wortmannin and LY-294002 as potent pan-PI3K inhibitors were the first to be used, but did not carry further than preclinical trials because of their non-specificity within the PIKK-family and high toxicity profile (Akinleye et al. 2013). In bladder cancer cells, they showed suppression of proliferation or radio sensitization (Gupta et al. 2003, Ortiz et al. 2004, Wu et al. 2011).
In this study we worked with the imidazoquinazoline pan-PI3K inhibitor PIK90 that potently inhibits p110α, p110γ and p110δ and has little less affinity to p110β with IC50s of 11nM, 18nM, 58nM and 350nM respectively. Being an ATP-competitive inhibitor, it forms hydrogen bonds with the ATP-binding pocket of the PI3K catalytic subunit. Although it also shows inhibitory activity against DNA-dependent protein kinase (DNA-PK) with an IC50 of 13nM, a concentration of 1.05µM is needed to inhibit mTORC1, with both targets being members of the PIKK- family (Knight et al. 2006). To date, PIK90 has only been tested in preclinical settings (Lonetti et al. 2015), whereas BKM120, another pan-PI3K inhibitor, was recently examined in a phase II trial for second-line bladder cancer therapy. The two-month-PFS could not be improved compared to chemotherapy, but SD was observed in 6 out of 13 patients and there was one case of PR. A TSC1 mutation was detected in this patient as well as in one patient with SD (Iyer et al. 2015). These results led to another study with BKM120 in patients with metastatic bladder cancer displaying PI3K pathway mutations (NCT01551030, https://clinicaltrials.gov/).

1.3.2.2 Inhibition of PDK1

Active-site PDK1 inhibitor GSK-2334470 has a higher specificity towards PDK1 than other inhibitors targeting this kinase. It potently inhibits PDK1 with an IC50 of 10nM, but when used at 500-fold higher concentrations, it does not display activity against a panel of 93 other protein kinases, of which 13 belong to the AGC-kinases and have structural similarity to PDK1 (Najafov et al. 2011). Although it reliably inhibited S6K1

phosphorylation, it failed to fully suppress AKT activation in conditions of strong activation of the PI3K pathway. This demonstrates that GSK-2334470 can inhibit downstream substrates of PDK1 to a different extent and that it can vary depending on the circumstances (Knight 2011). In preclinical trials, GSK-2334470 showed antitumor activity in different cancer entities and has proven to inhibit proliferation and induce apoptosis especially in multiple myeloma (Yang et al. 2017). To our knowledge this agent has not been used in bladder cancer studies so far.

1.3.2.3 Inhibition of mTOR

1.3.2.3.1 Steric inhibition of mTORC1 with rapalogs

Rapamycin was first isolated in 1975 from Streptomyces hygroscopius found in a soil sample on Easter Island (Rapa Nui) and led to the discovery of TOR1 and 2 in yeast and later mammalian TOR about 25 years ago (Benjamin et al. 2011). It is a specific inhibitor of mTORC1, although it was described to inhibit mTORC2 in some cell lines upon an extended period of incubation (Laplante et al. 2012). Rapamycin allosterically inhibits mTORC1 by forming a complex with the 12kDA FK506-binding protein (FKBP12). Analysis of the crystal structure of mTOR-mLST8 complex demonstrated that FKBP12-rapamycin binds to the FRB- (FKBP12-Rapamycin Binding) domain of mTOR. This domain normally interacts with substrates to facilitate access to the restricted active site. Upon rapamycin inhibition, the accessibility to the catalytic cleft is further reduced and recruitment of targets via the FRB-domain is blocked (Figure 4) (Yang et al. 2013). To improve pharmacokinetic properties and solubility, analogues of rapamycin, so-called rapalogs, were developed. Two representatives, temsirolimus and everolimus (RAD001), received FDA-approval in therapy of advanced renal cell carcinoma in 2007 and 2009 respectively. In the following years temsirolimus was approved for mantle cell lymphoma and everolimus for treatment of neuroendocrine tumors of pancreatic, gastrointestinal and lung origin, for subependymal giant cell astrocytoma and in combination with an aromatase inhibitor for advanced hormone receptor-positive HER2-negative breast cancer. However, compared to promising preclinical results, the anticancer effect of rapamycin in the clinical setting was limited (Li et al. 2014, Chan et al. 2017). In bladder cancer there have been, to date, several phase II clinical trials examining mTORC1 inhibitors after failure of platinum-based chemotherapy. Four of them showed no benefit of rapalogs as second-line therapy of bladder cancer, except for few patients with prolonged responses (Table 1). These disappointing results might be explained by different drawbacks linked to rapamycin treatment. An important reason might be that 4E-BP1 phosphorylation is not suppressed upon the use of this inhibitor. Another explanation is the rapamycin-triggered PI3K/AKT feedback-loop that leads to over-activation of PI3K/AKT-signaling (Saxton et al. 2017). Nevertheless a recent study on temsirolimus for second-line treatment of recurrent bladder cancer was able to meet their primary endpoint and showed clinical benefit for a subset of patients despite a high rate of adverse effects in total (Pulido et al. 2018). Temsirolimus and everolimus are still currently investigated in first- and second-line

settings for advanced urothelial carcinoma (NCT00805129, NCT01090466, NCT01215136, https://clinicaltrials.gov/).

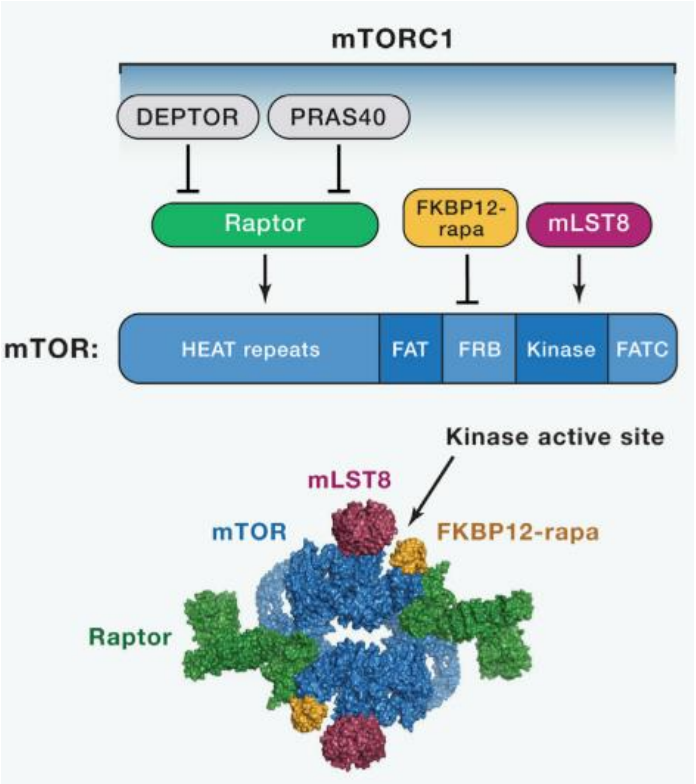

Figure 4: The structure of mTORC1. Subunits and binding sites and cryo-EM structure with binding of FKBP12-rapamycin (without PRAS40 and Deptor). Reproduced from (Saxton et al. 2017)

Study	Drug	n	Overall survival (months)	Complete response	Partial response	Stable disease
(Seront et al. 2012)	Everolimus	37	3.4	0	2	8
(Gerullis et al. 2012)	Temsirolimus	14	3.5	0	0	4
(Milowsky et al. 2013)	Everolimus	37	8.3	1	1	23
(Niegisch et al. 2015)	Everolimus, Paclitaxel	24	5.6	0	5	9
(Pulido et al. 2018)	Temsirolimus	45	7.2	0	3	19

Table 1: Clinical trials of rapalogs in bladder cancer. Number of patients assessed (n)

1.3.2.3.2 Active site inhibition of mTOR

ATP-competitive inhibitors of mTOR, for example Torin 1 and 2, PP242, AZD-8055 or INK128 were developed to overcome drawbacks of rapamycin inhibition, such as the lack of mTORC2 inhibition. They target the catalytic site of the mTOR kinase and therefore inhibit both mTORC1 and mTORC2 and suppress 4E-BP1 phosphorylation (Zaytseva et al. 2012). These features are made responsible for stronger antitumor activity in preclinical studies compared to rapalogs (Benjamin et al. 2011).
Although AKT phosphorylation is initially suppressed by ATP-competitive inhibitors due to mTORC2-inhibition, after longer incubation AKT is reactivated via the S6K1/PI3K feedback-loop (Rodrik-Outmezguine et al. 2011).
Because of the close structural similarity of the mTOR and the PI3K kinase domain some ATP-competitive mTOR inhibitors also suppress PI3K activity and vice versa, and efforts are made to improve selectivity (Benjamin et al. 2011).
INK128, also called MLN0128, TAK-228 or sapanisertib, is the compound we worked with in this study. It has an IC50 of 1nM for mTOR inhibition and an about 200-fold higher IC50 for inhibition of class I PI3Ks (Hsieh et al. 2012).
It was one of the first ATP-competitive inhibitors tested in clinical studies and almost 40 trials are currently ongoing in various cancer entities. One of these assesses INK128 in locally advanced or metastatic bladder cancer that bear TSC1 or 2 mutations and another one in combination with paclitaxel (Garcia-Echeverria 2010) (NCT03047213, NCT03745911 https://clinicaltrials.gov/).

1.3.2.4 Inhibition of AKT

ATP-competitive (AZD5363) and allosteric inhibitors of AKT (MK-2206) can be distinguished (Khan et al. 2013). The first ATP-competitive inhibitors showed poor kinase selectivity coupled with high toxicity leading to suspension of clinical development of some of the compounds. However, several second generation inhibitors aiming to improve these properties are currently in clinical development (Huck et al. 2017). The allosteric inhibition consists of preventing the active state of the kinase by keeping it in a closed conformation. This is achieved by binding of the small molecule into a hydrophobic pocket formed at the interface of the PH-domain and the kinase-domain (Fang et al. 2015). MK-2206 is one representative of allosteric AKT inhibitors that suppresses activation of AKT1, AKT2 and AKT3 with IC50s of 8nM, 12nM and 65nM respectively via dephosphorylation of both the threonine 308 and the serine 473 residue (Hirai et al. 2010). Around 30 phase II clinical studies for MK-2206 are currently ongoing in many different cancer entities, such as renal cell carcinoma, nasopharyngeal carcinoma, breast or prostate cancer (Pretre et al. 2018)(https://clinicaltrials.gov/). As antitumor-activity of a monotherapy was often limited, combination treatments were brought into sharper focus (Brown et al. 2017). For bladder cancer, MK-2206 was evaluated in preclinical studies, where sensitivity to this compound was associated with PIK3CA helical domain mutations (Sathe et al. 2014). A link between MK-2206 response and PIK3CA mutations, but also PTEN-deficiency was made in other cancer entities as well (Dienstmann et al. 2014). When

combined with cisplatin in bladder cancer cell lines, MK-2206 showed an increase of cytotoxicity and apoptosis (Sun et al. 2015).

1.3.2.5 Dual inhibition of PI3K and mTOR

Inhibitors that target the PI3K and the mTOR kinase domain to the same extent were developed in order to overcome the S6K1/PI3K feedback activation of the pathway observed upon single inhibition of mTOR.
One example is the imidazoquinoline NVP-BEZ235, which inhibits PI3K with an IC50 of 4nM (for p110α) and mTOR kinase activity with an IC50 of 20.7nM in an ATP-competitive manner (Maira et al. 2008). It was found to be superior to everolimus in a panel of 21 different cancer cell lines in terms of proliferation suppression (Serra et al. 2008). Consistently, the potential of downregulating S6K1 and 4E-BP1 phosphorylation simultaneously in different cancer entities, such as in ovarian carcinoma (Santiskulvong et al. 2011), glioblastoma (Yu et al. 2015), nasopharyngeal carcinoma (Ma et al. 2014) or endometrial carcinoma (Shoji et al. 2012), has been described in the literature and was also published for bladder cancer by our group (Nawroth et al. 2011). Whereas in some cancers, e.g. in mantle cell lymphoma, the inhibition of mTORC1 via rapalogs shows an effect on 4E-BP1 phosphorylation (Haritunians et al. 2007), in bladder cancer this is only the case for dual PI3K and mTOR inhibition via NVP-BEZ235 (Nawroth et al. 2011). The inhibitor was tested in multiple early clinical trials for different cancer entities with limited success or results still to be evaluated (https://clinicaltrials.gov/). In a phase II trial for second line therapy in bladder cancer, one partial response and two cases of stable disease were observed but also high toxicity, with half of the patients experiencing adverse events of grade 3 or 4 (Seront et al. 2016). Another second-line trial in bladder cancer patients was prematurely terminated because of Novartis' decision to stop the marketing of NVP-BEZ235 (NCT01856101, https://clinicaltrials.gov/). Limited clinical efficacy and high toxicity was also observed in pNET and renal cell carcinoma trials (Carlo et al. 2016, Fazio et al. 2016, Salazar et al. 2018). On the other hand, several other compounds inhibiting PI3K and mTOR simultaneously are currently being tested. The dual PI3K/mTOR inhibitor, GSK2126458, was investigated in a phase I trial in different advanced solid tumors. Amongst the 14 patients, 3 prolonged responses (1 SD and 2 PR), which were independent of PIK3CA mutations, could be observed (Munster et al. 2016). Gedatolisib, another PI3K/mTOR, produced by Pfizer, was tested in a phase I trial in different solid tumors and the results justified further investigations of this drug leading to several phase I and II trials currently recruiting patients (Wainberg et al. 2017) (NCT03698383, NCT03065062, NCT02626507, https://clinicaltrials.gov/). The novel agent PQR309 was tested for the first time in humans with different solid tumors and displayed anticancer activity, which could not clearly be linked to PI3K pathway alterations (Wicki et al. 2018). Phase II trials in lymphomas and head and neck cancer are currently ongoing (NCT03127020, NCT03740100, https://clinicaltrials.gov/). And also Novartis has developed a new inhibitor, LY3023414, targeting PI3K and mTOR. It has recently been tested in a first in-human phase I trial for advanced cancers and showed

favorable tolerability as well as antitumor activity (Bendell et al. 2018). It is further investigated in more than 10 different clinical trials at the present time (https://clinicaltrials.gov/).

1.3.3 Outlook

As summarized above, many clinical trials of small molecule inhibitors targeting the PI3K signaling pathway are currently ongoing in different tumor entities. Only a small subset of trials have been investigating these agents for treatment of bladder cancer, and the ones who have, showed discouraging clinical results. However, in some of these trials few patients with stable disease and partial or complete response could benefit from the respective treatment (Table 1). Seront et al. discovered that PTEN-loss was associated with resistance to everolimus, whereas two other trials using whole genome or exome sequencing detected an inactivating TSC1 mutation or activating mTOR mutations to predict response to this drug (Iyer et al. 2012, Seront et al. 2012, Wagle et al. 2014). Guo et al. could not confirm this relation between TSC1 loss and rapamycin sensitivity in a panel of bladder cancer cell lines without more ado (Guo et al. 2013). Ali et al. identified a NF2 mutation in an exceptional responder with advanced MIBC receiving everolimus and paclitaxel (Ali, Miller et al. 2015). These results led to two phase II trials with everolimus in solid tumors harbouring TSC1/2 or mTOR and NF1/2 mutations (NCT02201212, NCT02352844, https://clinicaltrials.gov/). In a phase I clinical trial for the dual PI3K/mTOR inhibitor GSK2126458 no correlation between objective response and PIK3CA mutations could be found (Munster et al. 2016). These attempts of identifying biomarkers to predict therapeutic response are rare examples that indicate what might be possible in terms of personalized medicine in the treatment of bladder cancer. However, these studies look at single responders in small patient cohorts and large prospective clinical trials with a prestratification of patients are needed, considering the enormous molecular heterogeneity of bladder cancer (da Costa et al. 2018). Two big biomarker-driven targeted therapy trials, the NCI-MATCH study in the USA and the ATLANTIS study in the UK in bladder cancer, are currently conducted for this purpose (Glaser et al. 2017) (NCT02465060, https://clinicaltrials.gov/).

Another approach to improve pharmaceutical results of targeting the PI3K signaling pathway is to deepen our understanding of its underlying molecular mechanisms that has constantly grown since the discovery of the PI3Ks in the 1980s (Vanhaesebroeck et al. 2012). This process is still ongoing and new insights to the pathways functioning are regularly made. Recently our group has observed that only S6K1, but not 4E-BP1 activation is downregulated upon inhibition of mTORC1 via rapamycin in bladder cancer cell lines. 4E-BP1 phosphorylation could successfully be suppressed when both PI3K and mTOR were inhibited with NVP-BEZ235, leading to the conclusion that 4E-BP1 is regulated by a PI3K- and mTOR-dependent mechanism. Moreover, an AKT-reactivating feedback loop that occurred upon long-term treatment with NVP-BEZ235 was identified that could be responsible for clinical failure of the drug (Nawroth et al. 2011, Sathe and Nawroth 2018). Despite this fact, dual PI3K/mTOR inhibitors are still of high interest as potential new agents in cancer

therapy and subject to a large panel of clinical trials. For that reason a more detailed understanding of the complex biochemical processes within the PI3K signaling pathway, as well as effects and limitations of targeting it, might be of significant relevance.

1.4 Aims of this project

The overall aim was to identify a therapy design to inhibit the PI3K signaling pathway in order to improve the treatment of advanced or metastatic bladder cancer. Based on the findings previously made by our group, two principal issues were raised and investigated in this study:

I) Identification of the underlying molecular mechanisms of 4E-BP1 regulation

   i) Examining the role of PI3K and mTORC1
   ii) Investigating the specificity of INK128 and the role of mTOR in regulating 4E-BP1
   iii) Characterizing the influence of potentially involved kinases in the regulation of 4E-BP1
   iv) Analyzing the biochemical effects of a simultaneous inhibition of PI3K and mTOR, Raptor or Rictor and determining the influence of AKT

II) Analysis of the operating principles of the AKT reactivating feedback loop upon dual PI3K/mTOR inhibition

   i) Demonstrating the AKT reactivation and its suppression in BLCA cell-line 647v
   ii) Analyzing the AKT/PDK1 feedback-loop by determining the roles of PI3K and mTOR
   iii) Analyzing the functional consequences of preventing AKT rephosphorylation

2 Materials and Methods

2.1 Materials

2.1.1 Basic laboratory equipment

Basic laboratory equipment	Manufacturer
3M durapore surgical tape	3M, Saint Paul, MN, USA
5430R microcentrifuge	Eppendorf GmbH, Hamburg, Germany
Analytical balance scale AT250	Mettler Toledo, Gießen, Germany
Analytical balance Sartorius 2254	Sartorius, Goettingen, Germany
Autoclave Sytec DX-65	Systec GmbH, Linden, Germany
Automatic film processor Curix CP1000	Agfa Healthcare, Mortsel, Belgium
AxioVert.135 microscope	Carl Zeiss, Oberkochen, Germany
AxioVert.A1 microscope	Carl Zeiss, Oberkochen, Germany
Biological safety cabinet Herasafe KS12	Thermo Scientific, Waltham, MA, USA
Block thermostat BT100	Kleinfeld Labortechnik, Gehrden, Germany
BVC professional laboratory fluid aspirator	Vacuubrand GmbH, Wertheim, Germany
Centrifuge ROTINA 35R	Hettich, Tuttlingen, Germany
ChemiDoc XRS+ system	Bio-Rad Laboratories GmbH, Munich, Germany
CO_2 incubator HERA Cell240	Thermo Scientific, Waltham, MA, USA
CO_2 incubator HERA Cell240i	Thermo Scientific, Waltham, MA, USA
Coulter mixer	Beckman Coulter, Brea, CA, USA
Cryogenic Freezing Container, 1 Deg C	Nalgene, Rochester, NY, USA
Electrophoresis Power Supply EPS 601	Amersham Pharmacia Biotech., Uppsala, Sweden
Heraeus Incubator B6 Function Line	Thermo Scientific, Waltham, MA, USA
Ice machine Manitowoc	Manitowoc Ice, Manitowoc, WI, USA
Intellimixer RM-2L	Elmi Ltd. Laboratory Equipment, Calabasas, CA, USA
Magnetic Stirrer with Heating	Heidolph Instruments GmbH, Schwabach, Germany
Microcentrifuge 5430R	Eppendorf GmbH, Hamburg, Germany
Microcentrifuge QikSpin QS7000 personal	Edwards Instrument Co., Narellan NSW, Australia
Micropipettes PIPETMAN P2, P10, P20, P200, P1000	Gilson Inc., Middleton, WI, USA
Microplate reader Vmax Kinetic	Molecular Devices, Sunnyvale, CA, USA
Mini Protean System	BioRad, Hercules, CA, USA
Mini Trans-blot cell transfer system	BioRad, Hercules, CA, USA
Mini-PROTEAN Tetra Cell gel system	BioRad, Hercules, CA, USA
Minishaker IKA MS2	IKA Works Inc., Staufen, Deutschland
Multilabel plate reader VICTOR X3	Perkin Elmer, Waltham, MA, USA
Neubauer chamber	LO, Laboroptik, Lancing, England
pH Meter 691	Metrohm, Filderstadt, Germany
PowerPac HC power supply	BioRad, Hercules, CA, USA
Vortex- Genie 2	Scientific Industries, Inc., Bohemia, NY, USA

Water bath W350	Memmert, Schwabach, Germany
Water purification system, Purelab	ELGA Lab water, Celle, Germany

Table 2: Basic laboratory equipment

2.1.2 Consumable supplies

Consumable supply	Manufacturer
0.5ml, 1.5ml reaction tubes	Sarstedt, Nümbrecht, Germany
1.8ml Nunc cryogenic vials	Thermo Scientific, Waltham, MA
Amersham hybond-P PVDF- Membrane	GE-Healthcare, Buckinghamshire, England
Cell culture plates 96 well, 6 well, 10cm	Corning Incorporated, Corning, NY, USA
Conical tubes 15ml and 50ml Falcon	Greiner GmbH, Frickenhauseen, Germany
Costar 96-well assay plates	Corning Incorporated, Corning, NY, USA
Microscope coverslips	Thermo Scientific, Waltham, MA, USA
Needles 27 Gauge	BD Biosciences, San Jose, CA, USA
Pipette tips with and without filter (10µl, 100µl, 200µl, 1000µl)	Sarstedt, Nümbrecht, Germany
Sigma cell lifter	Sigma-Aldrich, St. Louis, MO, USA
Serological pipettes (2ml, 5ml, 10ml, 25ml)	Greiner Bio-One International AG, Kremsmünster, Austria
Syringes 1ml Omnifix	B.Braun Melsungen AG, Melsungen, Germany
White polystyrene 96 well plates	Corning Incorporated, Corning, NY, USA
X-ray film CEA RP New	Agfa Healthcare, Mortsel, Belgium

Table 3: Consumable supplies

2.1.3 Chemicals and reagents

Chemical/ Reagent	**Manufacturer**
70% Ethanol	BrüggemannAlcohol Heilbronn GmbH, Heilbronn, Germany
Ammonium persulfate (APS)	Sigma-Aldrich, St. Louis, MO, USA
Bovine serum albumin (BSA)	Sigma-Aldrich, St. Louis, MO, USA
Bromophenol blue	Serva Electrophoresis GmbH, Heidelberg, Germany
Color Prestained Protein Standard, Broad Range	New England Biolabs, Ipswich, MA, USA
Complete Mini- Protease Inhibitor	Roche, Basel, Switzerland
Crystal violet, 0.5%	Sigma-Aldrich, St. Louis, MO, USA
Developing and fixation solutions Vision X GV60	Roentgen bender GmbH & Co. KG, Baden-Baden, Germany
Dimethyl sulfoxide (DMSO)	Sigma-Aldrich, St. Louis, MO, USA
Dithiothreitol (DTT)	Cell-Signaling, Cambridge, England
Ethylenediaminetetraacetic acid (EDTA), 0.5 M	AppliChem, Darmstadt, Germany
Fetal Bovine Serum (FBS)	Biochrom, Merck Millipore, Berlin, Germany
Glutaraldehyde, 6%	Sigma-Aldrich, St. Louis, MO, USA
Glycine	Sigma-Aldrich, St. Louis, MO, USA Carl Roth, Karlsruhe, Germany

Hydrogen chloride (HCl)	Merck, Darmstadt, Germany
Hydrogen peroxide (H_2O_2)	Merck, Darmstadt, Germany
Isopropanol	Sigma-Aldrich, St. Louis, MO, USA
Lipofectamine RNAimax	Life Technologies, Darmstadt, Germany
Luminol	Sigma-Aldrich, St. Louis, MO, USA
Methanol (MeOH)	Sigma-Aldrich, St. Louis, MO, USA
Non-essential amino acids (NEAA), 100x	Biochrom, Merck Millipore, Berlin, Germany
Opti-MEM	Invitrogen, Carlsbad, CA, USA
Penicillin/Streptomycin (P/S)	Biochrom, Merck Millipore, Berlin, Germany
Phosphate buffered saline (PBS), 1x, 10x	Biochrom, Merck Millipore, Berlin, Germany Sigma-Aldrich, St. Louis, MO, USA
p-Coumaric acid	Sigma-Aldrich, St. Louis, MO, USA
Phosphatase inhibitor Mix II	Serva Electrophoresis GmbH, Heidelberg, Germany
Roswell Park Memorial Insitute Medium (RPMI)	Biochrom, Merck Millipore, Berlin, Germany Sigma-Aldrich, St. Louis, MO, USA
Rotiphorese gel 30	Carl Roth, Karlsruhe, Germany
Skimmed milk powder	Nestlé, Vevey, Switzerland
Sodium azide	Sigma-Aldrich, St. Louis, MO, USA
Sodium chloride (NaCl)	Merck Chemicals GmbH, Hessen, Germany
Sodium dodecyl sulfate (SDS)	Sigma-Aldrich, St. Louis, MO, USA
Tetramethylethylenediamine (TEMED)	Carl Roth, Karlsruhe, Germany
Tris(hydroxymethyl)-aminomethan	Merck, Darmstadt, Germany
Triton X-100	Sigma-Aldrich, St. Louis, MO, USA
Trypan blue, 0.5%	Biochrom, Merck Millipore, Berlin, Germany
Trypsin/ EDTA	Biochrom, Merck Millipore, Berlin, Germany
Tween-20 (Polysorbat)	Serva Electrophoresis GmbH, Heidelberg, Germany

Table 4: Chemicals and reagents

2.1.4 Small molecule inhibitors

Small molecule inhibitor	Manufacturer
GSK2334470	Selleckchem, Munich, Germany
INK-128 (MLN-0128)	Active Biochem, Bonn, Germany
KU 60019	Tocris Bioscience, Bristol, United Kingdom
MK-2206	Active Biochem, Bonn, Germany
NU 7441	Tocris Bioscience, Bristol, United Kingdom
NVP-BEZ235	Selleckchem, Munich, Germany
PIK90	Merck Chemicals Ltd, Nottingham, United Kingdom
RAD001	Selleckchem, Munich, Germany

Table 5: Small molecule inhibitors

2.1.5 Assays

Assay	Manufacturer
Amersham ECL Prime Western Blotting Detection Reagent	GE Healthcare Europe GmbH, Freiburg, Germany
Caspase-Glo 3/7 Assay	Promega, Madison, WI, USA
CellTiter-Blue Cell Viability Assay	Promega, Madison, WI, USA
Pierce BCA Protein Assay	Thermo Scientific, Waltham, MA, USA

Table 6: Assays

2.1.6 Buffers and solutions

Buffer	Components
0.05% SDS Protein lysis buffer	150mM NaCl 50mM Tris/HCl pH 7.2 1% Triton X-100 0.05% SDS 5mM EDTA 1 Complete Mini-Protease Inhibitor tablet and 100µl phosphatase inhibitor for every 10ml of protein lysis buffer (add prior to use)
Chemiluminescence reagent part A	0.1M Tris/HCl pH 8.5 2.5mM Luminol 0.4mM p-Coumaric acid
Chemiluminescence reagent part B	0.1M Tris/HCl pH 8.5 0.18% H_2O_2
Culture medium for cells 5% CO_2	RPMI 5% FBS 1% NEAA 1% P/S
Freezing medium	50% RPMI 40% FBS 10% DMSO
Immunoblotting blocking solution	5% non-fat milk powder in TBST
Immunoblotting antibody dilution buffer	5% BSA in TBST 0.02% Sodium Azide
Protein loading buffer (4x)	0.25M Tris/HCl, pH 6.8 8% SDS 0.04% Bromophenol blue 40% Glycerine 100µl of 1M DTT to 500µl of 4x protein loading buffer (add prior to use)
SDS page running buffer (10x)	25nM Tris 192mM Glycine 0.1% w/v SDS pH 8.3
Separating gel buffer	1.5M Tris/HCl, pH 8.8
Stacking gel buffer	0.5M Tris/HCl, pH 6.8
TBS (10x)	0.5M Tris/HCl, pH 7.6
TBST	1x TBS 0.001% Tween-20

Transfer buffer (10x)	25nM Tris 192mM Glycine
Transfer buffer (1x)	10% 10x Transfer buffer 20% Methanol

Table 7: Buffers and solutions

2.1.7 Antibodies

Target protein	Catalogue number	Dilution	Manufacturer
4-EBP1	9452	1:1000	CST, Beverly, MA, USA
Phospho-4E-BP1 (Thr 37/46)	9459	1:1000	CST, Beverly, MA, USA
Akt (pan)	4685	1:1000	CST, Beverly, MA, USA
Bad	9239	1:1000	CST, Beverly, MA, USA
Phospho-Bad (Ser 136)	4366	1:1000	CST, Beverly, MA, USA
Phospho-Akt (Ser473)	3787	1:1000	CST, Beverly, MA, USA
Phospho-Akt (Thr308)	2965	1:1000	CST, Beverly, MA, USA
GAPDH	2118	1:1000	CST, Beverly, MA, USA
mTOR	2972	1:1000	CST, Beverly, MA, USA
p70-S6Kinase	9202	1:1000	CST, Beverly, MA, USA
Phospho-p70-S6Kinase (Thr389)	9234	1:1000	CST, Beverly, MA, USA
Raptor	2280	1:1000	CST, Beverly, MA, USA
Rictor	2140	1:1000	CST, Beverly, MA, USA
Peroxidase-conjugated Anti-Rabbit IgG	711-036-152	1:10.000	Dianova GmbH, Hamburg, Germany

Table 8: Antibodies

2.1.8 siRNA and shRNA sequences

10nM small interfering RNA (siRNA) oligonucleotides against Raptor and Rictor were obtained by Qiagen, Hiden, Germany, and negative control stealth RNAi high GC duplex #2 was obtained by Life Technologies, Darmstadt, Germany.

Target gene	Sequence	Modification	Catalogue number	Manufacturer
Raptor	CCCGUCGAUCUUCGUCUACGA	none	SI 03186260	Qiagen, Hiden, Germany
Rictor	UACGAGCGCUUCGAUAUCUCA	none	SI 04250561	Qiagen, Hiden, Germany
Negative Control	RNAi high GC duplex #2 Proprietary sequence	stealth	12935114	Life Technologies, Darmstadt, Germany

Table 9: siRNA sequences

shRNA	Sequence	Catalogue number	Manufacturer
Ad-sh-mTOR	GCATGGAAGAATACACCTGTA	SB-P-AV-004958-01	SIRION Biotech. GmbH, Martinsried, Germany
Control shRNA	CTTACAATCAGACTGGCGA	SB-P-AV-146-01	SIRION Biotech. GmbH, Martinsried, Germany

Table 10: shRNA sequences

2.1.9 Software

Assay	Manufacturer
CompusSyn	Combo Syn Inc., Parasmus, NJ, USA
Perkin Elmer 2030 Explorer	PerkinElmer, Waltham, MA, USA
Quantity One 1-D	Bio-Rad Laboratories GmbH, Munich, Germany

Table 11: Software

2.2 Methods

2.2.1 Cell Culture

2.2.1.1 Cell lines

Cell line	Culture medium	CO2 concentration	Source
647v	RPMI, 10% FBS, 1% NEAA, 1% P/S	5%	Leibniz Institute German collection of microorganisms and cell culture, Braunschweig Germany
RT112	RPMI, 10% FBS, 1% NEAA, 1% P/S	5%	Leibniz Institute German collection of microorganisms and cell culture, Braunschweig Germany
T24	RPMI, 10% FBS, 1% NEAA, 1% P/S	5%	American type culture collection, Manassas, VA, USA

Table 12: Cell lines

2.2.1.2 Splitting of cells

Cells were maintained in a sub-confluent condition with previously described medium in 10cm dishes. At 5% CO_2, 37ºC and saturated humidity the dishes were kept in Hera cell culture incubators (Thermo Scientific). The cells were used at early passage numbers. All culturing steps were performed in laminar flow biological safety cabinets under sterile conditions. Medium, PBS and Trypsin/EDTA were prewarmed in the 37ºC water bath and a disinfection of the bottles, the working place and the needed equipment was carried out before culturing. To perform a routine split, the medium was aspirated and cells were washed twice with PBS containing 5% 0.5M EDTA. After removal of the PBS, cells were incubated with trypsin/EDTA at 37ºC until most of the cells appeared to have lost adherence to the plate. The trypsin was subsequently neutralized with fresh medium and this suspension was centrifuged in a tube at 300 rcf for 5 minutes. The supernatant was aspirated and the cell pellet was

resuspended with fresh medium. A determined fraction was evenly distributed onto a new cell culture dish containing medium and was then restored in the incubator.

2.2.1.3 Cryopreservation and thawing of cells

For a cryopreservation of cells all steps were performed as described above, but the pellet was resuspended in 1ml of freezing medium and transferred into cryoviles. Before storage in the liquid nitrogen, the viles were kept for 2-3 days in a special freezing container at -80ºC.

In order to take a BLCA cell line in culture, the cryogenic vile from the liquid nitrogen tank containing the desired cell line in freezing medium was put in a 37ºC water bath for quick thawing. The thawed suspension was added to a tube with fresh medium, centrifuged and again resuspended in fresh medium after the supernatant had been aspirated.

2.2.1.4 Counting and seeding of cells

In order to have the same amount of cells per condition, cells were counted and $1x10^6$, $2x10^6$ or 500-1000 cells were seeded equally in 10cm, 6-well or 96-well plates respectively the day before treatment.

For counting cells, a small amount of the suspension was diluted with 0.5% trypan blue and transferred to a Neubauer chamber. The number of unstained cells that were considered viable was determined in four big squares. With following equation the amount of cells in 1ml of the suspension could be calculated:

$$\text{No. of cells in 1ml of cell suspension} = \frac{\text{No. of cells in 4 big squares}}{4} \text{ x dilution factor } x10^4$$

The formula to calculate the required volume of the cell suspension was the following:

$$\text{Required volume of cell suspension} = \frac{\text{No. of cells required for seeding}}{\text{No. of cells in 1ml cell suspension}}$$

The required volume was then added to the amount of medium needed to make up 10ml for 10cm dishes, 2ml for each well of a 6-well plate or 100µl for each well of a 96-well plate. To be as accurate as possible the volume for seeding of all plates or wells and some extra volume was mixed in one tube by gentle pipetting and then evenly distributed to the plates.

2.2.2 Treatment of BLCA cells with small molecule inhibitors

All small molecule inhibitors were dissolved in DMSO. The inhibitors GSK2334470, MK-2206 and RAD001 were stored as 10mM stock solutions at -20ºC. The 10mM stock of NVP-BEZ235 was kept at 4ºC. PIK90 was stored as a 2.5mM stock solution at -20ºC.
Prior to treatment, working concentrations were prepared by diluting the stock solution with a specific amount of fresh, pre-warmed medium. For the control an amount of DMSO that was equal to the highest concentration of the respective

inhibitor was used. The diluted inhibitor or control was pipetted onto the 10cm, 6-well or 96-well plates respectively and an even distribution was ensured by cautious movement of the dish.

2.2.3 Transfection of BLCA cells with siRNA

Transfection of bladder cancer cell lines with siRNA was performed with Lipofectamine RNAiMAx transfection reagent according to the manufacturer's protocol. One day before transfection, 0.5 x 10^5 or 1 x 10^5 cells were seeded in duplicates for each treatment condition in a 6 well plate. A final concentration of 10nM siRNA per well and Lipofectamine both diluted in Opti-MEM were pipetted onto the cells. After 10 minutes of incubation and occasional pivoting of the plates, 2.5ml of Opti-MEM were added, and the plates were incubated for 48 hours before analyzing protein expression via immunoblotting. For preparation of the transfection reagent dilution, it was directly pipetted into the Opti-MEM avoiding contact with the wall of the plastic tube. In order to prevent dissociation of the complexes, gentle pipetting or inversion of the tubes was used to mix.

2.2.4 Transducing cells with adenoviral shRNA

For Transduction, 1x10^5 cells were seeded one day before in a 6-well plate. Cells were transduced with mTOR shRNA or control shRNA adenovirus particles at a multiplicity of infection of 30. 100U mTOR shRNA or control shRNA mixed with 400µl Opti-MEM were pipetted onto each well and incubated for 2 hours in the incubator before being removed. Fresh RPMI medium was added and protein expression was analyzed via immunoblotting after approximately 72 hours.

2.2.5 Immunoblotting

2.2.5.1 Lysis of the cells and protein extraction

After the individual incubation time for treatment had passed, the cells were looked at under the microscope to evaluate whether morphological changes had occurred due to the inhibitor. The following steps for protein extraction were carried out on ice to avoid protein degradation. The medium was aspirated and the cells were washed twice with precooled PBS (1x). After thorough removal of the PBS, 500µl or 100µl protease and phosphatase inhibitor containing lysis buffer were added to 10cm dishes or 6-well plates respectively. Using a cell scraper, the cells were detached from the plate and the suspension was transferred into reaction tubes. The tubes were rotated in a special wheel at 4ºC for 10 minutes to mix the content and to give time for lysis. Subsequently, the tubes were centrifuged for 30 minutes with 30000 rcf at 4ºC. The supernatant was transferred to a fresh vile and the pellet was discarded. Lysates could immediately undergo protein quantification or be stored at -80ºC.

2.2.5.2 Quantification of proteins and preparation of the samples

In order to load the same amount of protein to the gels later on, the protein concentration had to be quantified. To do so, the Pierce BCA Protein assay kit was used as per manufacturer's protocol. The lysate samples as well as a BSA-based

dilution series as a standard were pipetted in duplicates to a 96-well plate. The BSA working reagent was added to each well and the plate was incubated for 30 minutes at 37ºC. Absorbance measurement was done with the Vmax Kinetic microplate reader at 562 nm and the protein concentration was calculated by comparison of the absorbance values to the standard series. Once proteins were quantified the lysate was diluted with the lysis buffer so as to obtain the same amount of protein in each sample. After adding a mixture of 4x protein loading buffer and DTT, the samples were degraded for 5 minutes at 100ºC and could either be stored at -20ºC or immediately be used for electrophoresis.

2.2.5.3 Preparation of the gels

The gels for separation of the proteins via SDS-page were handmade in special gel casting chambers according to the following protocol.

Reagent	Volume for an 8% separating gel (ml)	Volume for a 12% separating gel (ml)
ddH2O	4.78	3.45
1.5 M Tris/HCL pH 8.8	2.5	2.5
30% Acrylamide	1.67	4
10% APS	0.05	0.05
TEMED	0.01	0.01

Table 13: Preparation for an 8% separating gel

Reagent	Volume for a 4% polyacrylamide stacking gel (ml)
ddH2O	3.07
1.5 M Tris/HCL pH 8.8	1.25
30% Acrylamide	0.65
10% APS	0.025
TEMED	0.005

Table 14: Preparation for a 4% polyacrylamide stacking gel

The polyacrylamide concentration of the gels was chosen according to the size of the proteins to be detected. After the mixture for the resolving gel had been poured into the chambers, it was covered with a layer of isopropanol to ensure a sharp border between the two gel phases and quick polymerization under air deprivation. As soon as the separating gel was polymerized, the isopropanol was removed and the stacking gel was poured on top of the separating gel between the glass plates. A comb was inserted and about 15 minutes were needed for full polymerization.

2.2.5.4 SDS-Page

The finished gels were then assembled in the electrophoresis chambers that had been filled with running buffer. The comb was removed and the pockets were rinsed with a syringe to eliminate unpolymerized acrylamide leftovers. Then 5µl of the protein standard and 40µl of each protein sample were loaded into the pockets of the gel and the electrophoresis was started with a voltage of 90V. Once the proteins entered the separating gel, the voltage was changed to 150V.

2.2.5.5 Western Blot and blocking

As soon as the proteins nearly reached the bottom of the gel, the electrophoresis was stopped, and the gels were removed from the chambers. To remove the SDS, the gels were immersed in blotting buffer for 5 minutes to guarantee an unhindered transfer. The PVDF membrane was soaked in methanol in the meantime for activation and subsequently steeped in blotting buffer along with the sponges and the blotting paper. The gel, the membrane, two pieces of blotting paper and two sponges were assembled in the transfer cassette and bubbles between the layers were removed. The transfer was carried out for 2 hours with 100V in the corresponding chambers filled with transfer buffer. The system was cooled down by ice packs to avoid expansion of the gels and a magnetic stirrer was used to guarantee an even temperature in the chambers.

2.2.5.6 Immunodetection

After completion of the transfer process, the membrane was incubated for 1 hour at room temperature in a 5% concentrated milk powder blocking buffer to avoid nonspecific binding of the antibodies. That was followed by a three-step washing process with TBST and addition of the primary antibody that had been diluted in a sodium azide TBST-solution beforehand. After an overnight incubation at 4ºC, the membranes were again washed 5 times with TBST and the secondary horseradish-peroxidase coupled antibody diluted in the blocking buffer was added for an incubation period of 1 hour at room temperature. After 5 more washing steps with TBST, the membranes were ready for protein detection. To do so, Chemiluminescence reagents A and B were prepared as described in the table above (Table 7) or the commercial ECL kit was used, and a 1:1 mixture was made shortly before it was put onto the membranes to induce the ECL reaction. In a darkroom, chemiluminescence was detected by X-ray films that were subsequently developed in the Agfa Healthcare film processor or by the ChemiDoc XRS+ system for quantification of the signal using the Quantity One 1-D software.

2.2.6 Cell viability assays

2.2.6.1 Cell titer blue assay

Cells were seeded in triplets per treatment condition on a 96-well assay plate and on a clear 96-well plate so that a confluency of 70% for the non-treated cells was reached at the time the viability was analyzed. 24 hours after seeding, the cells were treated with small molecule inhibitors in respective concentrations or DMSO for control. 72 hours later, the Cell-Titer blue viability assay was performed as described in the manufacturer's protocol using 20µl of the resazurin-based Cell-Titer blue reagent per well and incubating at 37ºC. After a period of 1, 2, 3 and 4 hours, the fluorescence excitation and emission was measured with the VICTOR X3 Multilabel platereader at wavelengths of 560nm and 580nm.
The detected values were deducted by the value of background signal determined by wells containing only medium and reagent, and the average of equally treated wells was built.

2.2.6.2 Clonogenic assay

The clonogenic assay was performed according to the protocol by Franken et al. (Franken et al. 2006). 150 RT112 cells were seeded in 6-well plates. The treatment with the respective inhibitor was performed every 48 or 72 hours for 12 days. After this period the medium was removed and cells were washed with PBS. A mixture of 6% glutaraldehyde for fixation of the colonies and 0.5% crystal violet for staining were added to the plates and left for an incubation time of 30 minutes at room temperature. The mixture was then removed and the plates were rinsed by immerging them in tap water to get rid of the residues. The plates were left at room temperature until completely dried and were then scanned. The colonies were counted using an image editor.

2.2.7 Quantification of synergism

To assess the question whether a combination treatment with NVP-BEZ and GSK2334470 has a synergistic effect, the cell titer blue viability assay data were analyzed with the help of the CompuSyn software. This software determines the combination index (CI) in order to find out if a combination treatment is synergistic (CI <1), additive (CI=1) or antagonistic (CI>1) using the Chou-Talalay theorem (Chou 2006, Chou 2010). It is based on the following equation that determines the median-effect of a single drug:

$$\frac{F_a}{F_u} = \left(\frac{D}{D_m}\right)^m$$

F_a signifies the fraction that has been affected by the drug, whereas F_u is the unaffected fraction. D is the dose of the drug used in that experiment and D_m is the median effect dose. m is a coefficient that expresses if the slope of the curve is flat (m<1), hyperbolic (m=1) or sigmoidal (m>1).
The CI is calculated according to the following equation:

$$CI = \frac{D_1}{D_{x1}} + \frac{D_2}{D_{x2}}$$

D_{x1} and D_{x2} are the doses of a single drug that lead to an x% effect. Whereas D_1 and D_2 represent the doses used in the combination treatment that also result in an x% effect.
A dose reduction index (DRI) can be calculated to determine to which extent the dose of a drug can be reduced in a combination treatment to obtain the same effect as with a single treatment of this drug.

2.2.8 Apoptosis assay

Measuring of the apoptotic activity was carried out using the Caspase-Glo 3/7 assay from Promega according to their protocol. It determines the luminescence emitted in

lysed cells when the DEVD tetrapeptide sequence of the proluminescent substrate is cleaved by caspase 3 and 7. The intensity of the signal can therefore be correlated to the activity of these caspases and enables to draw conclusions on apoptosis.
647v and T24 cells were seeded in four wells per treatment condition in a white-walled 96-well plate and one well only containing medium was added to the plate serving as the blank. Cells were treated the following day with small molecule inhibitors NVP-BEZ235, MK-2206, a combination of these drugs or DMSO for control. After an incubation time of 48 hours, 50µl of the reagent that has been prepared as to manufacturer's protocol and brought to room temperature was added to each well in a light protected environment. The plate was subsequently shaken for about 30 seconds and incubated for half an hour in a dark place. Luminescence was then measured by the VICTOR X3 Multilabel Plate Reader. The blank value resulting from the wells only containing medium was subtracted and an average of the quadruplets per treatment condition was calculated before being normalized to the number of viable cells.

3 Results

3.1 Characterization of the regulation of 4E-BP1 in bladder cancer

Previous experiments have shown that an individual inhibition of either PI3K, AKT, mTOR or mTORC1 is not sufficient to regulate 4E-BP1 whereas dual PI3K/mTOR inhibition, as seen with NVP-BEZ235, suppresses phosphorylation of both S6K1 and 4E-BP1 (Nawroth et al. 2011, Sathe et al. 2014, Sathe, Chalaud, et al. 2018). Based on these findings, we wanted to identify the molecular components regulating 4E-BP1 in bladder cancer by further characterizing the role of PI3K and mTOR.

3.1.1 Identifying the role of dual PI3K and mTORC1 inhibition on 4E-BP1

To distinguish which mTOR complex in combination with PI3K is responsible for 4E-BP1 regulation we first tried to specifically inhibit PI3K and simultaneously mTORC1. We combined the PI3K inhibitor PIK90 with the specific mTORC1 inhibitor RAD001 (Figure 5A). Biochemically, the individual use of 5nM RAD001 had no effect on AKT phosphorylation. As published by our group before, this treatment led to a complete dephosphorylation of S6K1 but not 4E-BP1 (Nawroth et al. 2011). Treatment of T24 cells with 2000nM of PIK90 led to a complete suppression of AKT and S6K1 activity and to a reduction of phosphorylated 4E-BP1 (Figure 5A). When increasing doses of PIK90 were combined with fixed doses of RAD001, AKT threonine and serine phosphorylation decreased gradually with threonine phosphorylation showing a complete suppression at 500nM. S6K1 remained dephosphorylated throughout. Total protein levels were not affected due to any treatment. Concerning 4E-BP1, the combination of 1000nM and 2000nM of PIK90 with RAD001 clearly showed a further reduction of phosphorylation compared to the single treatment with PIK90. These results resemble data in other cell lines (Sathe, Chalaud, et al. 2018) and point to the fact that PI3K and mTORC1 have to be inhibited simultaneously in order to regulate 4E-BP1.

Next, we wanted to assess the effects of combining PIK90 and RAD001 in the context of cell survival. Hence, a viability assay with T24 cells was performed at the indicated concentrations of PIK90 and RAD001 (Figure 5B). RAD001 or PIK90 treatment alone already reduced viability by 50 to 60%. However, correlating with the biochemical data, the combination treatment of raising concentrations of PIK90 with 5nM of RAD001 resulted in a gradual decrease in viability beyond the effects seen with the single therapy of either of the compounds. Inhibition of mTORC1 combined with 500nM, 1000nM or 5000nM of PIK90 led to a 70%, 80% and 90% reduction in the number of surviving cells respectively.

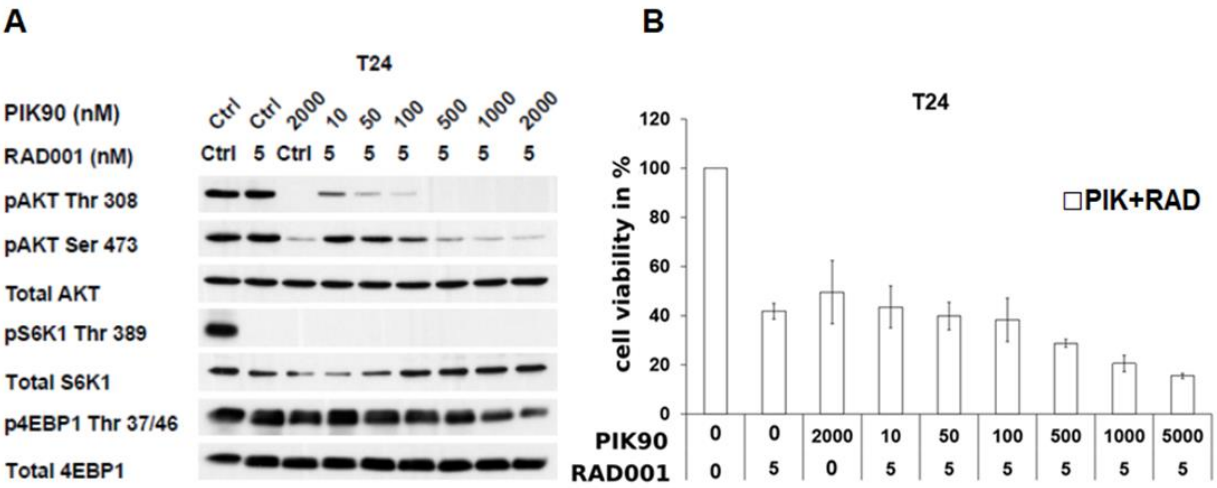

Figure 5: 4E-BP1 is dephosphorylated by dual inhibition of PI3K and mTORC1 with functional effects on cell viability. (A) BLCA cell line T24 was treated for one hour with PIK90 or RAD001 or a combination of 5nM RAD001 with increasing doses of PIK90. The biochemical effects were evaluated by a Western Blot analysis (B) The effects on cell viability of T24 cells in percent of the control after a 72h treatment with the indicated doses (in nM) of PIK90 and/or RAD001 were assessed.

3.1.2 Investigation of specificity of INK128

In order to further examine the molecular mechanisms that regulate 4E-BP1, we wanted to verify specificity of the mTOR catalytic site inhibitor INK128. In prior experiments of our group this inhibitor led to a dephosphorylation of 4E-BP1 at higher doses (Sathe, Chalaud, et al. 2018). To exclude that this dephosphorylation of 4E-BP1 was due to off-target effects of the inhibitor, we silenced mTOR expression via adenoviral shRNA and additionally applied INK128 in order to find out if the same effect as with the inhibitor alone can be observed when its target has been knocked down.

The expression level of mTOR protein was reduced by approximately 90% in all conditions mTOR shRNA was used (Figure 6). Consistent with published data from our group the knockdown of mTOR led to a decrease in phosphorylation of AKT threonine but not serine, while S6K1 was dephosphorylated. Remarkable is the fact that phosphorylation of 4E-BP1 was not affected by the knockdown of mTOR (Nawroth et al. 2011). The use of 250nM or 500nM of INK128 led to a complete dephosphorylation of all proteins examined, including 4E-BP1. When these two different doses of INK128 were combined with the mTOR knockdown the results were identical to the results seen with INK128 alone. At no point the levels of total proteins changed. Our data contribute to the assumption that 4E-BP1 regulation is not exclusively mediated via the mTOR kinase, but via a differential mechanism and that the effect seen with INK128 might be due to an additional inhibition of another molecule.

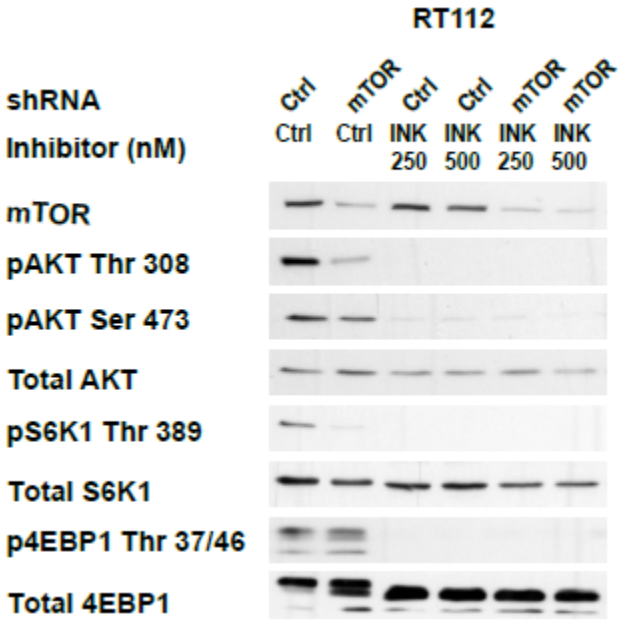

Figure 6: The inhibition of 4E-BP1 phosphorylation upon INK128 treatment at higher doses is due to off-target effects of the inhibitor. 72h after transduction with either mTOR or control shRNA RT112 cells were treated with 250 or 500nM of INK128 or an equivalent concentration of DMSO for one hour and phosphorylation levels and protein expression was analyzed via immunoblotting

3.1.3 Evaluating the role of PDK1, ATM and DNA-PK on 4E-BP1 regulation

Our data suggest that a dual inhibition of PI3K and mTORC1 is required to downregulate 4E-BP1 signaling. Before further analysis of the underlying mechanisms, we wanted to rule out that other kinases such as PDK1, ATM and DNA-PK are directly involved in the regulation of 4E-BP1 and that the dephosphorylation seen with NVP-BEZ235 is due to possible off-target effects. Therefore we inhibited these kinases with specific small molecule inhibitors and performed dose response assays in order to define a cell line dependent concentration with biochemical activity on AKT, S6K1 and 4E-BP1. The cells were treated for one hour and the phosphorylation status of 4E-BP1, S6K1 and AKT as well as the total proteins were examined via immunoblotting.

To inhibit PDK1, the compound GSK2334470 was used in the indicated doses (Figure 7A). Dephosphorylation of AKT at threonine 308 residue (AKT Thr) was observed in a dose-dependent manner. The estimated biochemical IC50 was detected at 5nM and the estimated IC100 at 1000nM (Table 15). The phosphorylation level of the Serine 473 residue of AKT was not influenced upon PDK1 inhibition. A similar dose dependent decrease as for the AKT threonine residue phosphorylation was also observed for S6K1 phosphorylation. Although a complete dephosphorylation of S6K1 was reached at a concentration of 250nM, no effect on 4E-BP1 phosphorylation could be detected by inhibiting PDK1. The expression of all corresponding total proteins was not affected.

For specific inhibition of ATM, we used the small molecule inhibitor KU60019 (Figure 7B). At concentrations between 1nM and 5000nM no dephosphorylation of AKT at both amino acid residues could be observed, although it has been described that basal AKT Ser phosphorylation is blocked by 70% in glioma cells and fibroblasts at a concentration of 3µM (Golding et al. 2009). A slight reduction of S6K1 phosphorylation occurred at a dose of 5000nM. Total protein expression was not affected by the treatment. The inhibition of ATM did not influence the phosphorylation status of 4E-BP1 indicating that ATM can be neglected as a direct regulator of 4E-BP1.

DNA-dependent protein kinase catalytic subunit was inhibited by using NU 7441 (Figure 7C). At a dose of 10.000nM a dephosphorylation of the AKT threonine 308 residue and a minor effect on the serine 473 phosphorylation could be seen. The reduction of S6K1 phosphorylation started at 2000nM and was completely suppressed at 5000nM. Upon DNA-PKcs inhibition the phosphorylation pattern of 4E-BP1 remained unchanged throughout as well as the expression levels of all total proteins. Hence, this kinase does not directly regulate the activity of 4E-BP1.

Table 15 summarizes the biochemical IC50 and IC100 concentrations of the different compounds needed for inhibition of AKT Thr, AKT Ser, S6K1 and 4EBP1 according to our results.

	PDK1- inhibition GSK2334470		**ATM- inhibition KU60019**		**DNA-PK- inhibition NU 7441**	
	IC50	**IC100**	**IC50**	**IC100**	**IC50**	**IC100**
pAKT Thr 308	5nM	1000nM	-	-	5000nM	10000nM
pAKT Ser 473	-	-	-	-	10000nM	-
pS6K1 Thr 389	10nM	250nM	5000nM	-	1000nM	5000nM
p4EBP1 Thr 37/46	-	-	-	-	-	-

Table 15: IC50 and IC100 concentrations for AKT, S6K1 and 4E-BP1 for different inhibitors according to our results

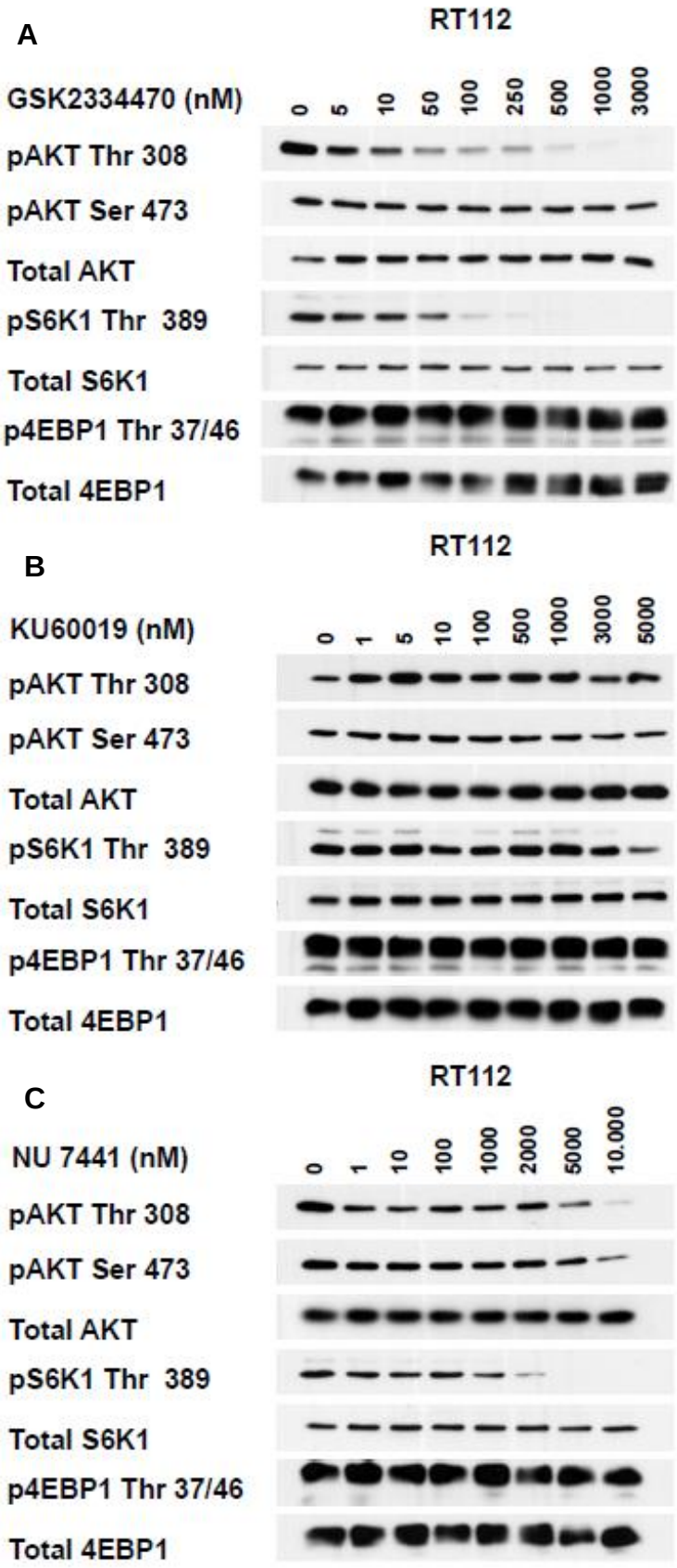

Figure 7: PDK1, ATM and DNA-PK do not directly regulate 4E-BP1. BLCA cell line RT112 was incubated with indicated doses of either (A) GSK2334470, (B) KU60019 or (C) NU 7441 for one hour and phosphorylation levels and protein expression was analyzed by immunoblotting.

3.1.4 Dual inhibition of PI3K and mTOR, Raptor or Rictor and dual inhibition of AKT and Raptor

We have observed that 4E-BP1 signaling can be suppressed by PI3K/mTOR inhibition with NVP-BEZ235 (Nawroth et al. 2011) as well as by PI3K/mTORC1 inhibition with PIK90 and RAD001 (Figure 5). Besides, we have indications that the mTOR molecule itself might not be the determining factor in the phosphorylation process of 4E-BP1 (Figure 6). To extend these data, we combined PIK90, the small molecule inhibitor against PI3K, with adenoviral mTOR shRNA and quantified the relative intensity of phosphorylated 4E-BP1 (Figure 8A). Detection of total mTOR protein expression showed a successful silencing of the protein in the respective conditions. The results observed with single silencing of mTOR in earlier experiments (Figure 6) could be confirmed. The effects of a single treatment with 2000nM of PIK90 on the selected molecular components in RT112 cells have already been described above (Figure 5). When mTOR and PIK90 were inhibited at the same time, AKT and S6K1 remained inactivated and 4E-BP1 showed a 77% suppression of phosphorylation compared to the control. The levels of total protein expression, such as GAPDH, used as a loading control, remained equal.

In order to distinguish whether mTORC1 or mTORC2 is responsible for the observed effect on 4E-BP1, we then combined PIK90 with siRNA against Raptor to achieve a specific disruption of the mTORC1 protein complex (Figure 8B). The results of the single treatment with 2000nM of PIK90 resembled the previous experiment (Figure 8A). When Raptor siRNA was applied, the detection of its expression level via immunoblotting showed a successful silencing. The individual Raptor knockdown led to a hyperphosphorylation of both AKT residues compared to the control. Phosphorylation of S6K1 was completely suppressed and the phosphorylation of 4E-BP1 was slightly reduced by 19%. When Raptor siRNA was combined with PIK90, AKT and S6K1 phosphorylation was completely abolished. Interestingly, a relative 4E-BP1 phosphorylation suppression of 89% compared to the control was attained by this combination treatment. The expression levels of total AKT, total S6K1 and total 4E-BP1 were not affected by the different treatment conditions.

To evaluate the role of mTORC2 in the regulation of 4E-BP1, the same experimental set-up as in Figure 8B was used but this time performing silencing of Rictor, a specific component of mTORC2, using a specific siRNA (Figure 8C). This siRNA led to a complete suppression of Rictor expression. All other protein levels remained stable, independent of the applied treatment. The Rictor knockdown was followed by an almost complete suppression of AKT phosphorylation without affecting S6K1 or 4E-BP1 activation. Combination of PI3K inhibition and additional mTORC2 disruption resulted in AKT and S6K1 dephosphorylation. No further reduction of 4E-BP1 phosphorylation was detected indicating that mTORC2 combined with a PI3K inhibition is not able to induce dephosphorylation of 4E-BP1.

Our next question was to examine if the regulation of 4E-BP1 by PI3K and mTORC1 involves AKT. Therefore Raptor was silenced and in parallel AKT kinase activity was

inhibited using the small molecule inhibitor MK-2206 (Figure 8D). The effects on AKT, S6K1 and 4E-BP1 phosphorylation with a single Raptor knockdown were described above. AKT inhibition by MK-2206 led to dephosphorylation of both AKT residues as well as of S6K1. 4E-BP1 was not affected by this treatment, as it was previously published by our group (Sathe et al. 2014). When the mTORC1 complex was disrupted via Raptor siRNA and AKT was additionally inhibited, AKT and S6K1 were still dephosphorylated, but 4E-BP1 remained in an activated state. No variation in total protein levels could be detected.

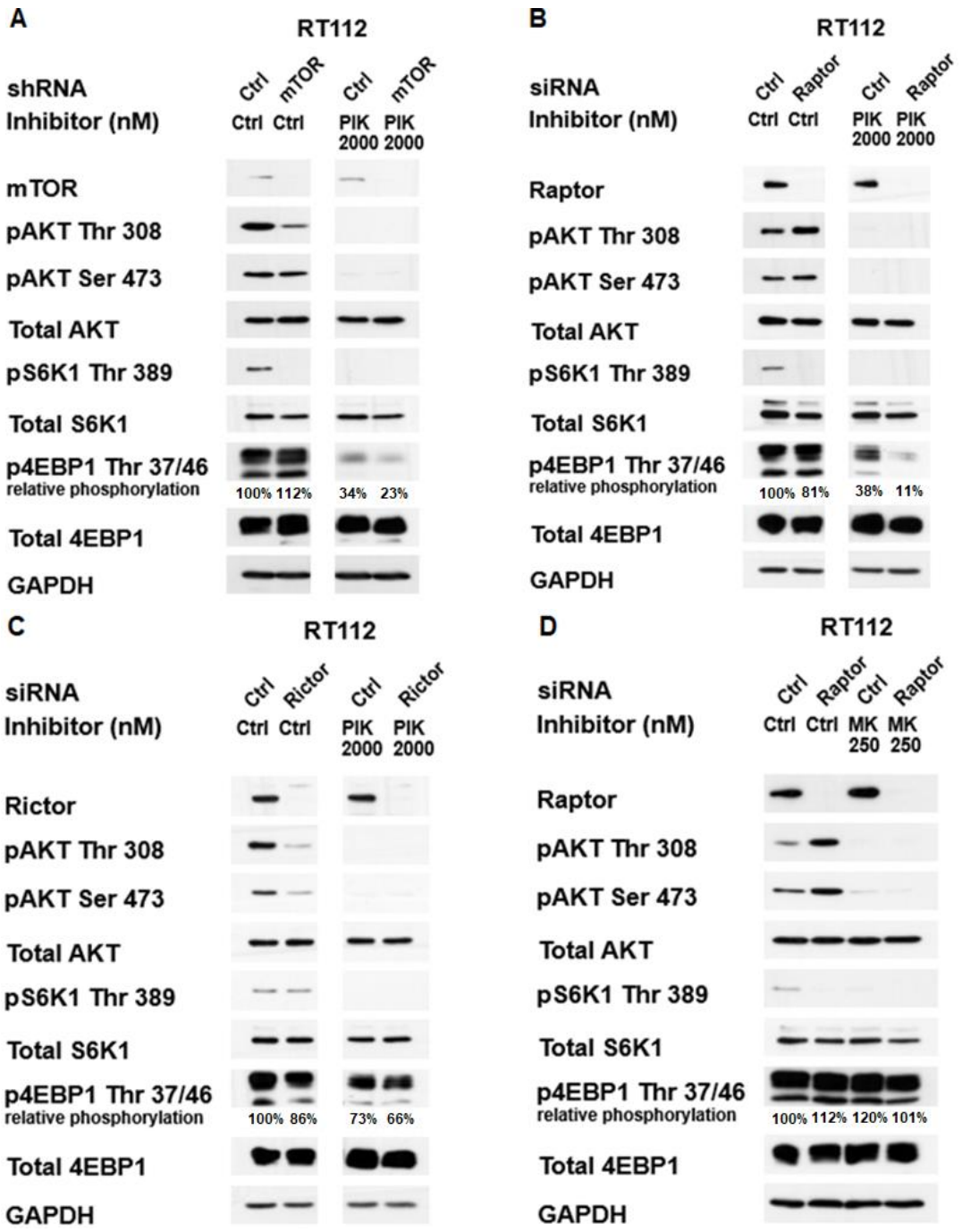

Figure 8: 4E-BP1 is regulated via PI3K and mTORC1, independent of AKT. (A) RT112 BLCA cell line was transduced for 72h with mTOR shRNA or control shRNA and additionally treated for one hour with 2000nM of PIK90 (PIK) or an equal amount of DMSO. (B) Transfection of RT112 cells with Raptor or control siRNA for 48 hours was performed, followed by a one hour treatment of 2000nM of PIK or DMSO as control. (C) Representative RT112 cells were transfected with Rictor or control RNA for 48h. Then cells were treated for one hour with 2000nM of PIK or an equal amount of DMSO. (D) RT112 cells were transfected with Raptor or control siRNA for 48 hours and additionally treated with 250nM of MK-2206 (MK) or an equal amount of DMSO for 1 hour. (A-D) The relative intensity of phosphorylated 4E-BP1 bands on immunoblots compared to the control band were quantified via QuantityOne.

3.2 Characterization of the feedback-loop leading to reactivation of AKT under extended treatment with NVP-BEZ235

We observed previously that treatment of the BLCA cell lines T24, RT112 or 253J with NVP-BEZ235 over an extended period of time results in an initial dephosphorylation of AKT followed by a rephosphorylation of its threonine residue after 4 to 6 hours and a hyperphosphorylation after 24 to 48 hours (Nawroth et al. 2011, Sathe, Chalaud, et al. 2018). Our aim was to analyze this feedback-loop in detail to identify the proteins involved as well as to point out the functional consequences of preventing it.

3.2.1 Rephosphorylation of AKT under treatment with NVP-BEZ235 in BLCA cell line 647v

We wanted to know if the phenomenon of AKT rephosphorylation under PI3K/mTOR inhibition could also be confirmed in other cell lines such as 647v cells. So a concentration of 200nM NVP-BEZ235 was applied for increasing periods of time. After a complete inhibition of AKT Thr 308 phosphorylation after one hour, this residue was slightly rephosphorylated after 4 hours and hyperphosphorylated after 48 hours. Fresh inhibitor was added in the last hour of the 24 and 48 hour treatment respectively. This was not sufficient to reverse the observed effect indicating that the reactivation of AKT was not due to a loss of the inhibitory effect of the compound. The phosphorylation of the serine residue was strongly reduced compared to the control and remained on a low level throughout the time course. The activation of 4E-BP1 and S6K1 was completely downregulated after 1h of 200nM NVP-BEZ235 treatment and remained suppressed over time. The amount of total protein expression of all three investigated targets was not influenced.

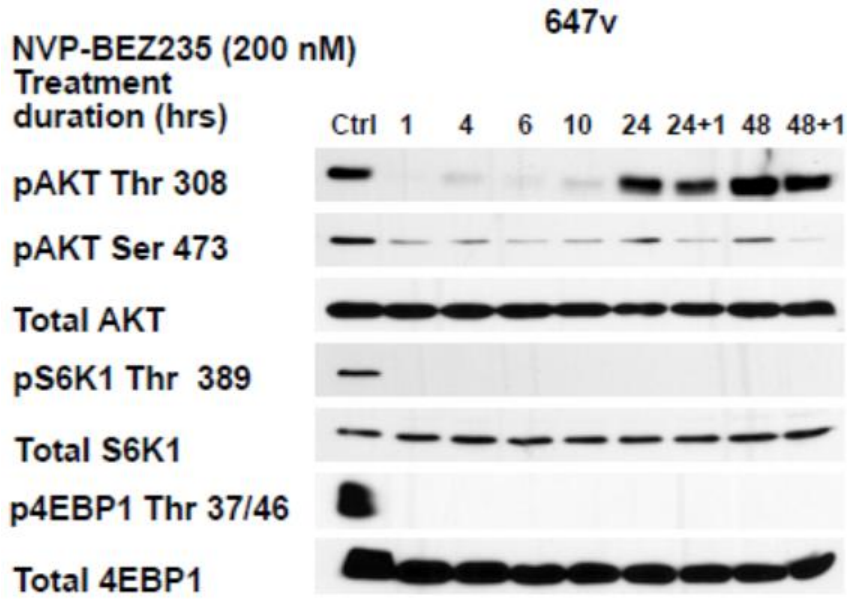

Figure 9: Rephosphorylation of AKT after treatment with NVP-BEZ235 for an extended period of time. BLCA cell line 647v was treated with 200nM of NVP-

BEZ235 for different time periods indicated above and selected proteins and their phosphorylation levels were analyzed by immunoblotting.

3.2.2 Overcoming AKT rephosphorylation by combining NVP-BEZ235 with an inhibition of PDK1

In the BLCA cell line RT112 it was shown that resphosphorylation of AKT occurring upon NVP-BEZ235 treatment could be reversed when PDK1 was additionally inhibited (Sathe, Chalaud, et al. 2018). In order to evaluate if this principle can be transferred to 647v cells, they were treated with 200nM of NVP-BEZ235 for 1 or 24 hours and/ or with GSK2334470 for 1 or 24 hours (Figure 10). Consistent with described data (Figure 9) the chosen concentration of NVP-BEZ235 was sufficient to completely suppress AKT threonine phosphorylation after one hour that recovered in the extended treatment of 24 hours. A strong reduction in AKT Ser 473 phosphorylation occurred and remained at this level 24 hours later. The individual inhibition of PDK1 for one hour was followed by a suppression of AKT phosphorylation in the threonine residue with a reactivation of the threonine residue after 24 hours. Phosphorylation of the serine residue was slightly reduced by monotherapy with GSK2334470 after one hour and remained at the same level after 24 hours. When GSK2334470 was added freshly for one hour before the 24 hour NVP-BEZ235 treatment was terminated, no rephosphorylation of AKT occurred and could as well be prevented when both inhibitors were used for 24 hours. Levels of total AKT and GAPDH protein remained stable in all conditions. These findings suggest that a feedback-loop reactivating AKT under PI3K and mTOR inhibition can be overcome by additional inhibition of PDK1.

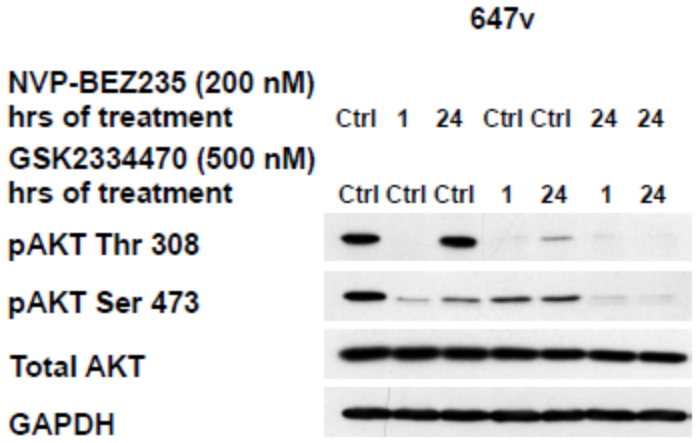

Figure 10: Preventing AKT rephosphorylation by inhibiting PI3K, mTOR and PDK1. 647v cells were subjected to a treatment of 200nM NVP-BEZ235 for one or 24 hours and/or a treatment with 500nM GSK2334470 for one or 24 hours. AKT in total and its phosphorylated residues and GAPDH as a loading control were analyzed via immunoblotting.

3.2.3 Analyzing molecular mechanisms of AKT rephosphorylation

The next aim was to further investigate the underlying molecular mechanisms of the AKT-reactivating feedback loop. As the combination of NVP-BEZ235 and PDK1

treatment prevent AKT rephosphorylation, we wanted to sort out which component targeted by NVP-BEZ235 is responsible for this phenomenon.

3.2.3.1 The role of mTOR in AKT rephosphorylation

To determine if the feedback-loop that leads to rephosphorylation of AKT upon NVP-BEZ235 treatment is mediated via mTOR, we inhibited this protein with the kinase inhibitor INK128 alone or in combination with PDK1 in RT112 and T24 BLCA cell lines (Figure 11). In both cell lines we observed an almost complete suppression of AKT phosphorylation at both residues after one hour of INK128 treatment. After 24 hours, a strong rephosphorylation of AKT Thr 308 indicated a reactivation of this kinase. A recovery of the AKT Ser 473 phosphorylation could be observed as well, although the effect was more subtle compared to the AKT Thr 308 residue. Therefore it can be stated that a long-term inhibition of mTOR results in a rephosphorylation of AKT. PDK1 inhibition led to an initial suppression of AKT threonine phosphorylation that appeared reversed in the 24 hour treatment in both cell lines. Although the phosphorylation of AKT Ser 473 was barely affected after one hour of PDK1 inhibition, a clear rephosphorylation could be seen in T24 cell line and a hyperphosphorylation in RT112 cells after 24 hours of treatment, different than in cell line 647v (Figure 10). As described before (Figure 10), inhibition of PDK1 for an extended period of time resulted in reactivation of AKT.

When GSK2334470 was added for one hour after the cells had been treated with INK128 for 23 hours, AKT remained activated. Also the 24 hour combination treatment with both drugs was not able to fully suppress AKT rephosphorylation. The addition of fresh inhibitor INK128 (last lane) could not change this fact and excluded at the same time that rephosphorylation was caused by loss of biochemical activity of the compound. At no point the expression level of total AKT was influenced. To conclude, the reactivation of AKT seen under prolonged mTOR or PDK1 inhibition cannot be suppressed by the simultaneous inhibition of both kinases.

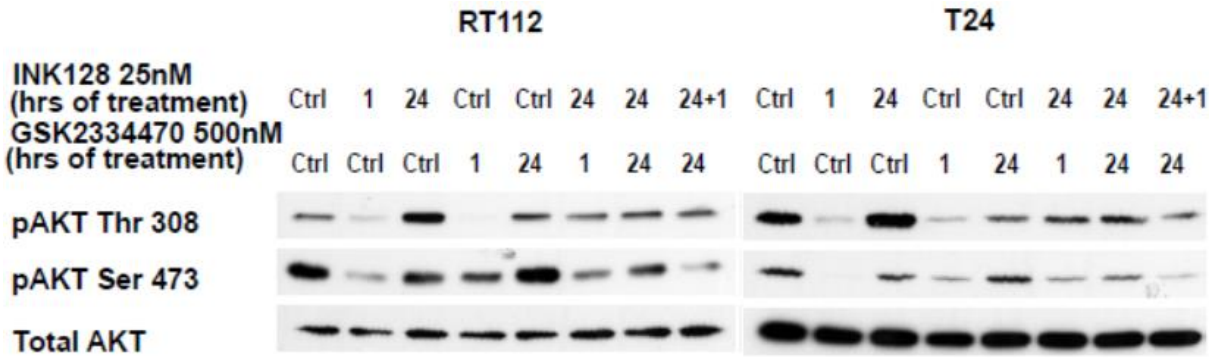

Figure 11: A dual inhibition of mTOR and PDK1 is not able to prevent AKT rephosphorylation. Respective cell lines were treated with indicated doses of INK128 and/ or GSK2334470 for 1 or 24 hours and the phosphorylation and expression status of AKT was analyzed in immunoblots.

3.2.3.2 The role of PI3K in AKT rephosphorylation

Since a dual inhibition of mTOR and PDK1 is not able to suppress AKT rephosphorylation, the aim was still to clarify the mechanisms of the feedback-loop observed with NVP-BEZ235. Therefore we wanted to address if this feedback-loop is induced by PI3K inhibition through activation of the PI3K/PIP2/PIP3/PDK1 axis rather than mTORC2 inactivation. Consequently, in RT112 cells either an inhibition of PI3K by PIK90 or of PDK1 by GSK2334470 or a combination of both treatments was performed for 1 or 48 hours (Figure 12). The individual use of the PI3K inhibitor resulted in a complete inhibition of AKT threonine phosphorylation after one hour followed by a rephosphorylation after two days of treatment. At both treatment points the phosphorylation of the serine residue was reduced by estimated 50%. The effects of PDK1 inhibition on AKT activation were consistent to the ones described before (Figure 11). The combined long-term inhibition of PI3K with short or long-term inhibition of PDK1 is able to successfully prevent rephosphorylation of the threonine residue of AKT, whereas the serine residue is still partially activated. Protein levels of total AKT itself, as well as the loading control GAPDH, remained stable. Thus, the feedback loop observed with NVP-BEZ235 is mediated via PI3K and PDK1 but not mTOR and can be overcome by inhibition of these two kinases.

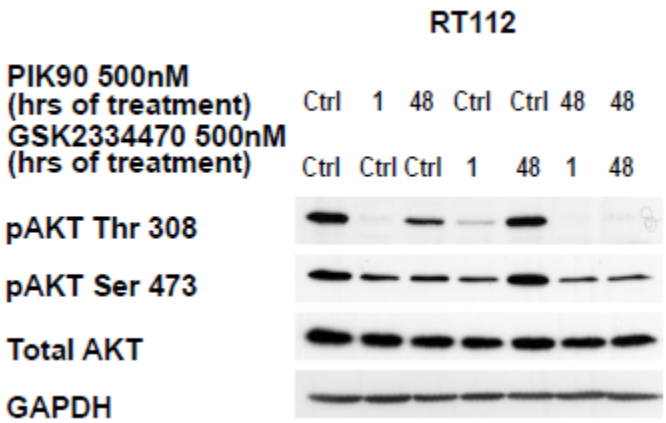

Figure 12: The simultaneous inhibition of PI3K and PDK1 prevents AKT rephosphorylation. RT112 cells were treated for 1 or 48 hours with either 500nM PIK90 or 500nM GSK2334470 or the combination of both. Subsequently, the phosphorylation and expression status of AKT was analyzed via immunoblotting. GAPDH served as a loading control.

3.2.4 Functional consequences of suppressing AKT rephosphorylation

As reactivation of AKT under NVP-BEZ235 treatment can be overcome by combining it with either a PDK1 or an AKT inhibitor, we addressed the question whether this therapeutic strategy is also of relevance regarding cell viability, colony formation and apoptosis.

3.2.4.1 Effects of preventing AKT rephosphorylation on cell viability

We wanted to compare the efficacy of a single treatment with NVP-BEZ235, GSK2334470 or MK-2206 to the combination of either NVP-BEZ235 with GSK2334470 or with MK-2206 in terms of cell viability. BLCA cell lines RT112, T24 and 647v were subjected for 72 hours to a treatment with the respective compounds (Figure 13).

In all three cell lines, the inhibition of either PDK1 or AKT alone only reduced the number of surviving cells by around 20 to 30%. The dual inhibition of PI3K and mTOR by NVP-BEZ235 in increasing doses was followed by a strong gradual decrease in viability by approximately 80% when 200nM of the inhibitor were used. When these raising concentrations of NVP-BEZ235 were combined with a fixed dose of 500nM GSK2334470 or 250nM MK-2206, a further decrease of viable cells for each condition could be observed. Especially for lower NVP-BEZ235 concentrations of 5nM, 10nM or 25nM, this effect was even more pronounced with a decrease of 30 to 50% compared to the single NVP-BEZ235 treatment. The efficacy of both combination therapies was very similar.

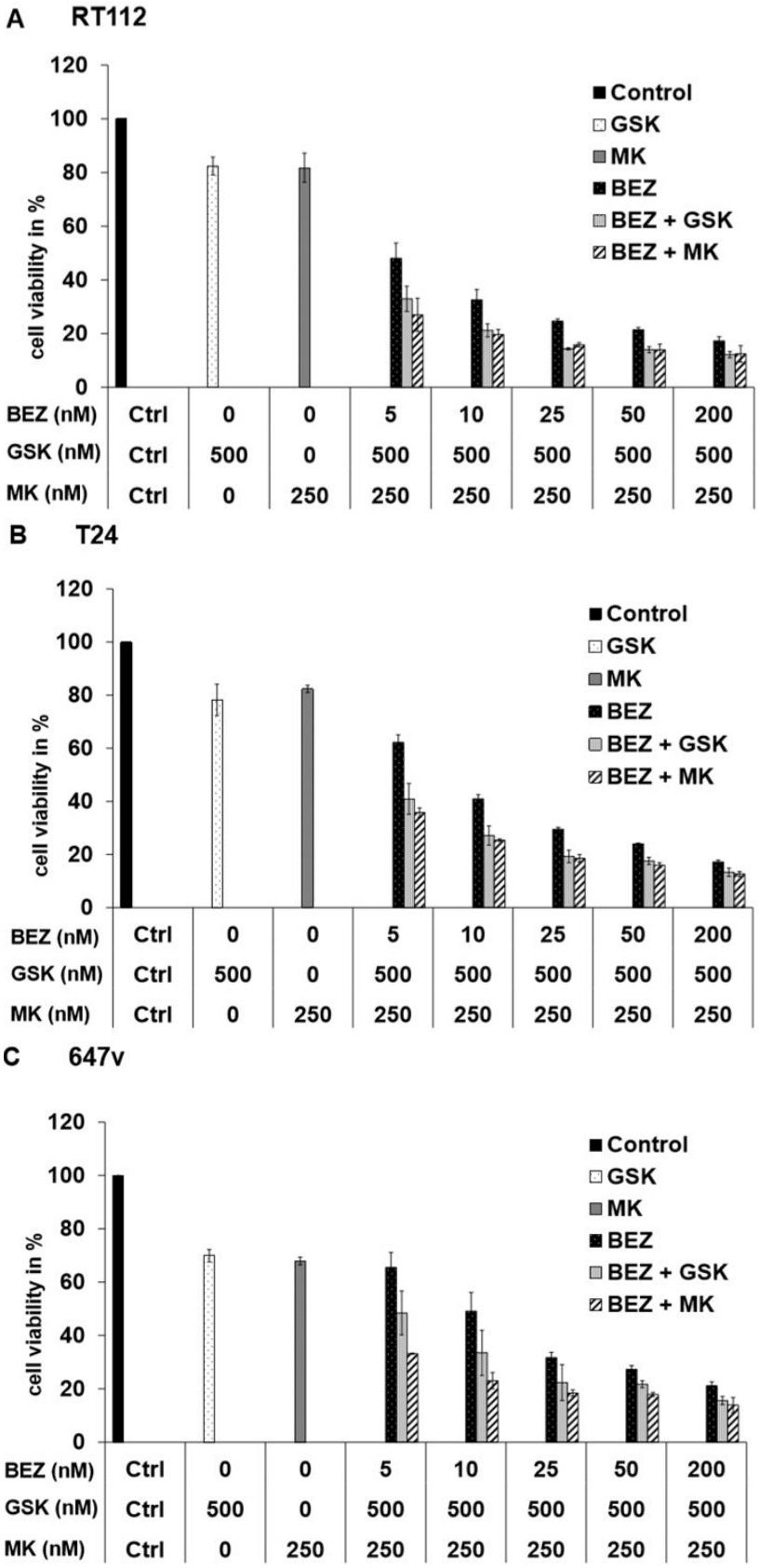

Figure 13: NVP-BEZ235 in combination with either GSK2334470 or MK-2206 decreases cell viability. RT112, T24 and 647v cells were treated with the indicated doses of NVP-BEZ235 (BEZ), GSK2334470 (GSK) and MK-2206 for 72 hours and the effects on cell survival in percent relative to the control were assessed by a cell titer blue viability assay.

3.2.4.2 Assessment of Synergism for the treatment combination of NVP-BEZ235 and GSK2334470

Previous data of our group show for RT112 and 253J cells that the combination of NVP-BEZ235 and MK-2206 is synergistic (Sathe, Chalaud, et al. 2018). We wanted to assess this question for the combination of NVP-BEZ235 and GSK2334470 as the second option to prevent AKT rephosphorylation (Figure 14). To do so, the data of the Cell Titer Blue viability assays were analyzed (Figure 13). The fraction affected (Fa) represents the percentage of cells successfully targeted by the combination therapy. With the help of the CompusSyn software, the combination index (CI) could be determined. It is a value that indicates if the combination of two drugs is synergistic (CI<1), antagonistic (CI>1) or has an additive effect (CI=0) (Chou 2006). Except for the combination of 200nM of NVP-BEZ235 and 50nM of GSK2334470, the combination of NVP-BEZ235 and GSK2334470 in different concentrations had a synergistic effect in all examined cell-lines. Correlating with the CI value, the drug reduction index (DRI) in these combinations was also greater than 1 (data not shown). This indicates that combining these drugs has an advantage over the individual use.

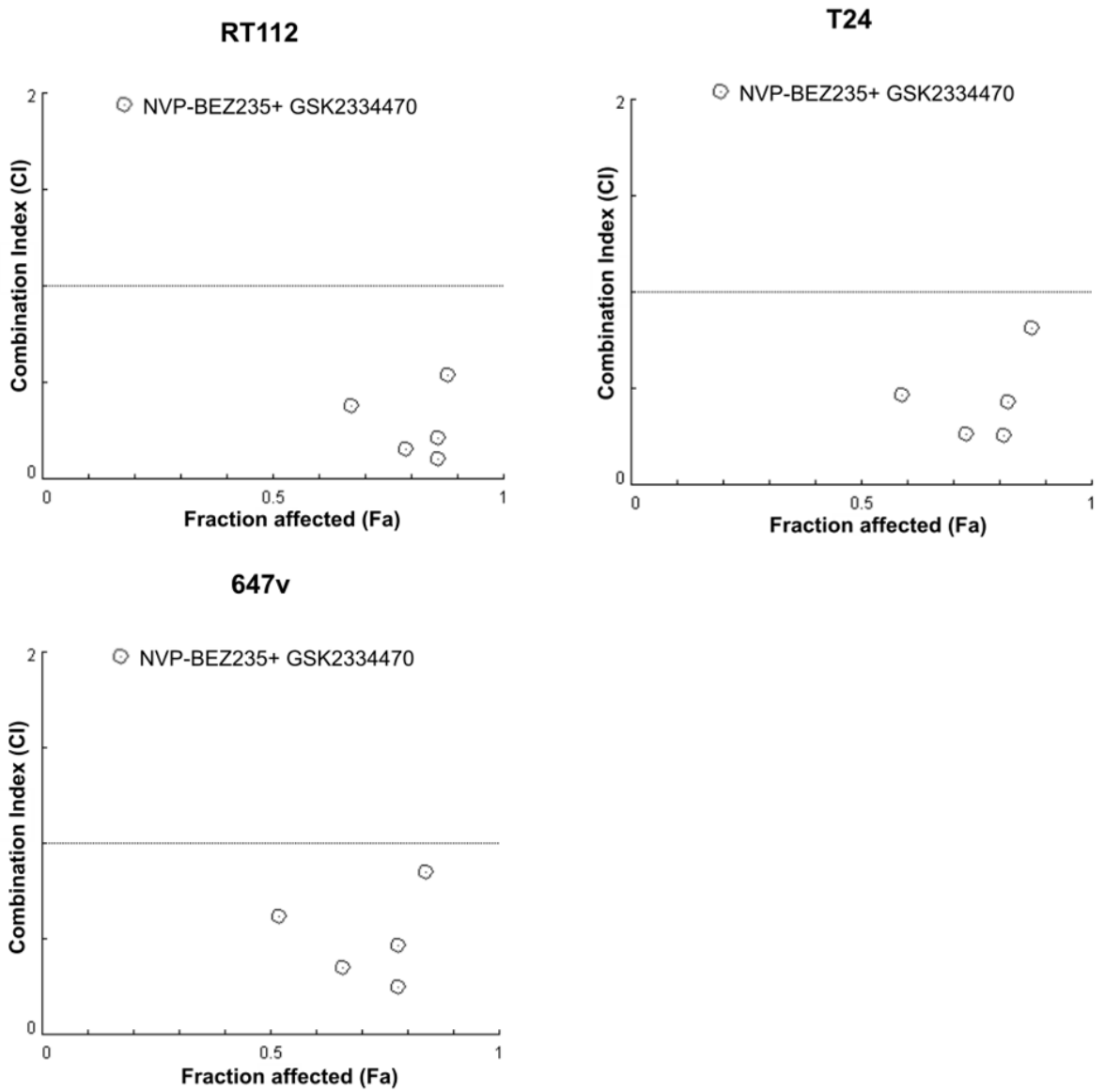

Figure 14: The combination of NVP-BEZ235 and GSK2334470 is synergistic. Synergism plots for the combination of increasing doses of NVP-BEZ235 as indicated in Figure 13 and 500nM of GSK2334470. The Fraction affected (Fa) was determined by 100 minus the percentage of viable cells. The CompusSyn software was used to calculate the combination index (CI).

3.2.4.3 Effects on preventing AKT rephosphorylation on colony formation

A different approach to address the question whether a combination therapy of NVP-BEZ235 and GSK2334470 or MK-2206 has an advantage over single treatment was to perform a clonogenic assay (Figure 15). RT112 cells were treated for 12 days with respective treatment strategies and subsequently the number of surviving colonies was quantified. Single long-term inhibition of PDK1 by GSK2334470 or AKT by MK-2206 had almost no effect on reducing colony growth. Treatment with NVP-BEZ235 resulted in a 35% reduction of colonies, but they were smaller in size. In contrast, both combination therapies resulted in a nearly complete suppression of colony

forming cells with 10% remaining colonies in the NVP-BEZ235 and GSK2334470 treatment and 0.2% in the combination with MK-2206.

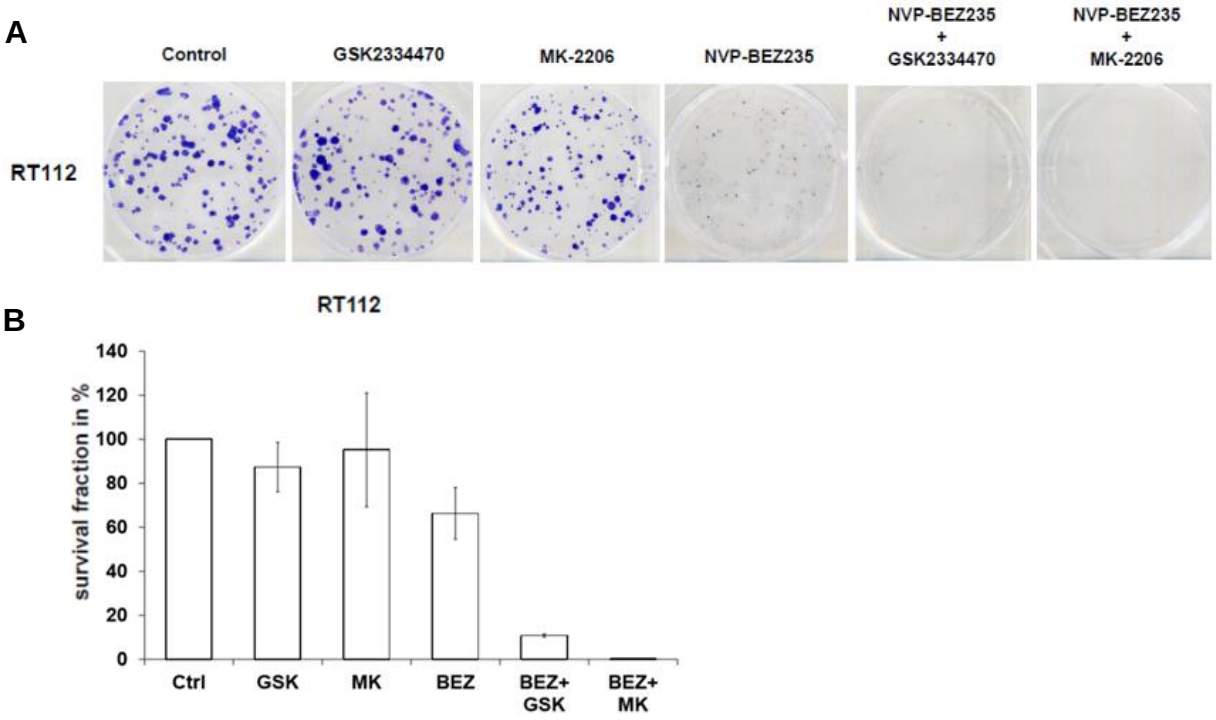

Figure 15: NVP-BEZ235 with either GSK2334470 or MK-2206 impedes colony formation. (A) A clonogenic assay of BLCA cell line RT112 was performed. 150 cells were seeded per well and treated for 12 days with either 500nm of GSK2334470 (GSK), 1000nm of MK-2206 (MK), 200nm of NVP-BEZ235 (BEZ) or a combination of BEZ and GSK or BEZ and MK. (B) The colonies were counted and the survival fraction relative to the control was calculated.

3.2.4.4 Effects on preventing AKT rephosphorylation on apoptosis

In a Caspase 3/7- Apoptosis assay performed in RT112 and 253J cells it has been shown that the Caspase 3/7 activity is significantly increased in the combination of NVP-BEZ235 and MK-2206 and might explain the observed functional data on cell viability (Sathe, Chalaud, et al. 2018) (Figure 13).

In order to extend our data, we used the Caspase 3/7 assay in BLCA cell lines 647v and T24 (Figure 16B). To normalize the level of apoptosis to the viable cells, counting of the surviving cells in each condition after 48 hours of treatment was performed (Figure 16A). The single therapy with NVP-BEZ235 reduced the number of cells to 61% or 52% in 647v and T24 respectively, whereas the single therapy with MK-2206 led to an 18% decrease in 647v cells and had no effect on the viability of T24 cells. Coherent with the data of the viability assay, the combination treatment led to a further reduction of cell viability compared to either of the treatments alone, being an 83% decrease for 647v and a 66% decrease for T24 cells compared to the control. In terms of apoptosis, in both cell lines the single treatments did not lead to an increase of Caspase 3/7 activity (Figure 16B). With the combination of NVP-BEZ235 and MK-

2206, a rise of apoptotic activity by 233% for the 647v cells and by 46% for the T24 cells could be observed.

We wanted to examine if this induction of apoptosis can also be proven biochemically. Therefore RT112 cells were treated either with 200nM of NVP-BEZ235 and/or 250nM of MK-2206 for 1 or 24h (Figure 16C). Besides the proteins of the PI3K pathway, we also analyzed the protein expression and phosphorylated form of the pro-apoptotic factor BAD.
As seen in 647v cells (Figure 9), the single therapy with NVP-BEZ235 induced a dephosphorylation of AKT in both residues after 1 hour followed by a hyperphosphorylation of only the threonine residue after 24 hours. As AKT was inhibited with MK-2206, no phosphorylation of AKT could be detected after 1 or 24 h. The 24 hour combination therapy could successfully prevent rephosphorylation of AKT threonine. S6K1 was in a dephosphorylated state upon NVP-BEZ235 treatment and upon the 1 hour MK-2206 treatment. A slight rephosphorylation occurred after 24 hours of AKT inhibition that could be reversed in the 24 hour combination treatment. As described above (Figure 9), 4E-BP1 phosphorylation in RT112 cells was also completely suppressed after 1 or 24 hours of NVP-BEZ235 treatment, but it was not influenced by AKT inhibition, consistent with a previous publication of our group (Sathe et al. 2014). BAD was phosphorylated at both time points upon NVP-BEZ235 treatment, although a minor decrease in BAD phosphorylation was observed after 24 hours treatment, indicating that apoptosis is slightly increased under these conditions. 1 hour AKT inhibition did not affect phosphorylated BAD, whereas similar to the 24 hour application of NVP-BEZ235 a subtle decrease in phosphorylation could be observed upon 24 hours of MK-2206 therapy. Notably, a complete dephosphorylation of BAD was observed in the combination therapy, suggesting that apoptosis is induced when NVP-BEZ235 and MK-2206 are simultaneously applied

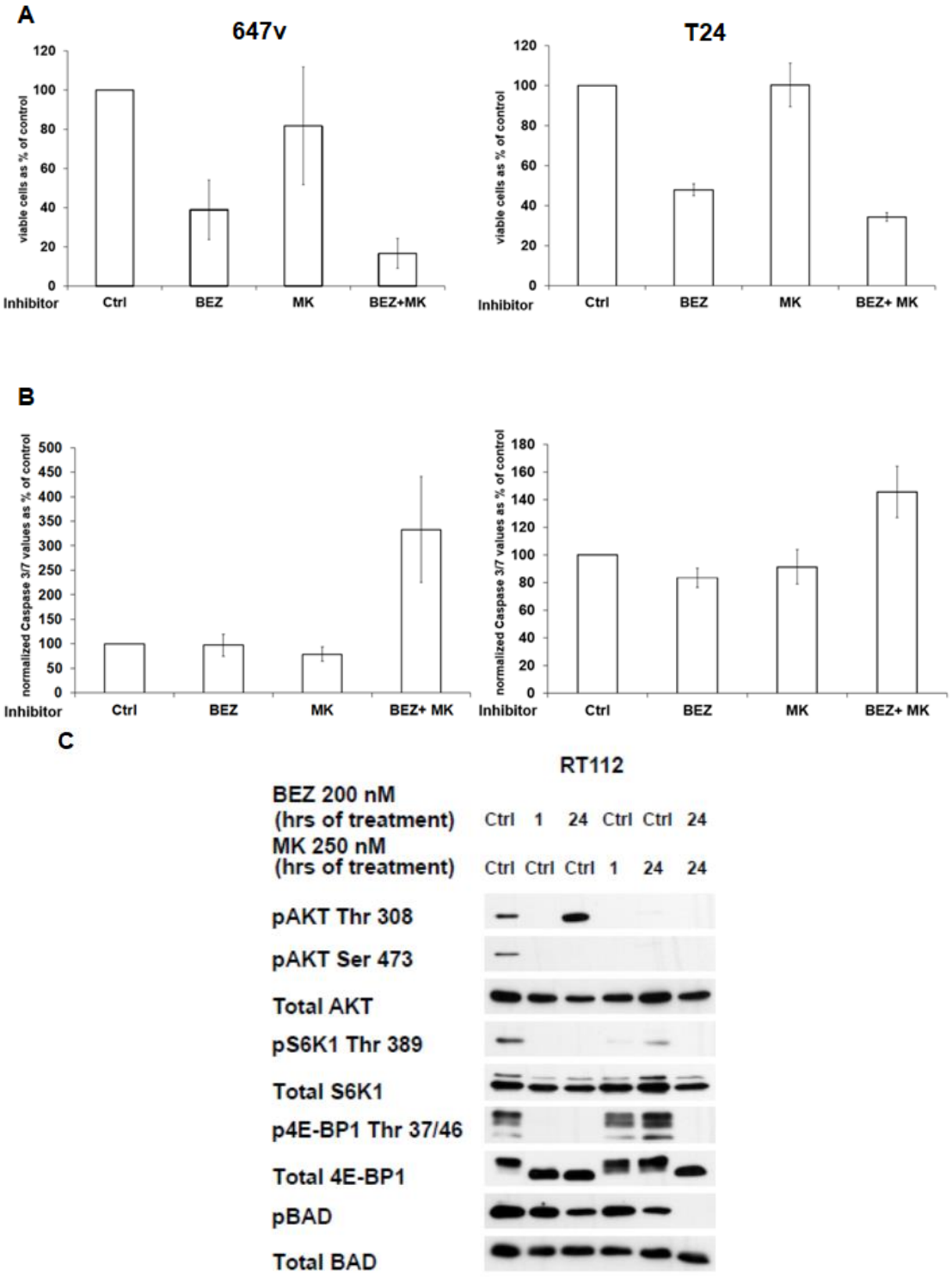

Figure 16: The combination of NVP-BEZ235 and MK-2206 increases apoptosis. (A+B) T24 cells were treated with 100nM of NVP-BEZ235 and/ or 1000nM of MK-2206. 647v cells were treated with 200nM of NVP-BEZ235 and/or 1000nM of MK-2206. (A) After 48 hours of treatment, the viable cells were counted. (B) The relative apoptosis activity was measured after 48 hours of treatment by a Caspase 3/7 assay and set as percentage of the control. (C) RT112 cells were treated with the indicated doses of NVP-BEZ235 and/or MK-2206 for 1 or 24 hours, and selected molecular components of the PI3K signaling pathway as well as BAD were analyzed concerning protein expression and phosphorylation via immunoblots.

4 Discussion

In this study, we investigated the effects of different target therapies on the PI3K/AKT/mTOR signaling pathway. Our aim was to identify molecular components regulating this pathway and that are crucial to target in order to develop an optimized therapy approach in bladder cancer.

4.1 Regulation of 4E-BP1

The first part of this thesis examined the regulation of the translation initiation factor 4E-BP1. According to the literature, 4E-BP1 is a direct downstream target of mTORC1 (Mamane et al. 2006, Ma et al. 2009, Laplante et al. 2012). Nevertheless, different groups as well as our group have shown that 4E-BP1 phosphorylation is not downregulated upon mTORC1 inhibition via rapamycin or rapalogs like RAD001 what could be an explanation for its disappointing clinical results (Nawroth et al. 2011, Zhang et al. 2012). Thoreen et al. described several mTORC1-dependent functions that are rapamycin-resistant, such as the regulation of 4E-BP1 (Thoreen et al. 2009), and also Feldmann et al. observed an incomplete inhibition of mTORC1 via rapamycin (Feldman et al. 2009). Kang et al. demonstrated that the capacity of mTORC1 to phosphorylate a protein is dependent on the affinity of mTORC1 towards the respective phosphorylation site. As mTORC1 strongly phosphorylates 4E-BP1, it is considered as a good substrate. That also leads to the fact that it is less sensitive to rapamycin treatment than S6K1 (Kang et al. 2013). Amongst others, these studies show that in contrast to rapamycin or rapalogs, ATP-competitive mTOR inhibitors like Torin1, PP242 or INK-128 are able to suppress 4E-BP1 activation (Feldman et al. 2009, Thoreen et al. 2009, Hsieh et al. 2012, Kang et al. 2013). Our group not only showed that mTORC1 inhibition via RAD001 is insufficient to regulate 4E-BP1 phosphorylation (Nawroth et al., 2011), but also that a single inhibition of AKT via MK-2206 (Sathe et al. 2014) or PI3K via PIK90 (Sathe, Chalaud, et al. 2018) could not efficiently downregulate 4E-BP1 activity. Only a dual inhibition of PI3K and mTOR with NVP-BEZ235 was able to sufficiently suppress 4E-BP1 signaling (Nawroth et al. 2011). These results might indicate a direct involvement of PI3K or related kinases in 4E-BP1 regulation.

Our group has previously demonstrated that dual PI3K and mTOR inhibition via the small molecule inhibitor NVP-BEZ235 can efficiently downregulate 4E-BP1 activity (Nawroth et al. 2011). In order to distinguish which of the molecular components inhibited by NVP-BEZ235 are responsible for 4E-BP1 dephosphorylation, we inhibited PI3K via PIK90 and mTORC1 via RAD001 (Figure 5A). We could observe a dephosphorylation of 4E-BP1 when 1000nM or 2000nM of PIK90 were combined with 5nM of RAD001. These data for BLCA cell line T24 suggest that PI3K and mTORC1 are involved in 4E-BP1 regulation and extend previous data of our group performed in other cell lines (Sathe, Chalaud, et al. 2018). Moreover the biochemical effects are reflected by the functional analysis concerning cell viability (Figure 5B). A significant reduction in surviving cells was observed in the combination treatment at concentrations, which affected both S6K1 and 4E-BP1 phosphorylation. At those

ranges there was a stronger decrease than with the single treatments. These results match the independent findings of several groups that attribute an important role in cell survival to S6K1 in combination with 4E-BP1 (Fingar et al. 2004, Nawroth et al. 2011, Kyou Kwon et al. 2014). Correlating with our results, Ni et al. came to the conclusion that inhibiting PI3K and mTORC1 is a promising treatment strategy in HER2-positive breast cancer brain metastases due to their efficient suppression of both S6K1 and 4E-BP1 phosphorylation (Ni et al. 2016).

Hsieh et al. and previous results of our group demonstrate a decrease in 4E-BP1 phosphorylation upon the mTOR ATP-site inhibitor INK128, a derivate of PP242 at concentrations 10-fold higher than those needed for AKT or S6K1 dephosphorylation (Hsieh et al. 2012, Sathe, Chalaud, et al. 2018). We wanted to rule out that these effects are due to nonspecific activity of the drug. As 4E-BP1 dephosphorylation occurred at concentrations of 100nM, we are in the range of PI3K inhibition (Sathe, Chalaud, et al. 2018). In our experiment, we silenced mTOR via shRNA and combined it with 250 or 500nM of INK128 (Figure 6). Interestingly, the knockdown of the mTOR protein did not have any effect on the phosphorylation of 4E-BP1, but the single treatment with INK128 completely suppressed 4E-BP1 signaling. If INK128 was a specific mTOR inhibitor, the effects of combining INK128 and mTOR silencing should be similar to the mTOR silencing alone, but instead 4E-BP1 is dephosphorylated upon the combination treatment. This effect could be due to remaining mTOR activity seen with the shRNA knockdown that is sufficient to phosphorylate 4E-BP1 and that gets abolished by using INK128. Alternatively, it might indicate that the effects on 4E-BP1 seen with INK128 alone might be due to inhibition of mTOR and additional inhibition of other kinases, such as PI3K. Although INK128 is claimed to be a specific mTOR inhibitor with an IC50 concentration of 1nM, it also displays inhibitory activity against PI3K with an IC50 that is more than 100-fold higher (Liu, Thoreen, et al. 2009, Hsieh et al. 2012). Hence, these results provide further evidence that 4E-BP1 is not solely regulated by mTORC1, but that other proteins like PI3K, might be involved. Moreover, they contribute to the assumption that the mechanism of phosphorylation is not exclusively dependent on the presence of the mTOR molecule.

Before examining this hypothesis in detail, we first wanted to rule out that other kinases, which are linked to the PI3K/AKT/mTOR pathway and are upstream of 4E-BP1, might be involved in its regulation. We therefore inhibited PDK1, ATM and DNA-PK with the small molecular inhibitors GSK2334470, KU60019 and NU 7441 respectively (Figure 7A-C, Table 15). In the literature PDK1 and ATM were linked to 4E-BP1 phosphorylation (Yang et al. 2000, Pons et al. 2012). ATM and DNA-PK as members of the PIKK-family were described as targets of NVP-BEZ235 (Mukherjee et al. 2012). Hence, we also aimed to examine if the effects on 4E-BP1 phosphorylation seen with this inhibitor are due to inhibition of other kinases. Our results allow the exclusion of PDK1, ATM or DNA-PK as direct upstream-regulators of 4E-BP1, since their inhibition was not leading to a decrease in 4E-BP1 phosphorylation. PDK1 inhibition only resulted in a dephosphorylation of the AKT Thr

308 residue and S6K1 (Figure 7A). PDK1 is described to directly phosphorylate the AKT Thr 308 residue (Alessi et al. 1997), whereas mTORC2 is the major kinase for serine 473 phosphorylation (Copp et al. 2009). The observation that dephosphorylation of S6K1 occurred at lower concentrations than for AKT dephosphorylation suggests that S6K1 inhibition is preceding and might be due to the fact that S6K1 is a direct downstream target of PDK1 (Wang et al. 2013). The effects on AKT and S6K1 phosphorylation upon DNA-PK inhibition are probably caused by off-target effects of the inhibitor, since DNA-PK is a member of the PIKK-familiy and NU 7441 was shown to inhibit PI3K with an IC50 of 5µM and mTOR with an IC50 of 1.7µM (Leahy et al. 2004).

The results show that dual inhibition of PI3K and mTORC1 via RAD001 can downregulate 4E-BP1 activity (Figure 5), although the effect seen with NVP-BEZ235 could not be imitated to its full extent. This pointed to the need of a more detailed investigation of molecular mechanisms involved in 4E-BP1 regulation. In order to do this, we worked with shRNA and siRNA to silence mTOR, Raptor or Rictor combined with inhibition of PI3K by PIK90 (Figure 8A-C). The knockdown of either mTOR, Raptor or Rictor alone had no impact on 4E-BP1 activation, but mTOR or Raptor silencing led to complete dephosphorylation of S6K1, emphasizing a different underlying mechanism of regulation for 4E-BP1 and S6K1. This is in contrast to findings of other groups that observed a downregulation of 4E-BP1 phosphorylation upon mTOR silencing (Green et al. 2010) or upon Raptor or mTOR silencing (Thoreen et al. 2009) attributing 4E-BP1 regulation to the catalytic activity of mTOR or mTORC1 respectively. Our results of mTOR knockdown combined with the experiment that proved off-target effects of the mTOR catalytic site inhibitor INK128 (Figure 6) indicate a different mechanism for 4E-BP1 regulation in bladder cancer.
The simultaneous inhibition of mTOR and PI3K led to a 30% further reduction of 4E-BP1 phosphorylation compared to single PI3K inhibition (Figure 8A), whereas combining Raptor siRNA with PIK90 led to a 70% further decrease (Figure 8B). Although this combination is similar to the PIK90 and RAD001 treatment, the effect on 4E-BP1 phosphorylation of PIK90 combined with Raptor is much stronger. This could be due to the different biochemical mechanisms of mTORC1 inhibition. RAD001 mediates a steric inhibition and binds to the FRB region of mTORC1 in complex with FKBP12 to achieve a conformational change, but does not directly act at the catalytic center (Choo et al. 2009). In contrast, Raptor silencing leads to a complete disruption of the complex that might ensure a stronger inhibition of mTORC1 activity.
The combination of Rictor siRNA with PIK90 had no effect on 4E-BP1 phosphorylation (Figure 8C), indicating that 4E-BP1 is not regulated via mTORC2. In order to investigate whether AKT is involved in this regulatory mechanism, we combined Raptor siRNA with the AKT inhibitor MK-2206 (Figure 8D). If the signaling pathway would be mediated via AKT, we would expect the same effect on 4E-BP1 as seen with the inhibition of PI3K and Raptor. Of note, the inhibition of AKT and Raptor did not lead to dephosphorylation of 4E-BP1, suggesting that its regulation is not dependent on AKT. This is in contrast to the observations of Mi et al. who

demonstrate that phosphorylation can be efficiently downregulated by mTORC1 inhibition with rapamycin combined with MK-2206 in human breast and colon cancer cells. They say that this effect is mediated via PRAS40, a negative regulator of mTORC1 (Mi et al. 2015). Nonetheless, our results lead to the conclusion that 4E-BP1 phosphorylation is independent of AKT activity.

Overall, our data revealed that the mechanism of 4E-BP1 phosphorylation in bladder cancer is dependent on PI3K and the formation of the mTORC1 protein complex, more than on the actual mTOR kinase activity, as the inhibition of PI3K and Raptor resulted in a stronger reduction of 4E-BP1 activity than inhibition of PI3K and mTOR. However, neither mTOR nor Raptor inhibition alone resulted in a dephosphorylation of 4E-BP1, but the simultaneous inhibition of PI3K was required, leading to the assumption that PI3K might have an influence on mTORC1 mediated via Raptor (Sathe, Chalaud, et al. 2018). We therefore suggest the following revised simplified model of 4E-BP1 regulation in urothelial carcinoma (Figure 17). These findings mark another step towards a detailed understanding of the complex structures of PI3K signaling. Furthermore, it is of clinical significance, since the expression levels of 4E-BP1, eIF4E and phosphorylated 4E-BP1 seem to be crucial markers for a prediction of the clinical outcome in different cancer entities (Musa et al. 2016). Only a profound knowledge of the biochemical context can lead to the development of an optimized therapeutic strategy as well as the identification of suitable biomarkers to detect potential responders to the different compounds.

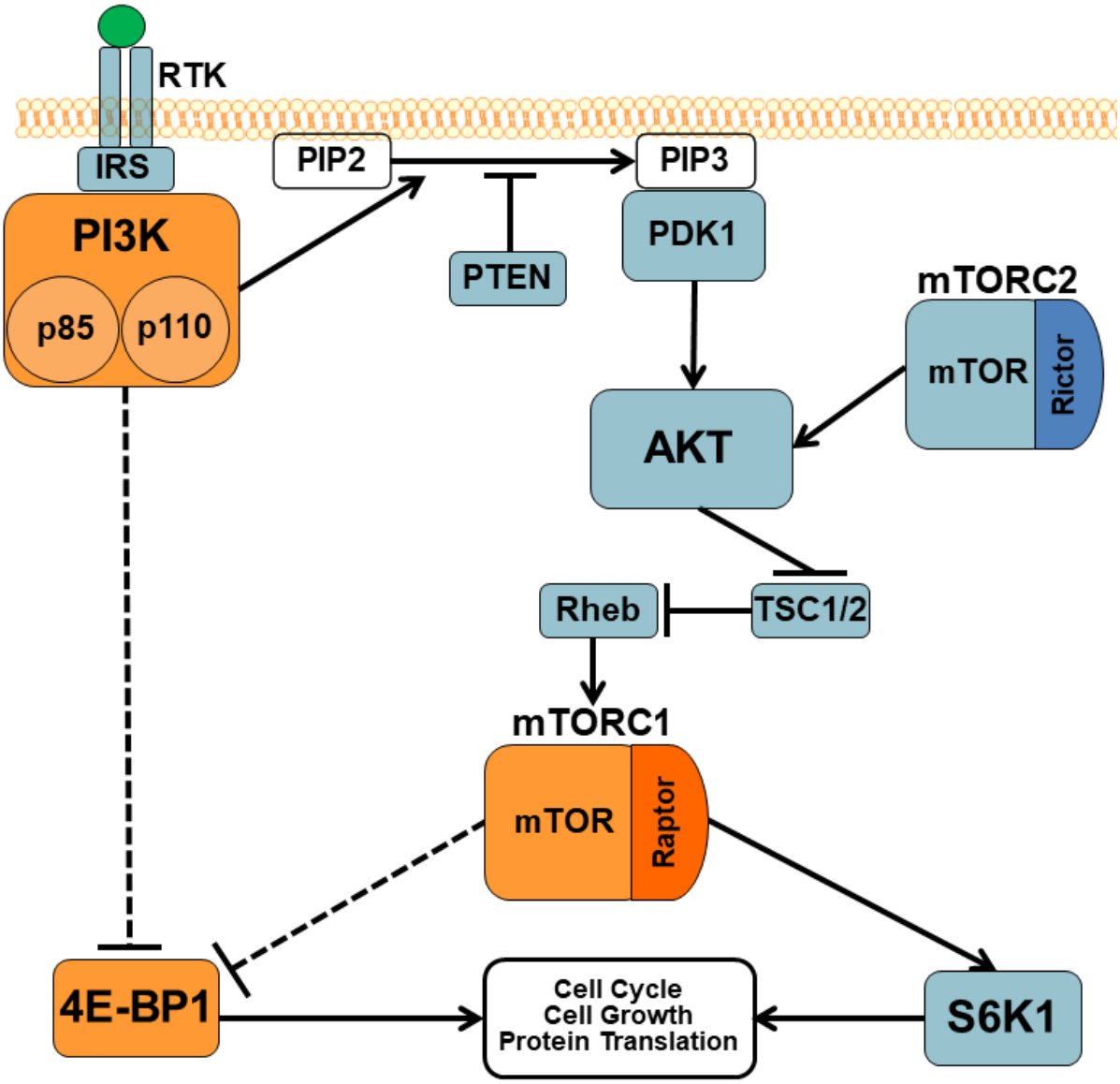

Figure 17: 4E-BP1 is regulated via PI3K and mTORC1, independent of AKT

4.2 Rephosphorylation of AKT upon treatment with NVP-BEZ235

Previously published data show a AKT threonine rephosphorylation in the cell lines RT112, T24, 253J and 647v when a time kinetic treatment with NVP-BEZ235 is applied (Nawroth et al. 2011) (Figure 9). In 647v cells an initial dephosphorylation of AKT at its threonine residue was followed by a slight recovery of phosphorylation after 4 hours and a hyperphosphorylation after 48 hours. We could exclude that this effect was caused by an activity loss of the inhibitor by freshly adding the compound after 23 or 47 hours of treatment respectively without rephosphorylation being reversed. This rephosphorylation under NVP-BEZ235 over time has also been observed in burkitt lymphoma (Li et al. 2015), gliomas (Liu, Koul, et al. 2009) and in breast cancer (Serra et al. 2008). Serra et al. claim that rephosphorylation occurs at doses that do not inhibit PI3K. For our experiments we worked with 100nM for T24 cells and 200nM for RT112, 253J and 647v cells. Besides the fact that p110α is inhibited by NVP-BEZ235 with an IC50 of 4nM (Maira et al. 2008), we can assume

that PI3K is inhibited at the concentrations used because AKT, S6K1 and 4E-BP1 phosphorylation is suppressed throughout the time course, which was, in case of 4E-BP1, shown above to only occur under dual PI3K and mTORC1 inhibition. S6K1 also remains dephosphorylated probably due to sustained mTORC1 inhibition. It has to be emphasized that this rephosphorylation of AKT cannot be explained by the S6K1 IRS-1 feedback loop, as the latter can be prevented by simultaneous PI3K and mTORC1 inhibition (O'Reilly et al. 2006). Unlike the threonine residue of AKT, the phosphorylation of the serine residue does not recover in 647v cells that might be explained by the persistent mTORC2 inhibition and indicates that the AKT reactivation loop is not mediated via mTORC2.
It has to be further examined to which degree the phenomenon of AKT reactivation following long-term use of NVP-BEZ235 is contributing to clinical failure of the drug (Seront et al. 2016).
We demonstrate here that AKT rephosphorylation under dual PI3K/mTOR inhibition via NVP-BEZ235 can be prevented when it is combined with the PDK1 inhibitor GSK2334470 (Sathe, Chalaud, et al. 2018) (Figure 10). Not only did the 24 hour treatment of 647v cells with NVP-BEZ235 lead to AKT rephosphorylation at the threonine residue, but also the 24h treatment with GSK2334470 showed this effect after an initial dephosphorylation at 1 hour. This indicates that PDK1 inhibition alone can trigger reactivation of AKT, a phenomenon that has already been described by Najafov et al. (Najafov et al. 2011). They made PIP3 and PIF-pocket dependent mechanisms of AKT phosphorylation responsible for PDK1 resistance (Najafov et al. 2012). Lately, other kinases like IKBKE or TBK1 have been discussed as kinases phosphorylating AKT independent of PDK1 (Guo et al. 2011, Xie et al. 2011). Nevertheless, the exact mechanism of AKT rephosphorylation upon PDK1 inhibition remains elusive for bladder cancer. At both time points the serine residue phosphorylation was only slightly affected, consistent with the fact that this residue is mainly phosphorylated via mTORC2 (Copp et al. 2009). Nevertheless, there seems to be a rephosphorylation of AKT Ser 473 after 24 hours of PDK1 inhibition in T24 cells and a hyperphosphorylation of this residue in the cell line RT112 (Figure 11). This effect cannot be seen in 647v cells emphasizing the fact that differences not only between the different tumor entities but also between different cell lines within one cancer entity exist. Following the results in RT112 and T24 (Sathe, Chalaud, et al. 2018), we observed that also in 647v cells rephosphorylation of AKT under NVP-BEZ235 treatment can be prevented when PDK1 is additionally inhibited (Figure 10). This indicates that PDK1 plays an important role in the feedback-loop that rephosphorylates AKT upon PI3K/mTOR inhibition.

For a more detailed understanding of this feedback-mechanism, we wanted to distinguish through which components AKT rephosphorylation is conducted. Therefore PI3K and mTOR that are both inhibited by NVP-BEZ235 were individually targeted by a small molecule inhibitor and combined with a PDK1 inhibition in BLCA cell lines T24 and RT112. First, the role of mTOR was determined by combining INK128 with GSK2334470 (Figure 11). The reason for the AKT rephosphorylation upon INK128 treatment for 24 hours can be explained by the described PIP3-

dependent S6K1 feedback-loop, which occurs upon activation of receptor tyrosine kinases (Rodrik-Outmezguine et al. 2011). Importantly, a simultaneous inhibition of mTOR and PDK1 was not sufficient to prevent reactivation of AKT, indicating that activated PI3K is the key factor for mediating the feedback-loop observed upon NVP-BEZ235 inhibition. Najafoj et al. demonstrate that the combination of an mTOR inhibitor and GSK2334470 represents a promising therapeutic strategy but without looking at the effects of a prolonged treatment with both compounds (Najafov et al. 2012).

Costa et al. described in their study in luminal breast cancer that rephosphorylation of AKT upon p110α inhibition is mediated by a p110β induced re-accumulation of PIP3 and is dependent on PDK1 (Costa et al. 2015). A similar mechanism could be a possible explanation for our findings in bladder cancer, as NVP-BEZ235 affinity for p110β inhibition is almost 20-fold lower than for p110α (Maira et al. 2008), meaning that p110β could only be partially inhibited. However, an ELISA-based PIP3 quantification assay was performed by our group and showed that the PIP2/PIP3 ratio decreased by 95% upon a one-hour NVP-BEZ235 treatment and stayed on a low level after 24 hours. This excludes the involvement of PIP3 in the feedback-loop observed with NVP-BEZ235 and reveals a novel mechanism for the regulation of AKT via PI3K and PDK1 that is not dependent of PIP3 (Sathe, Chalaud, et al. 2018). In the literature, Calleja et al. present a PIP3-independent way of AKT activation by PDK1 based on the formation of a protein complex in the cytoplasm, which might be a possible operating principle (Calleja et al. 2007).

We could exclude that AKT reactivation loop upon NVP-BEZ235 treatment is mediated via mTORC2 (Figure 11). So we had to confirm our assumption that it is induced through activation of the PI3K/PDK1 axis by dual inhibition of PI3K and PDK1 (Figure 12).
Similar to the situation with NVP-BEZ235 the application of PIK90 led to an initial dephosphorylation of AKT followed by a rephosphorylation after 24 hours. A possible explanation for this rephosphorylation could be a PI3K independent phosphorylation of AKT threonine by PDK1, compliant with the study of Ding et al. (Ding et al. 2010). This would also explain why no rephosphorylation of the serine residue can be observed upon PIK90 treatment. Noteworthy, the dual inhibition of PI3K and PDK1 was able to suppress AKT threonine rephosphorylation, but it was not sufficient to fully inhibit serine phosphorylation, probably because of a sustained mTORC2 function. Our data lead to the conclusion that the feedback-loop for AKT rephosphorylation at the threonine residue is conducted via PI3K and PDK1 (Figure 18). Nevertheless, the simultaneous inhibition of PI3K, PDK1 and mTOR, as realized with NVP-BEZ235 and GSK2334470, might be the more favorable strategy as phosphorylation of both AKT residues are efficiently suppressed.

Besides the combination of NVP-BEZ235 with a PDK1 inhibitor, our group has previously demonstrated that treatment with NVP-BEZ235 and MK-2206 is another effective drug combination. Not only AKT is directly targeted and therefore its rephosphorylation is suppressed, but also apoptosis is induced and tumor weight is

reduced in vivo (Sathe, Chalaud, et al. 2018). We wanted to compare these two different treatment strategies NVP-BEZ235 with either GSK-2334470 or MK-22006 in terms of viability with one another as well as with the single treatments for three BLCA cell lines (Figure 13). GSK2334470 and MK-2206 alone did not lead to a great reduction in cell viability. This is in accordance with previous results of our group because both compounds only inhibit S6K1 activity without affecting 4E-BP1 phosphorylation and both proteins have to be suppressed for an efficient reduction of cell proliferation (Nawroth et al. 2011). As described by Sathe et al. RT112, T24 and 647v are cell lines resistant to MK-2206, which was explained by their lack of mutation in the PIK3CA gene and could be confirmed by the viability data depicted in Figure 13. Although NVP-BEZ induces a feedback-loop that reactivates AKT, the number of surviving cells was reduced dose-dependently. However, both combination therapies were more efficient than the NVP-BEZ235 treatment alone concerning viability. Especially for low dose NVP-BEZ235 this difference was particularly pronounced. This finding could be of special interest in terms of a dose reduction of NVP-BEZ235 in a combination therapy, since NVP-BEZ235 displayed a high degree of toxicity in the concentration used in the clinical trial (Seront et al. 2016). Moreover, we could show that the combinations of NVP-BEZ235 and MK-2206 (Sathe, Chalaud, et al. 2018) or NVP-BEZ235 with GSK-2334470 (Figure 14) show synergistic effects. Thus, both combination therapies allow a reduction in concentration of the compounds that would probably lower the risk of dose-dependent toxicity.

To assess the ability of colony formation under these different treatment strategies, a clonogenic assay was performed in RT112 cells (Figure 15). According to our viability data, the minor influence on cell survival due to PDK1 or AKT inhibition was also reflected in this assay, as the number of formed colonies was comparable to the control. Interestingly, the number of surviving colonies in the NVP-BEZ235 treatment condition was not dramatically decreased as it might have been expected considering the viability data, but rather the size of the colonies was reduced. This could be explained by previous findings of our group that cell viability is decreased but more because of a cell cycle arrest in G0/G1 phase than because of an induction of apoptosis upon single treatment with NVP-BEZ235 (Sathe, Chalaud, et al. 2018). Both treatment combinations led to a drastic decrease in living colonies, which reflects the viability data (Figure 13).

As it was observed by our group, the combination of NVP-BEZ235 and MK-2206 can increase Caspase 3/7 activity in different bladder cancer cell lines (Sathe, Chalaud, et al. 2018)(Figure 16B). We provided additional biochemical evidence that the combination of NVP-BEZ235 and MK-2206 can induce apoptosis by examining the phosphorylation status of the proapoptotic factor BAD (Figure 16C). In a dephosphorylated state BAD is able to bind anti-apoptotic factors Bcl-2 and Bcl-xL so that Bax/Bak mediated apoptosis is induced (Yang et al. 1995). Moreover, BAD is a direct downstream target of AKT and suppresses apoptosis once it is phosphorylated, representing one of the many examples of how AKT promotes cell

survival (Datta et al. 1997). Only the treatment with both compounds, NVP-BEZ235 and MK-2206, result in complete dephosphorylation of AKT, S6K1 and 4E-BP1 and also in a complete dephosphorylation of BAD synonymous with an induction of apoptosis, as it has also been demonstrated by the Caspase 3/7 assay.

Overall, we have characterized a novel mechanism for 4E-BP1 regulation in bladder cancer as mediated via PI3K and mTORC1, but not via AKT (Figure 17). We have also described the PI3K/PDK1-dependent feedback-loop that leads to reactivation of AKT upon dual PI3K/mTOR inhibition (Figure 18). Taking these two aspects into consideration, we suggest a simultaneous inhibition of PI3K, mTOR and either AKT or PDK1. A possible drug combination would be NVP-BEZ235 applied with MK-2206 or GSK2334470. These therapy strategies assure a sustained suppression of AKT, S6K1 and 4E-BP1 signaling and decrease cell viability. We could further demonstrate that NVP-BEZ235 with MK-2206 is able to induce apoptosis. Our data lead to the conclusion that combined target therapies might be a promising approach in treatment of advanced urothelial carcinoma.

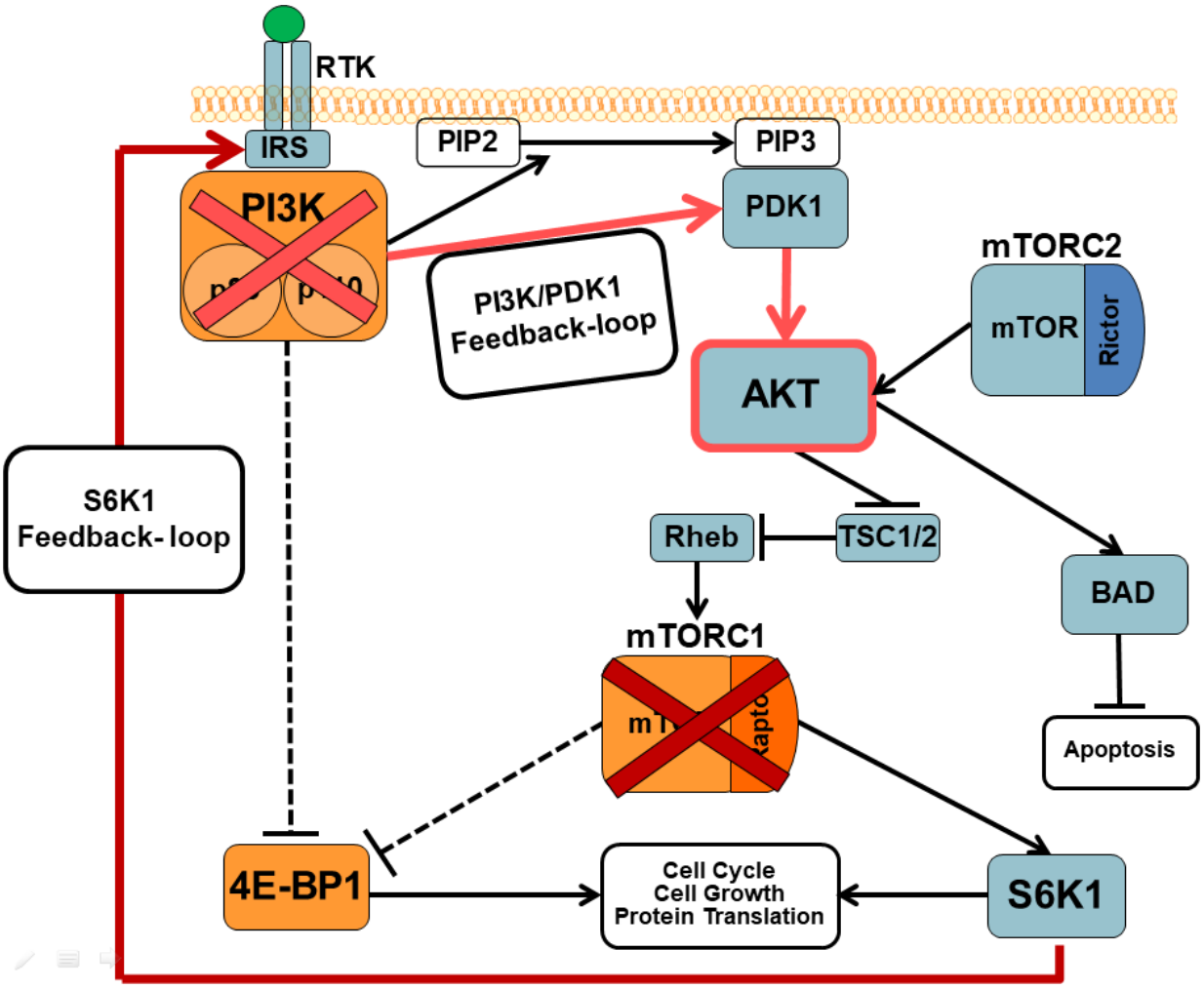

Figure 18: Modell of the S6K1- and the PI3K/PDK1- feedback loops.
Only the simultaneous inhibition of PI3K and PDK1 prevents rephosphorylation of AKT

Summary

Small molecular inhibitors that interfere with signaling pathways, such as the PI3K-signaling-cascade, in order to suppress cell viability and growth are already an integral part in the treatment of different tumor entities. However, in bladder cancer therapy clinical efficacy could not be proven to date and is still in the process of evaluation.
Creating an understanding of the underlying molecular processes could be the key in explaining and therefore circumventing limited response to available inhibitors of this pathway.
In this work, we focused on the regulation of 4E-BP1 in bladder cancer, as its inactivation is crucial for attaining the desired effects on cell survival. As previous results from our group show, it is not regulated via the PI3K/AKT/mTORC1 axis contrary to previously described findings in different tumor entities.
Dephosphorylation of 4E-BP1 was achieved by using the dual PI3K/mTOR inhibitor NVP-BEZ235. A combined inhibition of PI3K and with the steric mTORC1 inhibitor RAD001 could also downregulate 4E-BP1 activity. We further have indications that effects on 4E-BP1 phosphorylation seen with the mTOR inhibitor INK128 might be due to additional inhibition of other proteins. A direct influence of DNA-PK and ATM as members of the PIKK- family as well as the upstream kinase PDK1 on 4E-BP1 regulation could be excluded. We demonstrate that only an inhibition of PI3K and mTORC1 but not mTORC2 is required to downregulate 4E-BP1 phosphorylation and show that its regulation is independent from AKT signaling.
Although the simultaneous inhibition of PI3K and mTOR as effectuated by NVP-BEZ235 seems to be the ideal strategy to control both 4E-BP1 and S6K1 activity, the inhibitor bears the problem of AKT rephosphorylation after an extended treatment period. Our aim was to characterize this feedback-mechanism that could be one possible explanation for the limited success of NVP-BEZ235 in the clinic.
We first confirmed that reactivation of AKT upon NVP-BEZ235 treatment also occurs in 647v bladder cancer cells after an extended period of time and that it can be suppressed by additional inhibition of PDK1, as it was previously seen in other cell lines. We could further demonstrate that PI3K and PDK1 but not mTOR, are involved in this feedback-loop and that the combination of NVP-BEZ235 with an inhibitor of either AKT or PDK1 would be two suitable strategies to prevent it.
These biochemical findings could also be applied on a functional basis. Cell survival could be reduced to a greater extent with the combination of NVP-BEZ235 and the PDK1 inhibitor GSK2334470 or the AKT inhibitor MK-2206 than with the one of these compounds alone and colony formation could be almost completely suppressed by the combination therapies. Further, the use of NVP-BEZ235 along with GSK2334470 is synergistic and a dose reduction in order to reduce toxicity without affecting the efficacy of the treatment might be conceivable.
Combining NVP-BEZ235 with MK-2206 also showed an increased Caspase 3/7 activity compared to monotherapy, which was biochemically reflected by a dephosphorylation of the proapoptotic factor BAD.

In summary, we showed that 4E-BP1 in bladder cancer is regulated via a PI3K- and mTORC1-dependent and AKT-independent mechanism, in contrast to other cancer entities. We further characterized the PI3K/PDK1-dependent AKT-feedback-loop and suggest a combination of NVP-BEZ235 with either a PDK1 or an AKT inhibitor as suitable treatment options in order to sufficiently suppress S6K1 and 4E-BP1 signaling as well as to sustain dephosphorylation of AKT. With these findings we contribute to a more detailed knowledge of cell signaling processes in bladder cancer that is a prerequisite to make progress in the field of target therapy as a new treatment strategy in advanced or metastatic bladder cancer.

Zusammenfassung

Niedermolekulare Inhibitoren, die Komponenten von Signaltransduktionswegen wie dem PI3K-Signalweg inhibieren, um Zellwachstum und –überleben zu hemmen, sind bereits ein integraler Bestandteil in der Therapie verschiedener Tumorentitäten. Dennoch konnte die klinische Wirksamkeit für das Blasenkarzinom bis zum heutigen Tage nicht belegt werden und ist im Augenblick noch Gegenstand von Untersuchungen.
Ein Verständnis der zugrundeliegenden molekularen Mechanismen könnte der Schlüssel dafür sein, das eingeschränkte klinische Ansprechen auf verfügbare Wirkstoffe zu erklären.
In dieser Arbeit haben wir uns auf die Regulierung von 4E-BP1 im Blasenkarzinom konzentriert, da seine Herunterregulierung wesentlich für die gewünschten Effekte auf das Zellüberleben ist.
Wie Ergebnisse unserer Gruppe zeigen, wird es nicht über die PI3K/AKT/mTORC1-Achse reguliert, im Gegensatz zu vorherigen Ergebnissen in Tumorzellen anderer Tumorentitäten.
Die Dephosphorylierung von 4E-BP1 wurde durch den dualen PI3K/mTOR Inhibitor NVP-BEZ235 erreicht. Außerdem konnte die Aktivität von 4E-BP1 durch eine gleichzeitige Inhibierung von PI3K und dem sterischen mTORC1 Inhibitor RAD001 herunterreguliert werden. Wir haben weiter Hinweise dafür, dass die Effekte auf die Phosphorylierung von 4E-BP1, die mit dem ATP-kompetitiven Inhibitor INK128 beobachtet wurden, durch unspezifische Inhibierung anderer Kinasen verursacht ist. Ein direkter Einfluss anderer Kinasen der PIKK-Familie, wie DNA-PK und ATM sowie die vorgeschaltete Kinase PDK1 auf die Regulation von 4E-BP1 konnte aber ausgeschlossen werden.
Wir demonstrieren, dass lediglich eine Inhibierung von PI3K und mTORC1, nicht aber von mTORC2, notwendig ist, um die Phosphorylierung von 4E-BP1 herunterzuregulieren und zeigen, dass diese Regulation unabhängig von AKT ist.
Obwohl die gleichzeitige Inhibierung von PI3K und mTOR, wie sie durch NVP-BEZ235 gewährleistet ist, die ideale Strategie zu sein scheint, um sowohl die Aktivität von 4E-BP1, als auch die von S6K1 zu kontrollieren, birgt der Inhibitor das Problem der Rephosphorylierung von AKT nach einer länger dauernden Behandlungsperiode. Unser Ziel war es, diesen Feedback-Mechanismus zu charakterisieren, der eine mögliche Erklärung für den begrenzten klinischen Erfolg von NVP-BEZ235 darstellen könnte.
Wir haben zunächst bestätigt, dass auch in der Blasenkrebs- Zelllinie 647v, wie es auch schon in anderen Zelllinien beobachtet wurde, die Reaktivierung von AKT unter einer längeren Behandlung mit NVP-BEZ235 auftritt und dass dies durch zusätzliche Inhibierung von PDK1 verhindert werden kann. Wir konnten ferner genauer festlegen, dass PI3K und PDK1, aber nicht mTOR, in diese Feedback-Schleife involviert sind und dass die Kombination von NVP-BEZ235 mit einem Inhibitor von entweder AKT oder PDK1 zwei geeignete Strategien darstellen, um sie zu verhindern.

Diese biochemischen Erkenntnisse konnten auch auf eine funktionale Ebene übertragen werden. Das Zellüberleben konnte mit der Kombination aus NVP-BEZ235 und dem PDK1- Inhibitor GSK2334470 oder dem AKT- Inhibitor MK-2206 stärker reduziert werden als mit den jeweiligen Substanzen alleine und die Koloniebildung konnte mit den Kombinationstherapien fast vollständig unterdrückt werden. Weiter ist der gemeinsame Einsatz von NVP-BEZ2334470 mit GSK2334470 synergistisch, sodass eine Dosisreduktion zur Reduzierung der Toxizität, jedoch ohne Minderung der Effektivität der Behandlung, denkbar wäre. Die Kombination von NVP-BEZ235 mit MK-2206 zeigte im Vergleich zur Monotherapie auch eine gesteigerte Caspase 3/7 Aktivität, was biochemisch durch die Dephosphorylierung des proapoptotischen Faktors BAD widergespiegelt wurde.

Insgesamt konnten wir zeigen, dass 4E-BP1 im Blasenkarzinom, im Gegensatz zu anderen Krebsarten, durch einen PI3K- und mTORC1-abhängigen und AKT-unabhängigen Mechanismus reguliert wird. Außerdem haben wir die PI3K/PDK1-abhängige AKT-Feedback-Schleife charakterisiert und empfehlen eine Kombination aus NVP-BEZ235 mit entweder einem PDK1- oder einem AKT-Inhibitor als geeignete Behandlungsoptionen, um sowohl die Aktivität von S6K1 und 4E-BP1 zu unterdrücken, als auch die Reaktivierung von AKT zu verhindern. Mit diesen Ergebnissen tragen wir zu einem detaillierteren Wissen zu Prozessen der Signaltransduktion in Blasenkrebszellen bei, das eine Voraussetzung darstellt, um einen Fortschritt im Bereich der gezielten Krebstherapie als neue Behandlungstrategie für das fortgeschrittene oder metastasierte Blasenkarzinom zu erzielen.

Bibliography

Akinleye, A., P. Avvaru, M. Furqan, Y. Song and D. Liu (2013). "Phosphatidylinositol 3-kinase (PI3K) inhibitors as cancer therapeutics." J Hematol Oncol **6**(1): 88.

Alessi, D. R., S. R. James, C. P. Downes, A. B. Holmes, P. R. Gaffney, C. B. Reese and P. Cohen (1997). "Characterization of a 3-phosphoinositide-dependent protein kinase which phosphorylates and activates protein kinase Balpha." Curr Biol **7**(4): 261-269.

Allory, Y., W. Beukers, A. Sagrera, M. Flandez, M. Marques, M. Marquez, K. A. van der Keur, L. Dyrskjot, I. Lurkin, M. Vermeij, A. Carrato, J. Lloreta, J. A. Lorente, E. Carrillo-de Santa Pau, R. G. Masius, M. Kogevinas, E. W. Steyerberg, A. A. van Tilborg, C. Abas, T. F. Orntoft, T. C. Zuiverloon, N. Malats, E. C. Zwarthoff and F. X. Real (2014). "Telomerase reverse transcriptase promoter mutations in bladder cancer: high frequency across stages, detection in urine, and lack of association with outcome." Eur Urol **65**(2): 360-366.

Antoni, S., J. Ferlay, I. Soerjomataram, A. Znaor, A. Jemal and F. Bray (2017). "Bladder Cancer Incidence and Mortality: A Global Overview and Recent Trends." Eur Urol **71**(1): 96-108.

Antonova, O., D. Toncheva and E. Grigorov (2015). "Bladder cancer risk from the perspective of genetic polymorphisms in the carcinogen metabolizing enzymes." J buon **20**(6): 1397-1406.

Aragon-Ching, J. B. and D. L. Trump (2017). "Targeted therapies in the treatment of urothelial cancers." Urol Oncol **35**(7): 465-472.

Audenet, F., K. Attalla and J. P. Sfakianos (2018). "The evolution of bladder cancer genomics: What have we learned and how can we use it?" Urol Oncol **36**(7): 313-320.

Babjuk, M., A. Bohle, M. Burger, O. Capoun, D. Cohen, E. M. Comperat, V. Hernandez, E. Kaasinen, J. Palou, M. Roupret, B. W. van Rhijn, S. F. Shariat, V. Soukup, R. J. Sylvester and R. Zigeuner (2017). "EAU Guidelines on Non-Muscle-invasive Urothelial Carcinoma of the Bladder: Update 2016." Eur Urol **71**(3): 447-461.

Bellacosa, A., C. C. Kumar, A. Di Cristofano and J. R. Testa (2005). "Activation of AKT kinases in cancer: implications for therapeutic targeting." Adv Cancer Res **94**: 29-86.

Bendell, J. C., A. M. Varghese, D. M. Hyman, T. M. Bauer, S. Pant, S. Callies, J. Lin, R. Martinez, E. Wickremsinhe, A. Fink, V. Wacheck and K. N. Moore (2018). "A First-in-Human Phase 1 Study of LY3023414, an Oral PI3K/mTOR Dual Inhibitor, in Patients with Advanced Cancer." Clin Cancer Res **24**(14): 3253-3262.

Benjamin, D., M. Colombi, C. Moroni and M. N. Hall (2011). "Rapamycin passes the torch: a new generation of mTOR inhibitors." Nat Rev Drug Discov **10**(11): 868-880.

Berdik, C. (2017). "Unlocking bladder cancer." Nature **551**(7679): 34-35.

Brierley, J. D., M. K. Gospodarowicz and C. Wittekind (2017). TNM classification of malignant tumours. UICC International Union Against Cancer. Oxford, John Wiley & Sons.

Brown, J. S. and U. Banerji (2017). "Maximising the potential of AKT inhibitors as anti-cancer treatments." Pharmacol Ther **172**: 101-115.

Burger, M., J. W. Catto, G. Dalbagni, H. B. Grossman, H. Herr, P. Karakiewicz, W. Kassouf, L. A. Kiemeney, C. La Vecchia, S. Shariat and Y. Lotan (2013). "Epidemiology and risk factors of urothelial bladder cancer." Eur Urol **63**(2): 234-241.

Calleja, V., D. Alcor, M. Laguerre, J. Park, B. Vojnovic, B. A. Hemmings, J. Downward, P. J. Parker and B. Larijani (2007). "Intramolecular and intermolecular interactions of protein kinase B define its activation in vivo." PLoS Biol **5**(4): e95.

Carlo, M. I., A. M. Molina, Y. Lakhman, S. Patil, K. Woo, J. DeLuca, C. H. Lee, J. J. Hsieh, D. R. Feldman, R. J. Motzer and M. H. Voss (2016). "A Phase Ib Study of BEZ235, a Dual Inhibitor of Phosphatidylinositol 3-Kinase (PI3K) and Mammalian Target of Rapamycin (mTOR), in Patients With Advanced Renal Cell Carcinoma." Oncologist **21**(7): 787-788.

Carneiro, B. A., J. J. Meeks, T. M. Kuzel, M. Scaranti, S. A. Abdulkadir and F. J. Giles (2015). "Emerging therapeutic targets in bladder cancer." Cancer Treat Rev **41**(2): 170-178.

Chan, D. L., E. Segelov and S. Singh (2017). "Everolimus in the management of metastatic neuroendocrine tumours." Therap Adv Gastroenterol **10**(1): 132-141.

Cheng, S., A. S. Andrew, P. C. Andrews and J. H. Moore (2016). "Complex systems analysis of bladder cancer susceptibility reveals a role for decarboxylase activity in two genome-wide association studies." BioData Min **9**: 40.

Choo, A. Y. and J. Blenis (2009). "Not all substrates are treated equally: implications for mTOR, rapamycin-resistance and cancer therapy." Cell Cycle **8**(4): 567-572.

Chou, T. C. (2006). "Theoretical basis, experimental design, and computerized simulation of synergism and antagonism in drug combination studies." Pharmacol Rev **58**(3): 621-681.

Chou, T. C. (2010). "Drug combination studies and their synergy quantification using the Chou-Talalay method." Cancer Res **70**(2): 440-446.

Comperat, E. M., M. Burger, P. Gontero, A. H. Mostafid, J. Palou, M. Roupret, B. W. G. van Rhijn, S. F. Shariat, R. J. Sylvester, R. Zigeuner and M. Babjuk. (2018, Jan 20). "Grading of Urothelial Carcinoma and The New "World Health Organisation Classification of Tumours of the Urinary System and Male Genital Organs 2016"." Eur Urol Focus 2018/01/26. Retrieved July 9, 2019, from https://doi.org/10.1016/j.euf.2018.01.003.

Copp, J., G. Manning and T. Hunter (2009). "TORC-specific phosphorylation of mammalian target of rapamycin (mTOR): phospho-Ser2481 is a marker for intact mTOR signaling complex 2." Cancer Res **69**(5): 1821-1827.

Costa, C., H. Ebi, M. Martini, S. A. Beausoleil, A. C. Faber, C. T. Jakubik, A. Huang, Y. Wang, M. Nishtala, B. Hall, K. Rikova, J. Zhao, E. Hirsch, C. H. Benes and J. A. Engelman (2015). "Measurement of PIP3 levels reveals an unexpected role for p110beta in early adaptive responses to p110alpha-specific inhibitors in luminal breast cancer." Cancer Cell **27**(1): 97-108.

Courtney, K. D., R. B. Corcoran and J. A. Engelman (2010). "The PI3K pathway as drug target in human cancer." J Clin Oncol **28**(6): 1075-1083.

Cumberbatch, M. G., M. Rota, J. W. Catto and C. La Vecchia (2016). "The Role of Tobacco Smoke in Bladder and Kidney Carcinogenesis: A Comparison of Exposures and Meta-analysis of Incidence and Mortality Risks." Eur Urol **70**(3): 458-466.

Cumberbatch, M. G. K., I. Jubber, P. C. Black, F. Esperto, J. D. Figueroa, A. M. Kamat, L. Kiemeney, Y. Lotan, K. Pang, D. T. Silverman, A. Znaor and J. W. F. Catto (2018). "Epidemiology of Bladder Cancer: A Systematic Review and Contemporary Update of Risk Factors in 2018." Eur Urol **74**(6): 784-795.

da Costa, J. B., E. A. Gibb, T. K. Nykopp, M. Mannas, A. W. Wyatt and P. C. Black. (2018, Dec 8). "Molecular tumor heterogeneity in muscle invasive bladder cancer: Biomarkers, subtypes, and implications for therapy." Urol Oncol 2018/12/12. Retrieved January 28, 2019, from https://doi.org/10.1016/j.urolonc.2018.11.015.

Dahm, P. and J. E. Gschwend (2003). "Malignant non-urothelial neoplasms of the urinary bladder: a review." Eur Urol **44**(6): 672-681.

Datta, S. R., H. Dudek, X. Tao, S. Masters, H. Fu, Y. Gotoh and M. E. Greenberg (1997). "Akt phosphorylation of BAD couples survival signals to the cell-intrinsic death machinery." Cell **91**(2): 231-241.

Dibble, C. C. and L. C. Cantley (2015). "Regulation of mTORC1 by PI3K signaling." Trends Cell Biol **25**(9): 545-555.

Dienstmann, R., J. Rodon, V. Serra and J. Tabernero (2014). "Picking the point of inhibition: a comparative review of PI3K/AKT/mTOR pathway inhibitors." Mol Cancer Ther **13**(5): 1021-1031.

Ding, Z., J. Liang, J. Li, Y. Lu, V. Ariyaratna, Z. Lu, M. A. Davies, J. K. Westwick and G. B. Mills (2010). "Physical association of PDK1 with AKT1 is sufficient for pathway activation independent of membrane localization and phosphatidylinositol 3 kinase." PLoS One **5**(3): e9910.

Engelman, J. A. (2009). "Targeting PI3K signalling in cancer: opportunities, challenges and limitations." Nat Rev Cancer **9**(8): 550-562.

Engelman, J. A., J. Luo and L. C. Cantley (2006). "The evolution of phosphatidylinositol 3-kinases as regulators of growth and metabolism." Nat Rev Genet **7**(8): 606-619.

Fajkovic, H., J. A. Halpern, E. K. Cha, A. Bahadori, T. F. Chromecki, P. I. Karakiewicz, E. Breinl, A. S. Merseburger and S. F. Shariat (2011). "Impact of gender on bladder cancer incidence, staging, and prognosis." World J Urol **29**(4): 457-463.

Fang, Z., J. R. Simard, D. Plenker, H. D. Nguyen, T. Phan, P. Wolle, S. Baumeister and D. Rauh (2015). "Discovery of inter-domain stabilizers-a novel assay system for allosteric akt inhibitors." ACS Chem Biol **10**(1): 279-288.

Fazio, N., R. Buzzoni, E. Baudin, L. Antonuzzo, R. A. Hubner, H. Lahner, D. E. H. WW, M. Raderer, A. Teule, J. Capdevila, S. K. Libutti, M. H. Kulke, M. Shah, D. Dey, S. Turri, P. Aimone, C. Massacesi and C. Verslype (2016). "A Phase II Study of BEZ235 in Patients with Everolimus-resistant, Advanced Pancreatic Neuroendocrine Tumours." Anticancer Res **36**(2): 713-719.

Feldman, M. E., B. Apsel, A. Uotila, R. Loewith, Z. A. Knight, D. Ruggero and K. M. Shokat (2009). "Active-site inhibitors of mTOR target rapamycin-resistant outputs of mTORC1 and mTORC2." PLoS Biol **7**(2): e38.

Fingar, D. C., C. J. Richardson, A. R. Tee, L. Cheatham, C. Tsou and J. Blenis (2004). "mTOR controls cell cycle progression through its cell growth effectors S6K1 and 4E-BP1/eukaryotic translation initiation factor 4E." Mol Cell Biol **24**(1): 200-216.

Franke, T. F. (2008). "PI3K/Akt: getting it right matters." Oncogene **27**(50): 6473-6488.

Franken, N. A., H. M. Rodermond, J. Stap, J. Haveman and C. van Bree (2006). "Clonogenic assay of cells in vitro." Nat Protoc **1**(5): 2315-2319.

Freedman, N. D., D. T. Silverman, A. R. Hollenbeck, A. Schatzkin and C. C. Abnet (2011). "Association between smoking and risk of bladder cancer among men and women." Jama **306**(7): 737-745.

Gallagher, D. J., M. I. Milowsky, S. R. Gerst, N. Ishill, J. Riches, A. Regazzi, M. G. Boyle, A. Trout, A. M. Flaherty and D. F. Bajorin (2010). "Phase II study of sunitinib in patients with metastatic urothelial cancer." J Clin Oncol **28**(8): 1373-1379.

Garcia-Closas, M., Y. Ye, N. Rothman, J. D. Figueroa, N. Malats, C. P. Dinney, N. Chatterjee, L. Prokunina-Olsson, Z. Wang, J. Lin, F. X. Real, K. B. Jacobs, D. Baris, M. Thun, I. De Vivo, D. Albanes, M. P. Purdue, M. Kogevinas, A. M. Kamat, S. P. Lerner, H. B. Grossman, J. Gu, X. Pu, A. Hutchinson, Y. P. Fu, L. Burdett, M. Yeager, W. Tang, A. Tardon, C. Serra, A. Carrato, R. Garcia-Closas, J. Lloreta, A. Johnson, M. Schwenn, M. R. Karagas, A. Schned, G. Andriole, Jr., R. Grubb, 3rd, A. Black, E. J. Jacobs, W. R. Diver, S. M. Gapstur, S. J. Weinstein, J. Virtamo, D. J. Hunter, N. Caporaso, M. T. Landi, J. F. Fraumeni, Jr., D. T. Silverman, S. J. Chanock and X. Wu (2011). "A genome-wide association study of bladder cancer identifies a new susceptibility locus within SLC14A1, a urea transporter gene on chromosome 18q12.3." Hum Mol Genet **20**(21): 4282-4289.

Garcia-Echeverria, C. (2010). "Allosteric and ATP-competitive kinase inhibitors of mTOR for cancer treatment." Bioorg Med Chem Lett **20**(15): 4308-4312.

Gerullis, H., C. Eimer, T. H. Ecke, E. Georgas, C. Freitas, S. Kastenholz, C. Arndt, C. Heusch and T. Otto (2012). "A phase II trial of temsirolimus in second-line metastatic urothelial cancer." Med Oncol **29**(4): 2870-2876.

Ghatalia, P., M. Zibelman, D. M. Geynisman and E. Plimack (2018). "Approved checkpoint inhibitors in bladder cancer: which drug should be used when?" Ther Adv Med Oncol **10**: n.pag.

Glaser, A. P., D. Fantini, A. Shilatifard, E. M. Schaeffer and J. J. Meeks (2017). "The evolving genomic landscape of urothelial carcinoma." Nat Rev Urol **14**(4): 215-229.

Golding, S. E., E. Rosenberg, N. Valerie, I. Hussaini, M. Frigerio, X. F. Cockcroft, W. Y. Chong, M. Hummersone, L. Rigoreau, K. A. Menear, M. J. O'Connor, L. F. Povirk, T. van Meter and K. Valerie (2009). "Improved ATM kinase inhibitor KU-60019 radiosensitizes glioma cells, compromises insulin, AKT and ERK prosurvival signaling, and inhibits migration and invasion." Mol Cancer Ther **8**(10): 2894-2902.

Green, A. S., N. Chapuis, T. T. Maciel, L. Willems, M. Lambert, C. Arnoult, O. Boyer, V. Bardet, S. Park, M. Foretz, B. Viollet, N. Ifrah, F. Dreyfus, O. Hermine, I. C. Moura, C. Lacombe, P. Mayeux, D. Bouscary and J. Tamburini (2010). "The LKB1/AMPK signaling pathway has tumor suppressor activity in acute myeloid leukemia through the repression of mTOR-dependent oncogenic mRNA translation." Blood **116**(20): 4262-4273.

Grivas, P. D., S. Daignault, S. T. Tagawa, D. M. Nanus, W. M. Stadler, R. Dreicer, M. Kohli, D. P. Petrylak, D. J. Vaughn, K. A. Bylow, S. G. Wong, J. L. Sottnik, E. T. Keller, M. Al-Hawary, D. C. Smith and M. Hussain (2014). "Double-blind, randomized, phase 2 trial of maintenance sunitinib versus placebo after response to chemotherapy in patients with advanced urothelial carcinoma." Cancer **120**(5): 692-701.

Guo, J. P., D. Coppola and J. Q. Cheng (2011). "IKBKE protein activates Akt independent of phosphatidylinositol 3-kinase/PDK1/mTORC2 and the pleckstrin homology domain to sustain malignant transformation." J Biol Chem **286**(43): 37389-37398.

Guo, Y., Y. Chekaluk, J. Zhang, J. Du, N. S. Gray, C. L. Wu and D. J. Kwiatkowski (2013). "TSC1 involvement in bladder cancer: diverse effects and therapeutic implications." J Pathol **230**(1): 17-27.

Gupta, A. K., G. J. Cerniglia, R. Mick, M. S. Ahmed, V. J. Bakanauskas, R. J. Muschel and W. G. McKenna (2003). "Radiation sensitization of human cancer cells in vivo by inhibiting the activity of PI3K using LY294002." Int J Radiat Oncol Biol Phys **56**(3): 846-853.

Hahn, N. M., W. M. Stadler, R. T. Zon, D. Waterhouse, J. Picus, S. Nattam, C. S. Johnson, S. M. Perkins, M. J. Waddell and C. J. Sweeney (2011). "Phase II trial of cisplatin, gemcitabine, and bevacizumab as first-line therapy for metastatic urothelial carcinoma: Hoosier Oncology Group GU 04-75." J Clin Oncol **29**(12): 1525-1530.

Haritunians, T., A. Mori, J. O'Kelly, Q. T. Luong, F. J. Giles and H. P. Koeffler (2007). "Antiproliferative activity of RAD001 (everolimus) as a single agent and combined with other agents in mantle cell lymphoma." Leukemia **21**(2): 333-339.

Harrington, L. S., G. M. Findlay, A. Gray, T. Tolkacheva, S. Wigfield, H. Rebholz, J. Barnett, N. R. Leslie, S. Cheng, P. R. Shepherd, I. Gout, C. P. Downes and R. F.

Lamb (2004). "The TSC1-2 tumor suppressor controls insulin-PI3K signaling via regulation of IRS proteins." J Cell Biol **166**(2): 213-223.

Hautmann, R. E., R. C. de Petriconi, C. Pfeiffer and B. G. Volkmer (2012). "Radical cystectomy for urothelial carcinoma of the bladder without neoadjuvant or adjuvant therapy: long-term results in 1100 patients." Eur Urol **61**(5): 1039-1047.

Hirai, H., H. Sootome, Y. Nakatsuru, K. Miyama, S. Taguchi, K. Tsujioka, Y. Ueno, H. Hatch, P. K. Majumder, B. S. Pan and H. Kotani (2010). "MK-2206, an allosteric Akt inhibitor, enhances antitumor efficacy by standard chemotherapeutic agents or molecular targeted drugs in vitro and in vivo." Mol Cancer Ther **9**(7): 1956-1967.

Houede, N. and P. Pourquier (2015). "Targeting the genetic alterations of the PI3K-AKT-mTOR pathway: its potential use in the treatment of bladder cancers." Pharmacol Ther **145**: 1-18.

Hsieh, A. C., Y. Liu, M. P. Edlind, N. T. Ingolia, M. R. Janes, A. Sher, E. Y. Shi, C. R. Stumpf, C. Christensen, M. J. Bonham, S. Wang, P. Ren, M. Martin, K. Jessen, M. E. Feldman, J. S. Weissman, K. M. Shokat, C. Rommel and D. Ruggero (2012). "The translational landscape of mTOR signalling steers cancer initiation and metastasis." Nature **485**(7396): 55-61.

Huck, B. R. and I. Mochalkin (2017). "Recent progress towards clinically relevant ATP-competitive Akt inhibitors." Bioorg Med Chem Lett **27**(13): 2838-2848.

Humphrey, P. A., H. Moch, A. L. Cubilla, T. M. Ulbright and V. E. Reuter (2016). "The 2016 WHO Classification of Tumours of the Urinary System and Male Genital Organs-Part B: Prostate and Bladder Tumours." Eur Urol **70**(1): 106-119.

Hussain, M., S. Daignault, N. Agarwal, P. D. Grivas, A. O. Siefker-Radtke, I. Puzanov, G. R. MacVicar, E. G. Levine, S. Srinivas, P. Twardowski, M. A. Eisenberger, D. I. Quinn, U. N. Vaishampayan, E. Y. Yu, S. Dawsey, K. C. Day, M. L. Day, M. Al-Hawary and D. C. Smith (2014). "A randomized phase 2 trial of gemcitabine/cisplatin with or without cetuximab in patients with advanced urothelial carcinoma." Cancer **120**(17): 2684-2693.

Inamura, K. (2018). "Bladder Cancer: New Insights into Its Molecular Pathology." Cancers (Basel) **10**(4).

Iyer, G., A. J. Hanrahan, M. I. Milowsky, H. Al-Ahmadie, S. N. Scott, M. Janakiraman, M. Pirun, C. Sander, N. D. Socci, I. Ostrovnaya, A. Viale, A. Heguy, L. Peng, T. A. Chan, B. Bochner, D. F. Bajorin, M. F. Berger, B. S. Taylor and D. B. Solit (2012). "Genome sequencing identifies a basis for everolimus sensitivity." Science **338**(6104): 221.

Iyer, G. and J. E. Rosenberg (2018). "Novel therapies in urothelial carcinoma: a biomarker-driven approach." Ann Oncol **29**(12): 2302-2312.

Iyer, G., C. M. Tully, I. R. Garcia-Grossman, S. N. Scott, M. E. Boyd, A. S. McCoy, M. F. Berger, H. Al-Ahmadie, D. B. Solit, J. E. Rosenberg and D. F. Bajorin (2015). "Phase 2 study of the pan-isoform PI3 kinase inhibitor BKM120 in metastatic urothelial carcinoma patients." Journal of Clinical Oncology **33**(7_suppl): 324-324.

Jones, R. J., S. A. Hussain, A. S. Protheroe, A. Birtle, P. Chakraborti, R. A. Huddart, S. Jagdev, A. Bahl, A. Stockdale, S. Sundar, S. J. Crabb, J. Dixon-Hughes, L. Alexander, A. Morris, C. Kelly, J. Stobo, J. Paul and T. Powles (2017). "Randomized Phase II Study Investigating Pazopanib Versus Weekly Paclitaxel in Relapsed or Progressive Urothelial Cancer." J Clin Oncol: Jco2016707828.

Kang, S. A., M. E. Pacold, C. L. Cervantes, D. Lim, H. J. Lou, K. Ottina, N. S. Gray, B. E. Turk, M. B. Yaffe and D. M. Sabatini (2013). "mTORC1 phosphorylation sites encode their sensitivity to starvation and rapamycin." Science **341**(6144): 1236566.

Khan, K. H., T. A. Yap, L. Yan and D. Cunningham (2013). "Targeting the PI3K-AKT-mTOR signaling network in cancer." Chin J Cancer **32**(5): 253-265.

Knight, Z. A. (2011). "For a PDK1 inhibitor, the substrate matters." Biochem J **433**(2): e1-2.

Knight, Z. A., B. Gonzalez, M. E. Feldman, E. R. Zunder, D. D. Goldenberg, O. Williams, R. Loewith, D. Stokoe, A. Balla, B. Toth, T. Balla, W. A. Weiss, R. L. Williams and K. M. Shokat (2006). "A pharmacological map of the PI3-K family defines a role for p110alpha in insulin signaling." Cell **125**(4): 733-747.

Knowles, M. A. and C. D. Hurst (2015). "Molecular biology of bladder cancer: new insights into pathogenesis and clinical diversity." Nat Rev Cancer **15**(1): 25-41.

Koch-Institut, R. (2017). Krebs in Deutschland für 2013/2014. Berlin, Robert Koch-Institut. **11**.

Kyou Kwon, J., S. J. Kim, J. Hoon Kim, K. Mee Lee and I. Ho Chang (2014). "Dual inhibition by S6K1 and Elf4E is essential for controlling cellular growth and invasion in bladder cancer." Urol Oncol **32**(1): 51.e27-35.

Laplante, M. and D. M. Sabatini (2009). "mTOR signaling at a glance." J Cell Sci **122**(Pt 20): 3589-3594.

Laplante, M. and D. M. Sabatini (2012). "mTOR Signaling." Cold Spring Harb Perspect Biol **4**(2).

Laplante, M. and D. M. Sabatini (2012). "mTOR signaling in growth control and disease." Cell **149**(2): 274-293.

Leahy, J. J., B. T. Golding, R. J. Griffin, I. R. Hardcastle, C. Richardson, L. Rigoreau and G. C. Smith (2004). "Identification of a highly potent and selective DNA-dependent protein kinase (DNA-PK) inhibitor (NU7441) by screening of chromenone libraries." Bioorg Med Chem Lett **14**(24): 6083-6087.

Lheureux, S., C. Denoyelle, P. S. Ohashi, J. S. De Bono and F. M. Mottaghy (2017). "Molecularly targeted therapies in cancer: a guide for the nuclear medicine physician." Eur J Nucl Med Mol Imaging **44**(Suppl 1): 41-54.

Li, C., P. Xin, H. Xiao, Y. Zheng, Y. Huang and X. Zhu (2015). "The dual PI3K/mTOR inhibitor NVP-BEZ235 inhibits proliferation and induces apoptosis of burkitt lymphoma cells." Cancer Cell Int **15**: 65.

Li, J., S. G. Kim and J. Blenis (2014). "Rapamycin: one drug, many effects." Cell Metab **19**(3): 373-379.

Lim, H. J., P. Crowe and J. L. Yang (2015). "Current clinical regulation of PI3K/PTEN/Akt/mTOR signalling in treatment of human cancer." J Cancer Res Clin Oncol **141**(4): 671-689.

Liu, P., W. Gan, Y. R. Chin, K. Ogura, J. Guo, J. Zhang, B. Wang, J. Blenis, L. C. Cantley, A. Toker, B. Su and W. Wei (2015). "PtdIns(3,4,5)P3-Dependent Activation of the mTORC2 Kinase Complex." Cancer Discov **5**(11): 1194-1209.

Liu, Q., C. Thoreen, J. Wang, D. Sabatini and N. S. Gray (2009). "mTOR Mediated Anti-Cancer Drug Discovery." Drug Discov Today Ther Strateg **6**(2): 47-55.

Liu, T. J., D. Koul, T. LaFortune, N. Tiao, R. J. Shen, S. M. Maira, C. Garcia-Echevrria and W. K. Yung (2009). "NVP-BEZ235, a novel dual phosphatidylinositol 3-kinase/mammalian target of rapamycin inhibitor, elicits multifaceted antitumor activities in human gliomas." Mol Cancer Ther **8**(8): 2204-2210.

Lonetti, A., A. Cappellini, A. M. Sparta, F. Chiarini, F. Buontempo, C. Evangelisti, C. Evangelisti, E. Orsini, J. A. McCubrey and A. M. Martelli (2015). "PI3K pan-inhibition impairs more efficiently proliferation and survival of T-cell acute lymphoblastic leukemia cell lines when compared to isoform-selective PI3K inhibitors." Oncotarget **6**(12): 10399-10414.

Ma, B. B., V. W. Lui, C. W. Hui, C. P. Lau, C. H. Wong, E. P. Hui, M. H. Ng, S. H. Cheng, S. W. Tsao, C. M. Tsang, C. S. Cheung, K. Ho and A. T. Chan (2014). "Preclinical evaluation of the mTOR-PI3K inhibitor BEZ235 in nasopharyngeal cancer models." Cancer Lett **343**(1): 24-32.

Ma, X. M. and J. Blenis (2009). "Molecular mechanisms of mTOR-mediated translational control." Nat Rev Mol Cell Biol **10**(5): 307-318.

Maira, S. M., F. Stauffer, J. Brueggen, P. Furet, C. Schnell, C. Fritsch, S. Brachmann, P. Chene, A. De Pover, K. Schoemaker, D. Fabbro, D. Gabriel, M. Simonen, L. Murphy, P. Finan, W. Sellers and C. Garcia-Echeverria (2008). "Identification and characterization of NVP-BEZ235, a new orally available dual phosphatidylinositol 3-kinase/mammalian target of rapamycin inhibitor with potent in vivo antitumor activity." Mol Cancer Ther **7**(7): 1851-1863.

Mamane, Y., E. Petroulakis, O. LeBacquer and N. Sonenberg (2006). "mTOR, translation initiation and cancer." Oncogene **25**(48): 6416-6422.

Martini, M., M. C. De Santis, L. Braccini, F. Gulluni and E. Hirsch (2014). "PI3K/AKT signaling pathway and cancer: an updated review." Ann Med **46**(6): 372-383.

Mayer, I. A. and C. L. Arteaga (2016). "The PI3K/AKT Pathway as a Target for Cancer Treatment." Annu Rev Med **67**: 11-28.

Mi, W., Q. Ye, S. Liu and Q. B. She (2015). "AKT inhibition overcomes rapamycin resistance by enhancing the repressive function of PRAS40 on mTORC1/4E-BP1 axis." Oncotarget **6**(16): 13962-13977.

Milowsky, M. I., G. Iyer, A. M. Regazzi, H. Al-Ahmadie, S. R. Gerst, I. Ostrovnaya, L. L. Gellert, R. Kaplan, I. R. Garcia-Grossman, D. Pendse, A. V. Balar, A. M. Flaherty, A. Trout, D. B. Solit and D. F. Bajorin (2013). "Phase II study of everolimus in metastatic urothelial cancer." BJU Int **112**(4): 462-470.

Mukherjee, B., N. Tomimatsu, K. Amancherla, C. V. Camacho, N. Pichamoorthy and S. Burma (2012). "The dual PI3K/mTOR inhibitor NVP-BEZ235 is a potent inhibitor of ATM- and DNA-PKCs-mediated DNA damage responses." Neoplasia **14**(1): 34-43.

Munster, P., R. Aggarwal, D. Hong, J. H. Schellens, R. van der Noll, J. Specht, P. O. Witteveen, T. L. Werner, E. C. Dees, E. Bergsland, N. Agarwal, J. F. Kleha, M. Durante, L. Adams, D. A. Smith, T. A. Lampkin, S. R. Morris and R. Kurzrock (2016). "First-in-Human Phase I Study of GSK2126458, an Oral Pan-Class I Phosphatidylinositol-3-Kinase Inhibitor, in Patients with Advanced Solid Tumor Malignancies." Clin Cancer Res **22**(8): 1932-1939.

Musa, J., M. F. Orth, M. Dallmayer, M. Baldauf, C. Pardo, B. Rotblat, T. Kirchner, G. Leprivier and T. G. Grunewald (2016). "Eukaryotic initiation factor 4E-binding protein 1 (4E-BP1): a master regulator of mRNA translation involved in tumorigenesis." Oncogene **35**(36): 4675-4688.

Najafov, A., N. Shpiro and D. R. Alessi (2012). "Akt is efficiently activated by PIF-pocket- and PtdIns(3,4,5)P3-dependent mechanisms leading to resistance to PDK1 inhibitors." Biochem J **448**(2): 285-295.

Najafov, A., E. M. Sommer, J. M. Axten, M. P. Deyoung and D. R. Alessi (2011). "Characterization of GSK2334470, a novel and highly specific inhibitor of PDK1." Biochem J **433**(2): 357-369.

Nawroth, R., F. Stellwagen, W. A. Schulz, R. Stoehr, A. Hartmann, B. J. Krause, J. E. Gschwend and M. Retz (2011). "S6K1 and 4E-BP1 are independent regulated and control cellular growth in bladder cancer." PLoS One **6**(11): e27509.

Ni, J., S. H. Ramkissoon, S. Xie, S. Goel, D. G. Stover, H. Guo, V. Luu, E. Marco, L. A. Ramkissoon, Y. J. Kang, M. Hayashi, Q. D. Nguyen, A. H. Ligon, R. Du, E. B. Claus, B. M. Alexander, G. C. Yuan, Z. C. Wang, J. D. Iglehart, I. E. Krop, T. M. Roberts, E. P. Winer, N. U. Lin, K. L. Ligon and J. J. Zhao (2016). "Combination inhibition of PI3K and mTORC1 yields durable remissions in mice bearing orthotopic patient-derived xenografts of HER2-positive breast cancer brain metastases." Nat Med **22**(7): 723-726.

Niegisch, G., M. Retz, M. Thalgott, S. Balabanov, F. Honecker, C. H. Ohlmann, M. Stockle, M. Bogemann, F. Vom Dorp, J. Gschwend, A. Hartmann, C. Ohmann and P. Albers (2015). "Second-Line Treatment of Advanced Urothelial Cancer with Paclitaxel and Everolimus in a German Phase II Trial (AUO Trial AB 35/09)." Oncology **89**(2): 70-78.

Ning, Y. M., D. Suzman, V. E. Maher, L. Zhang, S. Tang, T. Ricks, T. Palmby, W. Fu, Q. Liu, K. B. Goldberg, G. Kim and R. Pazdur (2017). "FDA Approval Summary: Atezolizumab for the Treatment of Patients with Progressive Advanced Urothelial Carcinoma after Platinum-Containing Chemotherapy." Oncologist **22**(6): 743-749.

Nojima, H., C. Tokunaga, S. Eguchi, N. Oshiro, S. Hidayat, K. Yoshino, K. Hara, N. Tanaka, J. Avruch and K. Yonezawa (2003). "The mammalian target of rapamycin (mTOR) partner, raptor, binds the mTOR substrates p70 S6 kinase and 4E-BP1 through their TOR signaling (TOS) motif." J Biol Chem **278**(18): 15461-15464.

O'Reilly, K. E., F. Rojo, Q. B. She, D. Solit, G. B. Mills, D. Smith, H. Lane, F. Hofmann, D. J. Hicklin, D. L. Ludwig, J. Baselga and N. Rosen (2006). "mTOR inhibition induces upstream receptor tyrosine kinase signaling and activates Akt." Cancer Res **66**(3): 1500-1508.

Oeyen, E., L. Hoekx, S. De Wachter, M. Baldewijns, F. Ameye and I. Mertens (2019). "Bladder Cancer Diagnosis and Follow-Up: The Current Status and Possible Role of Extracellular Vesicles." Int J Mol Sci **20**(4).

Ortiz, T., S. Lopez, M. A. Burguillos, A. Edreira and J. Pinero (2004). "Radiosensitizer effect of wortmannin in radioresistant bladder tumoral cell lines." Int J Oncol **24**(1): 169-175.

Oshiro, N., R. Takahashi, K. Yoshino, K. Tanimura, A. Nakashima, S. Eguchi, T. Miyamoto, K. Hara, K. Takehana, J. Avruch, U. Kikkawa and K. Yonezawa (2007). "The proline-rich Akt substrate of 40 kDa (PRAS40) is a physiological substrate of mammalian target of rapamycin complex 1." J Biol Chem **282**(28): 20329-20339.

Oudard, S., S. Culine, Y. Vano, F. Goldwasser, C. Theodore, T. Nguyen, E. Voog, E. Banu, A. Vieillefond, F. Priou, G. Deplanque, G. Gravis, A. Ravaud, J. M. Vannetzel, J. P. Machiels, X. Muracciole, M. F. Pichon, J. O. Bay, R. Elaidi, C. Teghom, F. Radvanyi and P. Beuzeboc (2015). "Multicentre randomised phase II trial of gemcitabine+platinum, with or without trastuzumab, in advanced or metastatic urothelial carcinoma overexpressing Her2." Eur J Cancer **51**(1): 45-54.

Paner, G. P., R. Montironi and M. B. Amin (2017). "Challenges in Pathologic Staging of Bladder Cancer: Proposals for Fresh Approaches of Assessing Pathologic Stage in Light of Recent Studies and Observations Pertaining to Bladder Histoanatomic Variances." Adv Anat Pathol **24**(3): 113-127.

Petrylak, D. P., S. T. Tagawa, M. Kohli, A. Eisen, C. Canil, S. S. Sridhar, A. Spira, E. Y. Yu, J. M. Burke, D. Shaffer, C. X. Pan, J. J. Kim, J. B. Aragon-Ching, D. I. Quinn, N. J. Vogelzang, S. Tang, H. Zhang, C. T. Cavanaugh, L. Gao, J. S. Kauh, R. A. Walgren and K. N. Chi (2016). "Docetaxel As Monotherapy or Combined With Ramucirumab or Icrucumab in Second-Line Treatment for Locally Advanced or Metastatic Urothelial Carcinoma: An Open-Label, Three-Arm, Randomized Controlled Phase II Trial." J Clin Oncol **34**(13): 1500-1509.

Philips, G. K., S. Halabi, B. L. Sanford, D. Bajorin and E. J. Small (2008). "A phase II trial of cisplatin, fixed dose-rate gemcitabine and gefitinib for advanced urothelial tract carcinoma: results of the Cancer and Leukaemia Group B 90102." BJU Int **101**(1): 20-25.

Pons, B., G. Armengol, M. Livingstone, L. Lopez, L. Coch, N. Sonenberg and S. Ramon y Cajal (2012). "Association between LRRK2 and 4E-BP1 protein levels in normal and malignant cells." Oncol Rep **27**(1): 225-231.

Powles, T., I. Duran, M. S. van der Heijden, Y. Loriot, N. J. Vogelzang, U. De Giorgi, S. Oudard, M. M. Retz, D. Castellano, A. Bamias, A. Flechon, G. Gravis, S. Hussain, T. Takano, N. Leng, E. E. Kadel, 3rd, R. Banchereau, P. S. Hegde, S. Mariathasan, N. Cui, X. Shen, C. L. Derleth, M. C. Green and A. Ravaud (2018). "Atezolizumab versus chemotherapy in patients with platinum-treated locally advanced or metastatic urothelial carcinoma (IMvigor211): a multicentre, open-label, phase 3 randomised controlled trial." Lancet **391**(10122): 748-757.

Powles, T., R. A. Huddart, T. Elliott, S. J. Sarker, C. Ackerman, R. Jones, S. Hussain, S. Crabb, S. Jagdev, J. Chester, S. Hilman, M. Beresford, G. Macdonald, S. Santhanam, J. A. Frew, A. Stockdale, S. Hughes, D. Berney and S. Chowdhury (2017). "Phase III, Double-Blind, Randomized Trial That Compared Maintenance Lapatinib Versus Placebo After First-Line Chemotherapy in Patients With Human Epidermal Growth Factor Receptor 1/2-Positive Metastatic Bladder Cancer." J Clin Oncol **35**(1): 48-55.

Pretre, V. and A. Wicki (2018). "Inhibition of Akt and other AGC kinases: A target for clinical cancer therapy?" Semin Cancer Biol **48**: 70-77.

Pulido, M., G. Roubaud, A. L. Cazeau, H. Mahammedi, L. Vedrine, F. Joly, L. Mourey, C. Pfister, A. Goberna, B. Lortal, C. Bellera, P. Pourquier and N. Houede (2018). "Safety and efficacy of temsirolimus as second line treatment for patients with recurrent bladder cancer." BMC Cancer **18**(1): 194.

Robertson, A. G., J. Kim, H. Al-Ahmadie, J. Bellmunt, G. Guo, A. D. Cherniack, T. Hinoue, P. W. Laird, K. A. Hoadley, R. Akbani, M. A. A. Castro, E. A. Gibb, R. S. Kanchi, D. A. Gordenin, S. A. Shukla, F. Sanchez-Vega, D. E. Hansel, B. A. Czerniak, V. E. Reuter, X. Su, B. de Sa Carvalho, V. S. Chagas, K. L. Mungall, S. Sadeghi, C. S. Pedamallu, Y. Lu, L. J. Klimczak, J. Zhang, C. Choo, A. I. Ojesina, S. Bullman, K. M. Leraas, T. M. Lichtenberg, C. J. Wu, N. Schultz, G. Getz, M. Meyerson, G. B. Mills, D. J. McConkey, J. N. Weinstein, D. J. Kwiatkowski and S. P. Lerner (2017). "Comprehensive Molecular Characterization of Muscle-Invasive Bladder Cancer." Cell **171**(3): 540-556.e525.

Rodriguez-Vida, A., S. P. Lerner and J. Bellmunt (2018). "The Cancer Genome Atlas Project in Bladder Cancer." Cancer Treat Res **175**: 259-271.

Rodrik-Outmezguine, V. S., S. Chandarlapaty, N. C. Pagano, P. I. Poulikakos, M. Scaltriti, E. Moskatel, J. Baselga, S. Guichard and N. Rosen (2011). "mTOR kinase inhibition causes feedback-dependent biphasic regulation of AKT signaling." Cancer Discov **1**(3): 248-259.

Rosenberg, J. E., P. R. Carroll and E. J. Small (2005). "Update on chemotherapy for advanced bladder cancer." J Urol **174**(1): 14-20.

Rosenberg, J. E., J. Hoffman-Censits, T. Powles, M. S. van der Heijden, A. V. Balar, A. Necchi, N. Dawson, P. H. O'Donnell, A. Balmanoukian, Y. Loriot, S. Srinivas, M. M. Retz, P. Grivas, R. W. Joseph, M. D. Galsky, M. T. Fleming, D. P. Petrylak, J. L. Perez-Gracia, H. A. Burris, D. Castellano, C. Canil, J. Bellmunt, D. Bajorin, D. Nickles, R. Bourgon, G. M. Frampton, N. Cui, S. Mariathasan, O. Abidoye, G. D. Fine and R. Dreicer (2016). "Atezolizumab in patients with locally advanced and metastatic urothelial carcinoma who have progressed following treatment with

platinum-based chemotherapy: a single-arm, multicentre, phase 2 trial." Lancet **387**(10031): 1909-1920.

Ross, J. S., K. Wang, D. Khaira, S. M. Ali, H. A. Fisher, B. Mian, T. Nazeer, J. A. Elvin, N. Palma, R. Yelensky, D. Lipson, V. A. Miller, P. J. Stephens, V. Subbiah and S. K. Pal (2016). "Comprehensive genomic profiling of 295 cases of clinically advanced urothelial carcinoma of the urinary bladder reveals a high frequency of clinically relevant genomic alterations." Cancer **122**(5): 702-711.

Salazar, R., R. Garcia-Carbonero, S. K. Libutti, A. E. Hendifar, A. Custodio, R. Guimbaud, C. Lombard-Bohas, S. Ricci, H. J. Klumpen, J. Capdevila, N. Reed, A. Walenkamp, E. Grande, S. Safina, T. Meyer, O. Kong, H. Salomon, R. Tavorath and J. C. Yao (2018). "Phase II Study of BEZ235 versus Everolimus in Patients with Mammalian Target of Rapamycin Inhibitor-Naive Advanced Pancreatic Neuroendocrine Tumors." Oncologist **23**(7): 766-e790.

Sanli, O., J. Dobruch, M. A. Knowles, M. Burger, M. Alemozaffar, M. E. Nielsen and Y. Lotan (2017). "Bladder cancer." Nat Rev Dis Primers **3**: 17022.

Santiskulvong, C., G. E. Konecny, M. Fekete, K. Y. Chen, A. Karam, D. Mulholland, C. Eng, H. Wu, M. Song and O. Dorigo (2011). "Dual targeting of phosphoinositide 3-kinase and mammalian target of rapamycin using NVP-BEZ235 as a novel therapeutic approach in human ovarian carcinoma." Clin Cancer Res **17**(8): 2373-2384.

Sathe, A., G. Chalaud, I. Oppolzer, K. Y. Wong, M. von Busch, S. C. Schmid, Z. Tong, M. Retz, J. E. Gschwend, W. A. Schulz and R. Nawroth (2018). "Parallel PI3K, AKT and mTOR inhibition is required to control feedback loops that limit tumor therapy." PLoS One **13**(1): e0190854.

Sathe, A., F. Guerth, M. V. Cronauer, M. M. Heck, M. Thalgott, J. E. Gschwend, M. Retz and R. Nawroth (2014). "Mutant PIK3CA controls DUSP1-dependent ERK 1/2 activity to confer response to AKT target therapy." Br J Cancer **111**(11): 2103-2113.

Sathe, A. and R. Nawroth (2018). "Targeting the PI3K/AKT/mTOR Pathway in Bladder Cancer." Methods Mol Biol **1655**: 335-350.

Saxton, R. A. and D. M. Sabatini (2017). "mTOR Signaling in Growth, Metabolism, and Disease." Cell **168**(6): 960-976.

Schalm, S. S., D. C. Fingar, D. M. Sabatini and J. Blenis (2003). "TOS motif-mediated raptor binding regulates 4E-BP1 multisite phosphorylation and function." Curr Biol **13**(10): 797-806.

Seront, E., S. Rottey, B. Filleul, P. Glorieux, J. C. Goeminne, V. Verschaeve, J. M. Vandenbulcke, B. Sautois, P. Boegner, A. Gillain, A. van Maanen and J. P. Machiels (2016). "Phase II study of dual phosphoinositol-3-kinase (PI3K) and mammalian target of rapamycin (mTOR) inhibitor BEZ235 in patients with locally advanced or metastatic transitional cell carcinoma." BJU Int **118**(3): 408-415.

Seront, E., S. Rottey, B. Sautois, J. Kerger, L. A. D'Hondt, V. Verschaeve, J. L. Canon, C. Dopchie, J. M. Vandenbulcke, N. Whenham, J. C. Goeminne, M. Clausse, D. Verhoeven, P. Glorieux, S. Branders, P. Dupont, J. Schoonjans, O. Feron and J.

P. Machiels (2012). "Phase II study of everolimus in patients with locally advanced or metastatic transitional cell carcinoma of the urothelial tract: clinical activity, molecular response, and biomarkers." Ann Oncol **23**(10): 2663-2670.

Serra, V., B. Markman, M. Scaltriti, P. J. Eichhorn, V. Valero, M. Guzman, M. L. Botero, E. Llonch, F. Atzori, S. Di Cosimo, M. Maira, C. Garcia-Echeverria, J. L. Parra, J. Arribas and J. Baselga (2008). "NVP-BEZ235, a dual PI3K/mTOR inhibitor, prevents PI3K signaling and inhibits the growth of cancer cells with activating PI3K mutations." Cancer Res **68**(19): 8022-8030.

Sharma, P., M. Retz, A. Siefker-Radtke, A. Baron, A. Necchi, J. Bedke, E. R. Plimack, D. Vaena, M. O. Grimm, S. Bracarda, J. A. Arranz, S. Pal, C. Ohyama, A. Saci, X. Qu, A. Lambert, S. Krishnan, A. Azrilevich and M. D. Galsky (2017). "Nivolumab in metastatic urothelial carcinoma after platinum therapy (CheckMate 275): a multicentre, single-arm, phase 2 trial." Lancet Oncol **18**(3): 312-322.

Shoji, K., K. Oda, T. Kashiyama, Y. Ikeda, S. Nakagawa, K. Sone, Y. Miyamoto, H. Hiraike, M. Tanikawa, A. Miyasaka, T. Koso, Y. Matsumoto, O. Wada-Hiraike, K. Kawana, H. Kuramoto, F. McCormick, H. Aburatani, T. Yano, S. Kozuma and Y. Taketani (2012). "Genotype-dependent efficacy of a dual PI3K/mTOR inhibitor, NVP-BEZ235, and an mTOR inhibitor, RAD001, in endometrial carcinomas." PLoS One **7**(5): e37431.

Siegel, R. L., K. D. Miller and A. Jemal (2019). "Cancer statistics, 2019." CA Cancer J Clin **69**(1): 7-34.

Sievert, K. D., B. Amend, U. Nagele, D. Schilling, J. Bedke, M. Horstmann, J. Hennenlotter, S. Kruck and A. Stenzl (2009). "Economic aspects of bladder cancer: what are the benefits and costs?" World J Urol **27**(3): 295-300.

Smith, A. B., A. M. Deal, M. E. Woods, E. M. Wallen, R. S. Pruthi, R. C. Chen, M. I. Milowsky and M. E. Nielsen (2014). "Muscle-invasive bladder cancer: evaluating treatment and survival in the National Cancer Data Base." BJU Int **114**(5): 719-726.

Solomon, J. P. and D. E. Hansel (2016). "The Emerging Molecular Landscape of Urothelial Carcinoma." Surg Pathol Clin **9**(3): 391-404.

Sun, D., A. Sawada, M. Nakashima, T. Kobayashi, O. Ogawa and Y. Matsui (2015). "MK2206 potentiates cisplatin-induced cytotoxicity and apoptosis through an interaction of inactivated Akt signaling pathway." Urol Oncol **33**(3): 111.e117-126.

Taylor, C. F., F. M. Platt, C. D. Hurst, H. H. Thygesen and M. A. Knowles (2014). "Frequent inactivating mutations of STAG2 in bladder cancer are associated with low tumour grade and stage and inversely related to chromosomal copy number changes." Hum Mol Genet **23**(8): 1964-1974.

TCGA (2014). "Comprehensive molecular characterization of urothelial bladder carcinoma." Nature **507**(7492): 315-322.

TCGA, C. G. A. R. N. (2014). "Comprehensive molecular characterization of urothelial bladder carcinoma." Nature **507**(7492): 315-322.

Thoreen, C. C., S. A. Kang, J. W. Chang, Q. Liu, J. Zhang, Y. Gao, L. J. Reichling, T. Sim, D. M. Sabatini and N. S. Gray (2009). "An ATP-competitive mammalian target of rapamycin inhibitor reveals rapamycin-resistant functions of mTORC1." J Biol Chem **284**(12): 8023-8032.

Tripathi, A. and E. R. Plimack (2018). "Immunotherapy for Urothelial Carcinoma: Current Evidence and Future Directions." Curr Urol Rep **19**(12): 109.

Vanhaesebroeck, B., J. Guillermet-Guibert, M. Graupera and B. Bilanges (2010). "The emerging mechanisms of isoform-specific PI3K signalling." Nat Rev Mol Cell Biol **11**(5): 329-341.

Vanhaesebroeck, B., L. Stephens and P. Hawkins (2012). "PI3K signalling: the path to discovery and understanding." Nat Rev Mol Cell Biol **13**(3): 195-203.

Volanis, D., T. Kadiyska, A. Galanis, D. Delakas, S. Logotheti and V. Zoumpourlis (2010). "Environmental factors and genetic susceptibility promote urinary bladder cancer." Toxicol Lett **193**(2): 131-137.

von der Maase, H., L. Sengelov, J. T. Roberts, S. Ricci, L. Dogliotti, T. Oliver, M. J. Moore, A. Zimmermann and M. Arning (2005). "Long-term survival results of a randomized trial comparing gemcitabine plus cisplatin, with methotrexate, vinblastine, doxorubicin, plus cisplatin in patients with bladder cancer." J Clin Oncol **23**(21): 4602-4608.

Wagle, N., B. C. Grabiner, E. M. Van Allen, E. Hodis, S. Jacobus, J. G. Supko, M. Stewart, T. K. Choueiri, L. Gandhi, J. M. Cleary, A. A. Elfiky, M. E. Taplin, E. C. Stack, S. Signoretti, M. Loda, G. I. Shapiro, D. M. Sabatini, E. S. Lander, S. B. Gabriel, P. W. Kantoff, L. A. Garraway and J. E. Rosenberg (2014). "Activating mTOR mutations in a patient with an extraordinary response on a phase I trial of everolimus and pazopanib." Cancer Discov **4**(5): 546-553.

Wainberg, Z. A., M. Alsina, H. P. Soares, I. Brana, C. D. Britten, G. Del Conte, P. Ezeh, B. Houk, K. A. Kern, S. Leong, N. Pathan, K. J. Pierce, L. L. Siu, J. Vermette and J. Tabernero (2017). "A Multi-Arm Phase I Study of the PI3K/mTOR Inhibitors PF-04691502 and Gedatolisib (PF-05212384) plus Irinotecan or the MEK Inhibitor PD-0325901 in Advanced Cancer." Target Oncol **12**(6): 775-785.

Wang, J., C. Zhong, F. Wang, F. Qu and J. Ding (2013). "Crystal structures of S6K1 provide insights into the regulation mechanism of S6K1 by the hydrophobic motif." Biochem J **454**(1): 39-47.

Wang, L., T. E. Harris, R. A. Roth and J. C. Lawrence, Jr. (2007). "PRAS40 regulates mTORC1 kinase activity by functioning as a direct inhibitor of substrate binding." J Biol Chem **282**(27): 20036-20044.

Wicki, A., N. Brown, A. Xyrafas, V. Bize, H. Hawle, S. Berardi, N. Cmiljanovic, V. Cmiljanovic, M. Stumm, S. Dimitrijevic, R. Herrmann, V. Pretre, R. Ritschard, A. Tzankov, V. Hess, A. Childs, C. Hierro, J. Rodon, D. Hess, M. Joerger, R. von Moos, C. Sessa and R. Kristeleit (2018). "First-in human, phase 1, dose-escalation pharmacokinetic and pharmacodynamic study of the oral dual PI3K and mTORC1/2 inhibitor PQR309 in patients with advanced solid tumors (SAKK 67/13)." Eur J Cancer **96**: 6-16.

Witjes, J. A., E. Comperat, N. C. Cowan, M. De Santis, G. Gakis, T. Lebret, M. J. Ribal, A. G. Van der Heijden and A. Sherif (2014). "EAU guidelines on muscle-invasive and metastatic bladder cancer: summary of the 2013 guidelines." Eur Urol **65**(4): 778-792.

Witjes, J. A., T. Lebret, E. M. Comperat, N. C. Cowan, M. De Santis, H. M. Bruins, V. Hernandez, E. L. Espinos, J. Dunn, M. Rouanne, Y. Neuzillet, E. Veskimae, A. G. van der Heijden, G. Gakis and M. J. Ribal (2017). "Updated 2016 EAU Guidelines on Muscle-invasive and Metastatic Bladder Cancer." Eur Urol **71**(3): 462-475.

Wu, D., J. Tao, B. Xu, W. Qing, P. Li, Q. Lu and W. Zhang (2011). "Phosphatidylinositol 3-kinase inhibitor LY294002 suppresses proliferation and sensitizes doxorubicin chemotherapy in bladder cancer cells." Urol Int **86**(3): 346-354.

Xie, X., D. Zhang, B. Zhao, M. K. Lu, M. You, G. Condorelli, C. Y. Wang and K. L. Guan (2011). "IkappaB kinase epsilon and TANK-binding kinase 1 activate AKT by direct phosphorylation." Proc Natl Acad Sci U S A **108**(16): 6474-6479.

Yang, C., X. Huang, H. Liu, F. Xiao, J. Wei, L. You and W. Qian (2017). "PDK1 inhibitor GSK2334470 exerts antitumor activity in multiple myeloma and forms a novel multitargeted combination with dual mTORC1/C2 inhibitor PP242." Oncotarget **8**(24): 39185-39197.

Yang, D. Q. and M. B. Kastan (2000). "Participation of ATM in insulin signalling through phosphorylation of eIF-4E-binding protein 1." Nat Cell Biol **2**(12): 893-898.

Yang, E., J. Zha, J. Jockel, L. H. Boise, C. B. Thompson and S. J. Korsmeyer (1995). "Bad, a heterodimeric partner for Bcl-XL and Bcl-2, displaces Bax and promotes cell death." Cell **80**(2): 285-291.

Yang, H., D. G. Rudge, J. D. Koos, B. Vaidialingam, H. J. Yang and N. P. Pavletich (2013). "mTOR kinase structure, mechanism and regulation." Nature **497**(7448): 217-223.

Yee, D. S., N. M. Ishill, W. T. Lowrance, H. W. Herr and E. B. Elkin (2011). "Ethnic differences in bladder cancer survival." Urology **78**(3): 544-549.

Yu, Z., G. Xie, G. Zhou, Y. Cheng, G. Zhang, G. Yao, Y. Chen, Y. Li and G. Zhao (2015). "NVP-BEZ235, a novel dual PI3K-mTOR inhibitor displays anti-glioma activity and reduces chemoresistance to temozolomide in human glioma cells." Cancer Lett **367**(1): 58-68.

Zaytseva, Y. Y., J. D. Valentino, P. Gulhati and B. M. Evers (2012). "mTOR inhibitors in cancer therapy." Cancer Lett **319**(1): 1-7.

Zhang, Y. and X. F. Zheng (2012). "mTOR-independent 4E-BP1 phosphorylation is associated with cancer resistance to mTOR kinase inhibitors." Cell Cycle **11**(3): 594-603.

Zhao, W., Y. Qiu and D. Kong (2017). "Class I phosphatidylinositol 3-kinase inhibitors for cancer therapy." Acta Pharm Sin B **7**(1): 27-37.

Publications

Sathe, A., G. Chalaud, I. Oppolzer, K. Y. Wong, M. von Busch, S. C. Schmid, Z. Tong, M. Retz, J. E. Gschwend, W. A. Schulz and R. Nawroth (2018). "Parallel PI3K, AKT and mTOR inhibition is required to control feedback loops that limit tumor therapy." PLoS One 13(1): e0190854. https://doi.org/ 10.1371/journal.pone.0190854